Université de Montréal

Enhancing Infotainment Applications Quality of Service in Vehicular Ad Hoc Networks

par
Togou Mohammed Amine

Département d'informatique et de recherche opérationnelle
Faculté des arts et des sciences

Thèse présentée à la Faculté des études supérieures
en vue de l'obtention du grade de Philosophiæ Doctor (Ph.D.)
en informatique

Février, 2017

RÉSUMÉ

Les réseaux ad hoc de véhicules accueillent une multitude d'applications intéressantes. Parmi celles-ci, les applications d'infodivertissement visent à améliorer l'expérience des passagers. Ces applications ont des exigences rigides en termes de délai de livraison et de débit. De nombreuses approches ont été proposées pour assurer la qualité du service des dites applications. Elles sont réparties en deux couches : réseau et contrôle d'accès. Toutefois, ces méthodes présentent plusieurs lacunes.

Cette thèse a trois volets. Le premier aborde la question du routage dans le milieu urbain. A cet égard, un nouveau protocole, appelé SCRP, a été proposé. Il exploite l'information sur la circulation des véhicules en temps réel pour créer des épines dorsales sur les routes et les connectées aux intersections à l'aide de nIJuds de pont. Ces derniers collectent des informations concernant la connectivité et le délai, utilisées pour choisir les chemins de routage ayant un délai de bout-en-bout faible. Le deuxième s'attaque au problème d'affectation des canaux de services afin d'augmenter le débit. A cet effet, un nouveau mécanisme, appelé ASSCH, a été conçu. ASSCH collecte des informations sur les canaux en temps réel et les donne à un modèle stochastique afin de prédire leur état dans l'avenir. Les canaux les moins encombrés sont sélectionnés pour être utilisés. Le dernier volet vise à proposer un modèle analytique pour examiner la performance du mécanisme EDCA de la norme IEEE 802.11p. Ce modèle tient en compte plusieurs facteurs, tels que l'opportunité de transmission, non exploitée dans IEEE 802.11p.

Mots clés: Réseaux ad hoc de véhicules, applications d'infodivertissement, routage (informatique), IEEE 802.11p (norme).

ABSTRACT

The fact that vehicular ad hoc network accommodates two types of communications, Vehicle-to-Vehicle and Vehicle-to-Infrastructure, has opened the door for a plethora of interesting applications to thrive. Some of these applications, known as infotainment applications, focus on enhancing the passengers' experience. They have rigid requirements in terms of delivery delay and throughput. Numerous approaches have been proposed, at medium access control and routing layers, to enhance the quality of service of such applications. However, existing schemes have several shortcomings. Subsequently, the design of new and efficient approaches is vital for the proper functioning of infotainment applications.

This work proposes three schemes. The first is a novel routing protocol, labeled SCRP. It leverages real-time vehicular traffic information to create backbones over road segments and connect them at intersections using bridge nodes. These nodes are responsible for collecting connectivity and delay information, which are used to select routing paths with low end-to-end delay. The second is an altruistic service channel selection scheme, labeled ASSCH. It first collects real-time service channels information and feeds it to a stochastic model that predicts the state of these channels in the near future. The least congested channels are then selected to be used. The third is an analytical model for the performance of the IEEE 802.11p Enhanced Distributed Channel Access mechanism that considers various factors, including the transmission opportunity (TXOP), unexploited by IEEE 802.11p.

Keywords: DSRC, EDCA, IEEE 802.11p standard, routing, WAVE.

CONTENTS

LIST OF TABLES

LIST OF FIGURES

LIST OF ABBREVIATIONS

AC	Access Category
ACD	Average Capture Delay
AES	Advanced Encryption Standard
AIFS	Arbitrary Inter-Frame Spacing
AODV	Arbitrary Inter-Frame Spacing
AP	Access Point
AVSI	Advanced Vehicle Safety Initiative
BSM	Basic Safety Message
BSS	Basic Service Set
BSSID	Basic Service Set Identifier
CAHSI	Cruise-Assist Highway System Initiative
CALM	Continuous Air interface for Long and Medium distance
CAR	Connectivity Aware Routing
CBC-MAC	Cipher Block Chaining Message Authentication Code
CCH	Control Channel
CCI	Control Channel Interval
CCW	Channel Collision Warning
CDS	Connected Dominating Set
CEPT	European Conference of Postal and Telecommunications Administrations
CH	Cluster Head
CICAS	Cooperative Intersection Collision Avoidance System
CSMA/CA	Carrier Sense Multiple Access/Collision Avoidance
CTS	Clear To Send

CW	Contention Window
DNS	Domain Name System
DOT	Department Of Transportation
DS	Distribution System
DSR	Dynamic Source Routing
DSRC	Dedicated Short Range Communication
E2ED	End-to-End Delay
ECIES	Elliptic Curve Integrated Encryption Scheme
EDCA	Enhanced Distributed Channel Access
FCC	Federal Communication Commission
FI	Frame Information
GI	Guard Interval
GPS	Geographic Positioning System
GPSR	Greedy Perimeter Stateless Routing
GPCR	Greedy Perimeter Coordinator Routing
GSR	Geographic Source Routing
HMM	Hidden Markov Model
IEEE	Institute of Electrical and Electronics Engineers
ITS	Intelligent Transportation Systems
LLC	Logical Link Control
LoS	Line-of-Sight
MAC	Medium Access Layer
MANET	Mobile Ad hoc Network
MCDS	Minimum CDS
MDC	Minimum Duration Counter
MDDV	Mobility-Centric Data Dissemination Algorithm for VANET

MT	Monitor Table
NOW	Network on Wheels
OBU	On-Board Unit
OCB	Outside the Context of BSS
OCT	Channel Occupancy Table
OFDM	Orthogonal Frequency Division Multiplexing
OSCHN	Overlapping SCH Notification
PBR	Position-based Routing
PHY	Physical Layer
PLCP	Physical Layer Convergence Procedure
PMD	Physical Medium Dependent
PPDU	Physical Protocol Data Unit
PSC	Provider Service Context
PSDU	PHY Service Data Unit
PSID	Provider Service IDentifier
QoS	Quality of Service
RCPI	Received Channel Power Indicator
RREQ	Route Request
RSSI	Received Signal Strength Indication
RSU	Road Side Unit
RTS	Ready To Send
SAE	Society of Automotive Engineers
SCH	Service Channel
SCI	Service Channel Interval
SI	Synchronization Interval
SIFS	Short Inter-Frame Space

TA	Timing Advertisement
TXOP	Transmission Opportunity
UTC	Coordinated Universal Time
V2V	Vehicle-to-Vehicle
V2I	Vehicle-to-Infrastructure
VANET	Vehicular Ad hoc Network
VII	Vehicle Infrastructure Integration
VSC-A	Vehicle Safety Communication Application
VSS	Vehicle-Based Safety Systems
WAVE	Wireless Access for Vehicular Environment
WBSS	WAVE Basic Service Set
WEC	World Energy Council
WHO	World Health Organization
WILLWARN	Wireless Local Danger Warning
WRA	WAVE Routing Advertisement
WSA	WAVE Service Advertisement
WSM	WAVE Short Message
WSMP	WAVE Short Message Protocol
ZOR	Zone of Relevance

NOTATION

SF_i	Stability Factor
R	Transmission Range
V_{nb}	average speed of the tagged vehicle's neighbors
d_{nb}	average distance between the tagged vehicle's and its neighbors
α, β	weighting coefficients
t_{cross}	Time needed by a vehicle to cross the intersection zone
t_{rem}	Remaining time of the green light phase
t_g	Green light phase
t_a	Time to reach traffic light
t_C	Traffic light cycle
d_p	Delay to incur for transmitting a new data packet over a road segment
d_{h_i}	Delay to incur at each backbone vehicle
T_q	Queuing delay
T_{tx}	Transmission delay
d_{rap}	RAP's delivery delay
t_{rx}	RAP's received time
T_{bc}	Time needed by RAP to travel a road segment with built-in backbone
h_{max}	Maximum number of backbone vehicles a road segment can hold
T_{cf}	Maximum time to wait for RAP when using carry-and-forward
$w_{S_{(i,j)}}$	Weight of road segment $S_{(i,j)}$
d_{cf}	Delay to incur when using carry-and-forward
l	Cell's length
l_{av}	Vehicle's average length
d_s	Average safety distance
v_{av}	Average speed of vehicles on $S_{i,j}$
p_{cf}	Probability of using the carry-and-forward
p_{cell}	Probability of having at least one vehicle in a cell
λ_i	Vehicles' arrival rate at road segment $S_{i,j}$

p_{dis}	Probability of disconnection
$WVP_{S_{i,j}}$	Weight validity period of $S_{i,j}$
w_{pth}	Weight of the routing path
WVP_{pth}	Weight validity period of the routing path
w_{th}	Routing path weight threshold
S_N	Set of vehicles on SCH 172
p_q^i	Probability of a provider Pv_i requesting a channel
$P_{m,j}$	Probability that the channel will be in state S_m in the next SCI given that it is in state S_j
P_{hold}^i	Probability that provider Pv_i holds the same channel in the next SCI
$P_{release}^i$	Probability that provider Pv_i releases the channel at the end of the current SCI
P_{nrq}^i	Probability that no provider of priority i requests the channel
$P_{rq\geq 1}^i$	Probability that at least one provider of priority i requests the channel
t_i	Time interval vehicles should wait before transmitting OSCHN
CW_{min}	Minimum contention window
CW_{max}	Maximum contention window
T_s	Duration of a time slot
r_i	Retransmission limit
CW_j^i	Contention window size of AC_i at backoff stage j
m_i	The backoff stage where $CW_m^i = CW_{max}^i$
p_b	Probability of a busy channel in a slot
p_{c_i}	Collision probability of AC_i in a slot
τ_i	Transmission probability of AC_i
p_{s_i}	Probability of successful transmission for AC_i
p_{f_i}	Probability of $TXOP_i$ not yet expired
T_L	Transmission time of a packet of size L
$\overline{T_i}$	Average expected time spent at all states by AC_i

(dedication) To my MOTHER, FATHER,

SISTERS, and BROTHER.

I am forever indebted to you.

ACKNOWLEDGMENTS

I would like to thank all the people who have encouraged me, in various ways, to pursue my goal. This dissertation would not have been possible without them.

My deep appreciation goes to Prof. Abdelhakim Hafid and Dr. Lyes Khoukhi for giving me the opportunity to work with them on one of the promising technologies that can make our world better. Their exemplary supervision, great support, valuable advice and constructive criticism have helped me become the researcher I am today.

Special thanks go to my PhD committee members, Prof. Hossam Hassanein, Prof. Rami Langar, Prof. Pierre Samuel, Prof. Philippe Langlais, and Prof. Dominique Gaiti for the constructive comments and suggestions, which helped improving the quality of the thesis.

I would like to thank Dr. Pratap Kumar Sahu for his guidance and encouragement during my first year as a Ph.D student. His explanations were easy to grasp and his feedback was highly appreciated. I am very glad to have worked with him.

I would like also to thank all my colleagues at LRC and ERA Research Laboratories for the beneficial discussions, research collaboration, and continuous exchange of knowledge. No doubt all LRC and ERA members are great people.

In addition, I would sincerely like to thank all my friends in Montreal, Canada and in Troyes, France, for their continuous support and encouragements. Special thanks for my brothers Mourad D'Himane and Mustapha Hrouga, who made my stay in Troyes comfortable and very enjoyable.

Last but not least, I would like to express my sincere gratitude to my family for their moral, financial, and never ending support for without them, none of this would have been possible.

CHAPTER 1

INTRODUCTION

1.1 Research Context

Road safety and traffic efficiency are among the major problems that governments worldwide have been attempting to settle in the last decades. The inadequacy of current methods, i.e., post-crash measures (e.g., airbags) and road network expansion (i.e., due to spatial, financial, and environmental constraints), has mobilized government agencies and the automotive industry to develop prominent solutions that aim at making transportation systems safer and more efficient. The key idea is to equip vehicles with cutting-edge technologies (e.g., sensors, geographical positioning system (GPS), network interface cards (NICs), and cameras), making them evolve from a simple mean of transportation into intelligent systems that can assist drivers in making refined decisions and avoiding hazardous events. An example of such vehicles is *KITT*, David Hasselhoff's car in the *Knight Rider (K2000)* TV show (1982-1986).

When deployed, these vehicles shall enable a new self-configuring wireless network known as vehicular ad hoc network (VANET). It is based on the Wireless Access for Vehicular Environment (WAVE) standards suite and is considered as the key enabling technology for future Intelligent Transportation Systems (ITS). VANET will enable several useful applications such as automatic road traffic alerts dissemination, dynamic route planning, service queries (e.g., parking availability), media sharing, and context-aware advertisement [1]. To provide such services, two communication modes are supported, including vehicle-to-vehicle (V2V) and vehicle-to-infrastructure (V2I).

In the next subsections, we start by briefly describing each communication mode. Then, we present the characteristics and challenges of VANET. Next, we describe VANET's various applications and we review some of its ongoing projects.

1.1.1 VANET Architecture

VANET supports two forms of communication: vehicle-to-infrastructure and vehicle-to-vehicle. In V2I, messages are exchanged between vehicles equipped with WAVE devices, called On-Board Units (OBUs), and stationary entities, called Road Side Units (RSUs), usually installed along road edges or in dedicated locations such as intersections and parking lots [2]. The basic functionality of RSUs is to extend the communication range of the vehicular network via relaying messages received from vehicles to other vehicles passing by (see Figure 1.1(a) [2]). They can also provide additional services such as real-time traffic statistics, weather forecast, and Internet access (see Figure 1.1(b) [2]).

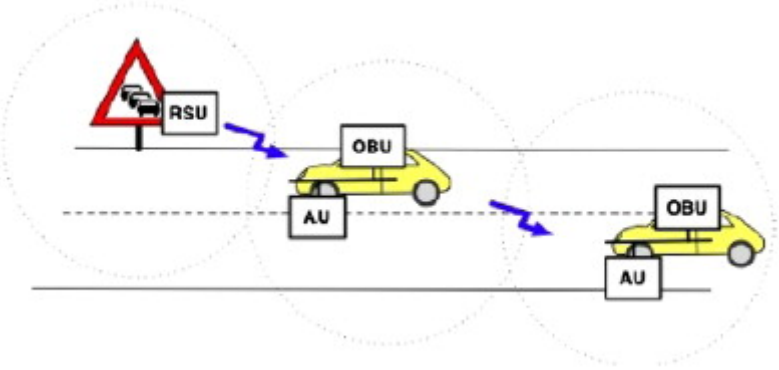

(a) RSU as safety information provider

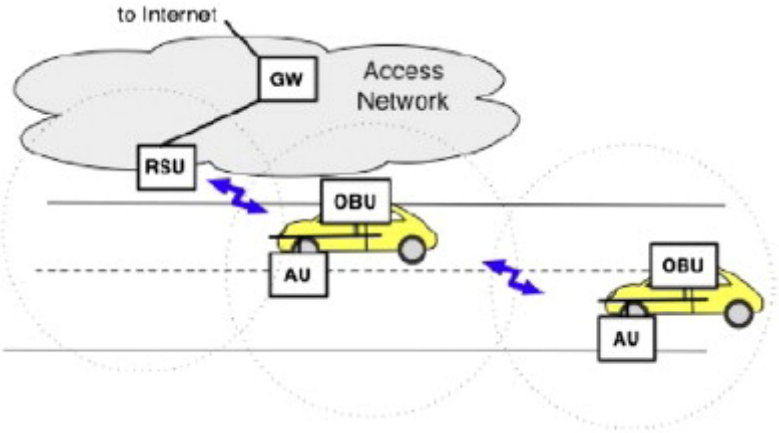

(b) RSU as Internet access provider

Figure 1.1: RSU functionalities

V2V is an infrastructure-less mode in which vehicles can directly communicate with one another when they are within transmission range (i.e., 300 to 1000 meters). They can also use multihop communication to reach out of range cars. At the heart of V2V is a basic technique, called beaconing. It consists of sending periodic messages, labeled *beacons*, containing various information such as vehicle's position, speed, and direction. The goal of beaconing is to make vehicles aware of their neighboring vehicles' current location in order to predict their future positions. This will help drivers make better decisions, avoiding therefore hazardous events.

1.1.2 VANET Characteristics

VANET has particular characteristics that distinguish it from other wireless networks. For instance, nodes [1] in VANET are highly mobile (i.e., up to 50 km/h in cities and 120 km/h in highways), causing frequent topological shifts. In addition, nodes movements are restricted by road layouts and shall abide to driving rules (e.g., traffic lights, stop signs, overtaking manoeuvres, etc.). Moreover, network density, which is directly linked to traffic flow, is observed to greatly fluctuate depending on time periods (i.e., night, day, and peak hours) as well as locations (i.e., downtown, highway, and suburban). Finally, VANET has no power nor computational capacity constraints. In fact, vehicles are equipped with batteries with a lifetime that spans between 3 to 5 years [3]. This allows for multiple gadgets to be installed such as high performance processors, high capacity memory cards, digital maps and GPS devices.

1.1.3 VANET Challenges

The aforementioned characteristics bring along new challenges that might affect the deployment of VANET in real life. For instance, high mobility and frequent topology shifts can lead to network fragmentation, resulting in sporadic connectivity. This forces routing protocols to build unstable routing paths that can extremely degrade the network's quality of service (QoS), delay and throughput in particular. Moreover, VANET

1. Nodes and vehicles will be used interchangeably in the rest of this dissertation.

has the potential to grow to a very large scale, imposing the need for new techniques (i.e., routing protocols, IP address configuration, and bandwidth allocation) as existing approaches for other wireless networks are not suitable for this highly agile environment. Furthermore, maintaining a global network topology is nearly impossible for a node in VANET. Traditional structures like trees cannot be used since they incur high maintenance cost. Instead, each vehicle keeps track of its local topology information (i.e., number of neighboring nodes, their locations, and their speed), collected via periodic beacon messages. Besides, signal propagation between communicating vehicles is affected by the presence of obstacles (e.g., buildings, trees, and even vehicles), increasing therefore its fading rate [2]. Finally, security and privacy are of crucial importance to VANET. Since packets encapsulate critical information, it is mandatory to make sure that they are neither injected nor altered by fraudulent users. Keeping in mind the requirements of VANET environment, cryptographic algorithms along with authentication schemes must be as fast as possible to allow for real-time data transfer [4].

1.1.4 VANET Applications

VANET was conceived primarily to enhance road safety and avoid accidents. Safety applications in VANET can be classified into event-driven and periodic, based on the frequency at which safety messages are transmitted. Event-driven applications require the transmission of safety messages only in case of an event taking place. For example, at intersections, messages regarding vehicles that are violating traffic lights or stop signs can be exchanged to prevent possible collisions. Similarly, in case of a car accident, messages are broadcasted quickly into the accident's vicinity urging drivers to slow down, averting therefore probable chain collisions (1 and 2 in Figure 1.2). These messages can also be used to notify vehicles near exits about the accident in order to avoid traffic jams (3 in Figure 1.2). Finally, paramedics and police officers can be notified immediately via RSUs to rapidly intervene and save people's lives. Periodic safety applications, on the other hand, require transmission of safety messages at regular time intervals. To illustrate, RSUs located at intersections can regularly notify approaching vehicles about road condition (e.g., slippery). They can also inform vehicles about the current traffic light

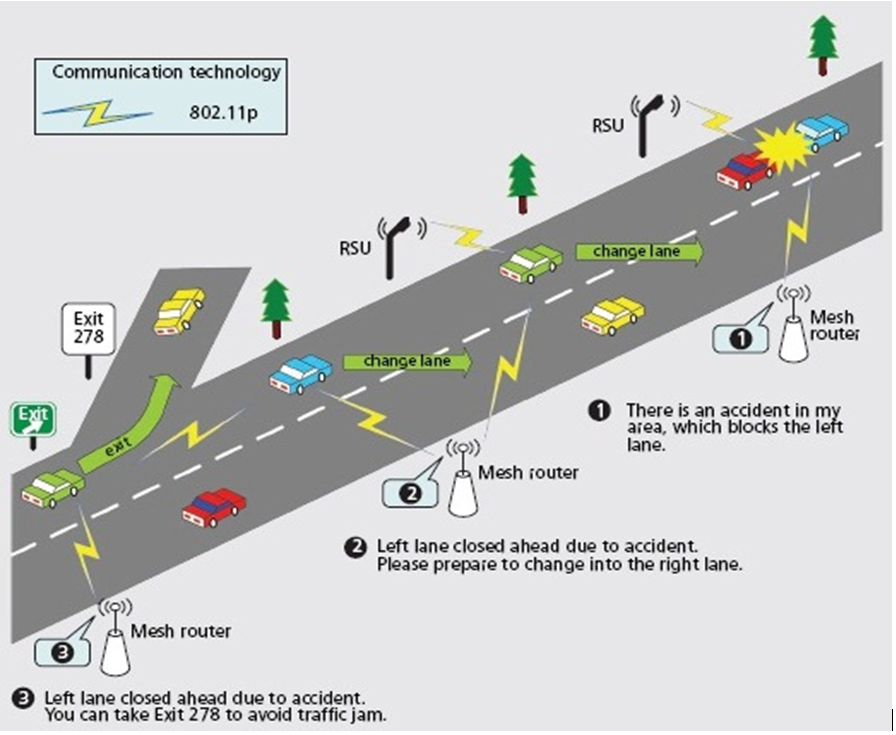

Figure 1.2: VANET applications

phase and the time remaining before switching to the next one. This information can be used by OBUs to suggest to drivers the stopping location or the optimal speed to cross the intersection without stopping at the traffic light.

Aside from safety-related applications, VANET allows for plenty of other services that offer tremendous potential for new business opportunities. These applications are of two types: traffic efficiency and infotainment. Traffic efficiency applications focus on enhancing route guidance and navigation. For instance, traffic statistics on various roads can be acquired in real-time and alternative routes can be provided to avoid traffic congestions. Likewise, controlling traffic lights via analyzing information collected through VANET (e.g., speed and density) can help smoothing traffic flows, therefore reducing traffic load on major roads. Infotainment applications, on the other hand, aims at improving the driving experience, making passengers' journey more enjoyable. For example, available services in nearby regions (e.g., malls, restaurants, gas stations, and parking lots) can be advertised using RSUs. These RSUs can also provide Internet access

to passengers in order to check their emails, download music, or make online transactions. Finally, media sharing (e.g., music, movies), social media applications, and online multiplayer games can be enabled between neighboring vehicles. Bear in mind that these applications may accelerate the deployment of VANET since people are more and more addicted to their smartphones and they want to be connected anywhere, anytime.

1.1.5 VANET Ongoing Projects

Since the early 90s, VANET activity in terms of research and development has been intensively growing. In this regard, several projects that aim at ensuring road safety have been jointly launched by governmental agencies and car manufacturers in different parts of the world. In the United States, the Federal Communication Commission (FCC) assigned 75 MHz bandwidth from the 5.9 GHz band as a freely licensed spectrum to enable safety applications using Dedicated Short Range Communication (DSRC) [5]. Since then, several projects have seen light. For instance, Vehicle Infrastructure Integration (VII), rebranded to IntelliDrive, focuses on establishing test beds to provide support for V2V and V2I under DSRC. It also studies non-technical issues regarding privacy, liability, and application of regulations. Similarly, the Vehicle Safety Communication-Application project (VSC-A) focuses on vehicle communication and relative positioning, with the goal of enabling interoperability among safety applications [6]. It identifies eight crash scenarios, including Emergency Electronic Brake Lights (EEBL), Forward Collision Warning (FCW), Blind Spot Warning (BSW), Intersection Movement Assist (IMA), and Do Not Pass Warning (DNP). The Integrated Vehicle-Based Safety Systems (IVBSS) project explores the human-machine interface issues when several safety applications, with potentially overlapping or contradictory advisories, are operated simultaneously [6]. Finally, the Cooperative Intersection Collision Avoidance System (CICAS) focuses on preventing dangers at intersections by allowing traffic lights to transmit phase and timing information to nearby vehicles. Each vehicle would then predict the likelihood of violating the red light; drivers are notified only when needed.

In Japan, a standard for V2I communication denoted also as DSRC System was issued in 2001. It was used in electronic toll collection, but the system was generalized to

support various services [6]. With the great success that this system has known, various ITS projects have been inaugurated to enhance V2I and V2V communications under the umbrella of Japan's national ITS Safety 2010 initiative. For example, the Advanced Vehicle Safety Initiative (AVSI) aims at warning drivers against road dangers ahead and preventing rear-end collisions. It also focuses on developing new techniques for position recognition of neighboring vehicles using V2V communication based on the Carrier Sense Multiple Access (CSMA) technology [6]. The Advanced Cruise-Assist Highway System (AHS) initiative focuses on reducing traffic accidents, enhancing safety, and improving transportation efficiency using RSUs.

In Europe, a 30 MHz bandwidth was allocated by the European Conference of Postal and Telecommunications Administrations (CEPT) to support road safety services [7]. Since then, several projects were initiated. Examples include COOPERS, CVIS, SAFESPOT, and PReVENT. The Co-operative Systems for Intelligent Road Safety project (COOPERS) focuses on developing innovative applications for cooperative traffic management using V2I communication. It makes use of Continuous Air interface for Long and Medium distance (CALM) standards, aiming at supporting continuous communications between vehicles via employing various media and communication interfaces [6]. The Co-operative Vehicle-Infrastructure Systems project (CVIS) aims at designing, developing, and testing new technologies to enable V2V and V2I communications following the CALM standards. It also makes use of the IEEE 802.11p interface, denoted as "Microwave 5 GHz" (M5) interface [6]. The SAFESPOT project focuses on enhancing the field's view of autonomous vehicles via developing sophisticated cooperative systems that are based on V2V and V2I communications. The communication technology used in SAFESPOT is IEEE 802.11a/p [6]. Finally, the Preventive and Active Safety Applications project (PReVENT) aims at developing, testing, and evaluating safety related applications using advanced sensing and communication devices integrated in OBUs. Within PReVENT, the Wireless Local Danger Warning subproject (WILLWARN) is based on IEEE 802.11a/p and uses the Network on Wheels (NOW) [8] communication platform.

1.2 Motivations and Objectives

Infotainment applications are supported by WAVE in order to accelerate VANET's deployment. Most of these applications have rigid QoS requirements (i.e., bandwidth, delay and throughput). Yet, meeting them is not straightforward, given the particular characteristics of VANET (e.g., high mobility, sporadic connectivity, and short links lifetime). Thus, the objective of this dissertation is to design and evaluate new solutions to ensure infotainment applications QoS. This is done at the network layer and the medium access control (MAC) sublayer. On the one hand, we propose a new routing protocol for infotainment applications that considers the end-to-end delay when forwarding data packets. On the other hand, we design and implement new mechanisms for managing resources, DSRC channels in particular, in order to enable service differentiation between different infotainment applications to further enhance their QoS.

The first part of this thesis addresses the problem of routing in urban VANET considering infotainment applications QoS requirements (e.g., short delivery delay and low packet loss ratio). Several routing strategies have been proposed to deal with this issue. Among them, position-based routing (PBR) ought to be the most convenient as it exhibits great resilience to network topology changes [9]. Various PBR schemes [10–21] have been proposed in the literature. They are either reactive or proactive. Reactive schemes aim at establishing routing paths whenever a data packet is to be transmitted while proactive approaches build virtual infrastructures (e.g., clusters and backbones), ahead of time, to relay messages. Despite their good performance, exiting schemes sustain major shortcomings. On the one hand, reactive protocols only acquire local network topology, making them prone to local maximum and data congestion problems (see Chapter 4 for more details). Proactive protocols, on the other hand, suffer large control message overhead when maintaining the infrastructure, which might lead to network congestion.

The second part of this dissertation focuses on the problem of DSRC channel selection to enhance the QoS of V2V infotainment applications. In the literature, several schemes [22–34] have been proposed to help service providers, mainly vehicles, of info-

tainment applications select service channels that guarantee the best QoS (e.g., throughput). They can be of two types: allocation-based and prediction-based. The former uses single or dual transceivers and requires vehicles to keep track of used service channels in their 1-hop and 2-hop ranges. This information is then exchanged on an event-driven basis and is used to select the least congested channel. The latter uses multiple transceivers to continuously monitor all channels and deploys prediction mechanisms to identify the best channel to be used. Although they assure certain level of QoS, schemes in both categories experience various limitations. On the one hand, channel occupancy information may be obsolete due to collisions, rendering the existing allocation-based schemes of limited value. On the other hand, prediction-based schemes suffer cross-channel interferences and are cost-inefficient, due to the use of multiple transceivers, making them infeasible, particularly during VANET's initial deployment [35].

The final part of this thesis addresses the problem of accurately modeling the performance of the enhanced distributed access channel (EDCA) mechanism for IEEE 802.11p. This problem shall take into account many criteria, including the saturation condition, the backoff procedure, the internal/external collisions, and the transmission opportunity (TXOP). Several models [36–42] have been proposed in the literature to analyze the IEEE 802.11p EDCA performance. While most of them were designed for safety applications, very few can be applied to non-safety applications. Yet, to the best of our knowledge, none of the proposed models have considered all the aforementioned factors.

1.3 Thesis Contributions and Organization

The aforementioned research topics have yielded several results that we have submitted or published as articles in international refereed journals and conferences. The thesis consists of three contributions made from three scientific articles (two journal article and one conference paper) which we considered the most significant and complete among the seven articles proposed. Four of these articles are already published (one journal article and three conference papers), two conference papers are accepted, and

one journal article is under review (minor revision).

To address the issue of routing in urban VANET, we proposes a novel routing protocol SCRP [43, 44]. It is a distributed geographic source routing scheme that takes advantage of the network topology to select routing paths with low end-to-end delay (E2ED). SCRP starts by building backbones over road segments considering vehicles' speed and spatial distribution. These backbones are then connected at intersections via bridge nodes that keep an up-to-date network topology while monitoring the delay to incur for transmitting new data packets over road segments. Based on this information, SCRP assigns weights to road segments; the ones with the lowest weights are selected to construct routing paths.

We then describe the service channel selection mechanism, called Altruistic Service Channel Selection Scheme (ASSCH), a hybrid approach that aims at improving V2V infotainment applications performance without affecting the delivery of safety messages. It is WAVE-compliant and has three phases: 1) collecting real-time information about channels state via compelling vehicles to collaborate; 2) feeding the collected information to a Markovian model that predicts the state of each channel in the near future; and 3) selecting the least congested/used channel.

Finally, we present a theoretical and simulation-based analysis of the IEEE 802.11p EDCA mechanism. In this regard, two Markovian models are proposed, taking into consideration various factors (e.g., saturation condition, the backoff procedure, the internal/external collisions). The first model describes the backoff procedure as well as the contention phase of the different traffic classes. The second model [45] extends the first one by considering TXOP, unexploited by IEEE 802.11p. Using both models, we derive the probability of transmission and the probability of collision and we infer the normalized throughput for each traffic class. Simulations were conducted to verify the effectiveness of our analysis.

1.4 Thesis Organization

The remaining of this dissertation is structured as follows. After introducing VANET and its characteristics, we review the WAVE framework in chapter 2. We describe in details the different standards being developed for WAVE deployment in the United States, including the IEEE 802.11p standard, the IEEE 1609.X standards family, and the SAE J2735 Message set Dictionary. In Chapter 3, we outline the existing approaches in the literature that address the aforementioned issues (i.e., routing in urban VANET, DSRC channel allocation, and EDCA performance modeling). We then present SCRP in chapter 4, describe ASSCH in chapter 5, and detail the models proposed for IEEE 802.11p EDCA performance analysis in chapter 6. Finally, in chapter 7, we summarize the major contributions of this dissertation, outline future research directions, and present the list of articles produced during this thesis.

CHAPTER 2

WIRELESS ACCESS FOR VEHICULAR ENVIRONMENT (WAVE)

The automotive industry has been working to develop WAVE framework, which will be used to support both V2V and V2I. The effectiveness of this technology is highly dependent on cooperative standards for interoperability [5]. In this chapter, we aim at giving insights about the different technologies and standards being developed for WAVE deployment. This includes the Dedicated Short Range Communication (DSRC) technology; the IEEE 802.11p standard; IEEE 1609.2, 1609.3, 1609.4 standards for Security, Network Services, and Multichannel Operations; and the SAE J2735 Message Set Dictionary. Although WAVE is of interest to several countries, implementation models vary from one place to another. In the following sections, we shed light on the North American version of WAVE.

The rest of the chapter is organized as follows. Section 2.1 gives an overview of DSRC while Section 2.2 describes in details WAVE's protocol stack. Section 2.3 concludes the chapter.

2.1 DSRC Overview

In 1999, the U.S FCC has allocated 75 MHz of licensed spectrum in the 5.9 GHz band (i.e., from 5.85 GHz to 5.925 GHz) for DSRC communication [5]. This spectrum is divided into seven 10 MHz channels, as illustrated in Figure 2.1, and a 5 MHz guard band. Channels 172 and 184 are reserved for public safety applications. Channel 178 is referred to as the Control Channel (CCH) and is exclusively dedicated to transmitting

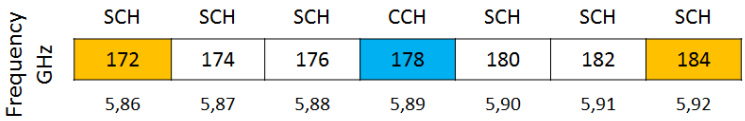

Figure 2.1: DSRC channels

safety and control messages. The remaining channels are referred to as Service Channels (SCHs) and are used for transmitting data packets of infotainment applications. Table 2.I [5, 46] shows DSRC characteristics in USA, Japan, and Europe.

Table 2.I: DSRC characteristics in USA, Japan, and Europe

Features	USA	Japan	Europe
Communication	Half-duplex	Half-duplex (OBU) full-duplex (RSU)	Half-duplex
Band	75 MHz	80 MHz	30 MHz
Channels	7	Downlink: 7, Uplink: 7	4
Transmission range	1000 m	30 m	15-20 m
Data Rate	3-27 Mbps	1, 4 Mbps	250-500 Kbps
Radio frequency	5.9 GHz	5.8 GHz	5.8 GHz
Channel separation	10 MHz	5 MHz	5 MHz

The primary motivation behind developing DSRC is to enable collision prevention applications. Indeed, the U.S Department of Transportation (DOT) has estimated that V2V communications based on DSRC can address up to 82% of all crashes in the United States involving unimpaired drivers, potentially saving thousands of lives and billions of dollars [5]. The reason is twofold: 1) DSRC is based on short-range (i.e., hundreds of meters) two-way Line-of-Sight (LoS) communication with sufficient bandwidth which is significantly cheap compared to other technologies such as cellular, WiMax or Satellite [35]; and 2) DSRC adopts WiFi standards, making operations related to V2V and V2I easier to integrate and implement.

DSRC can also be pivotal for many other applications beyond collision prevention. Most of these involve communication to and from RSUs [5]. For instance, DSRC can be used to assist navigation, make electronic payments (e.g., tolls, parking), reduce fuel consumption (i.e., reducing therefore CO_2 emissions), as well as collecting real-time traffic statistics and disseminating them. It can also be used for entertainment purposes such as Internet access, media sharing, and online gaming.

2.2 WAVE Standards Suite

Figure 2.2 [5] illustrates WAVE protocol stack. The physical and MAC layers are based on the IEEE 802.11p standard, which is a modified version of IEEE 802.11. At the upper layers, WAVE employs a suite of standards defined by the IEEE 1609 Working Group to enable safety applications: 1609.4 for multichannel operations, 1609.3 for network services (i.e., including WAVE Short Message Protocol (WSMP)), and 1609.2 for security services. Non-safety applications, on the other hand, use IPv6 and the TCP/UDP protocols in the network and transport layers, respectively. In the next subsections, we examine in more details the different standards, working from bottom to top.

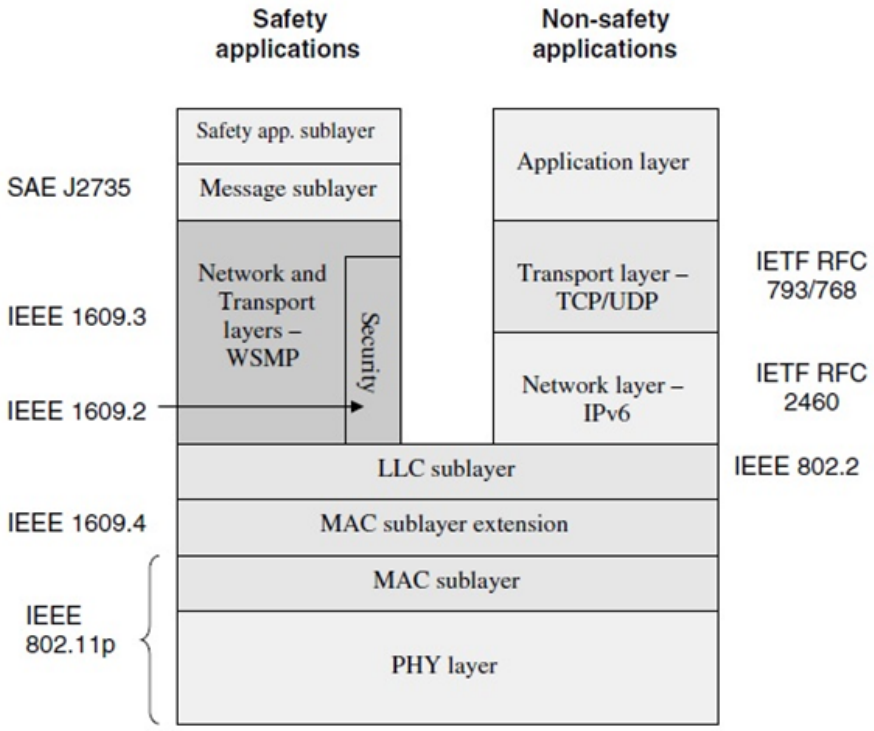

Figure 2.2: WAVE protocol stack

2.2.1 Physical Layer

WAVE's physical layer is based on the IEEE 802.11a standard. It uses Orthogonal Frequency Division Multiplexing (OFDM) modulation to provide different data rates (i.e., from 3 to 27 Mbps) and has two modules.

2.2.1.1 Physical Layer Convergence Procedure (PLCP)

At the transmitter, PLCP processes the bytes in a MAC frame to be transformed into OFDM symbols for transmission over the air by Physical Medium Dependent (PMD) module [5]. PLCP adds the physical layer overhead to the MAC frame to create a Physical Protocol Data Unit (PPDU), as illustrated in Figure 2.3 [47]. The *Preamble* is used to synchronize the signal at the receiver. while the *SIGNAL* field contains the data rate and the frame length, acquired from the MAC layer. The *SERVICE* and *TAIL* fields facilitate bit scrambling whereas the *PAD* field enures that the final OFDM symbol is properly encoded. The Physical Layer Service Data Unit (PSDU) field contains the MAC frame.

At the receiver, PLCP performs the inverse function to extract the MAC frame from the PPDU. It also provides the Received Signal Strength Indication (RSSI) to the MAC layer.

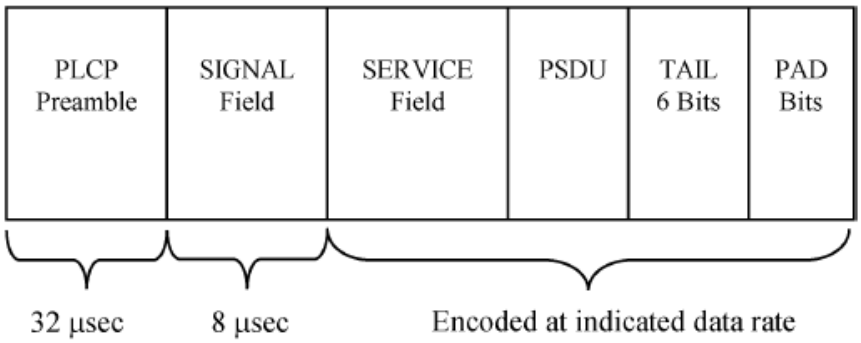

Figure 2.3: PPDU format

2.2.1.2 Physical Medium Dependent (PMD) Function

When PMD receives PPDU from PLCP, it performs OFDM modulation and transmits PPDU over the air. At the receiver, PMD performs demodulation and passes the received PPDU to PLCP along with RSSI. Note that, unlike IEEE 802.11a, DSRC uses 10 MHz channels to account for delay and Doppler spreads, likely to be encountered in the vehicular environment [48].

2.2.2 MAC Sublayer

Like IEEE 802.11, IEEE 802.11p uses Carrier Sense Multiple Access/Collision Avoidance (CSMA/CA) as the medium access mechanism. In addition, IEEE 802.11p utilizes the Enhanced Distributed Channel Access (EDCA) mechanism to provide service differentiation. In this paradigm, four access categories (ACs) are defined (i.e., AC_BK, AC_BE, AC_VI, and AC_VO), each having its own parameters (i.e., Arbitration Inter-Frame Space ($AIFS$), minimum contention window (CW_{min}) and maximum contention window (CW_{max})) with AC_VO having the highest priority, as show in Table 2.II. aCW_{min} and aCW_{max} are set to 15 and 1023, respectively [47].

Table 2.II: EDCA Parameter set

AC	CW_{min}	CW_{max}	AIFSN	TXOP
AC_BK	aCW_{min}	aCW_{max}	9	0
AC_BE	aCW_{min}	aCW_{max}	6	0
AC_VI	$\frac{aCW_{min}+1}{2}-1$	aCW_{min}	3	0
AC_VO	$\frac{aCW_{min}+1}{4}-1$	$\frac{aCW_{min}+1}{2}-1$	2	0

Each AC, with a frame to transmit, senses the channel first. If the channel is idle and stays idle for at least AIFS, AC starts transmitting its frame. If the channel is busy, AC invokes the backoff procedure by choosing a number of idle time slots (AIFSN) to wait before attempting to transmit its frame. The countdown begins when the channel becomes idle, is interrupted during any non-idle interval, and resumes when the medium stays idle for at least AIFS [5]. Once AC transmits its unicast frame, it waits for an

acknowledgement (ACK) from the recipient. If ACK is not received within a timeout interval, AC retransmits the frame after invoking the backoff process. A frame can be retransmitted as long as the retransmission limit is not yet reached. In case of unsuccessful retransmission given that the retransmission limit was attained, the frame is dropped. Note that each AC is allowed to send only one frame per channel access, i.e., transmission opportunity (TXOP) of each AC is set to 0.

The channel router module, illustrated in the top of Figure 2.4 [35], inserts data frames into ACs of the appropriate channel based on the channel identifier and the priority fields, contained in their headers. Data frames will then be dequeued and scheduled for external contention depending on their AC indices. The channel selector module, depicted in the bottom of Figure 2.4, is responsible for carrying out multiple decisions such as when to monitor a specific channel and for how long.

Besides, IEEE 802.11p introduces some enhancements to the traditional IEEE 802.11 standard in order to cope with VANET high mobility. Indeed, IEEE 802.11p defines a new type of communication, called *Outside Context of Basic Service Set (OCB)*, particularly for V2V, where exchanging data frames does not require neither authentication nor association. To distinguish frames sent in OCB mode, IEEE 802.11p sets the value of BSSID field in the frame header to 0xFFFFFF, also known as the wildcard value. A receiver with OCB mode enabled will pass up the stack any data frame that has the wildcard value as BSSID and will ignore any data frame with different BSSID. Data frames sent in OCB mode are transmitted between nodes that do not belong to any Basic Service Set (BSS). IEEE 802.11p defines the context of having such exchange as WAVE BSS (WBSS), which will be investigated in chapter 5. In addition, IEEE 802.11p introduces a new management frame, labeled Timing Advertisement (TA), which can be used to distribute time synchronization information [49] in the absence of GPS devices.

2.2.3 IEEE 1609.4

IEEE 1609.4 defines a management extension to IEEE 802.11p that enables DSRC devices to switch between different channels (i.e., CCH and SCHs). Under this extension, IEEE 1609.4 maintains a separate logical instance of the IEEE 802.11p MAC,

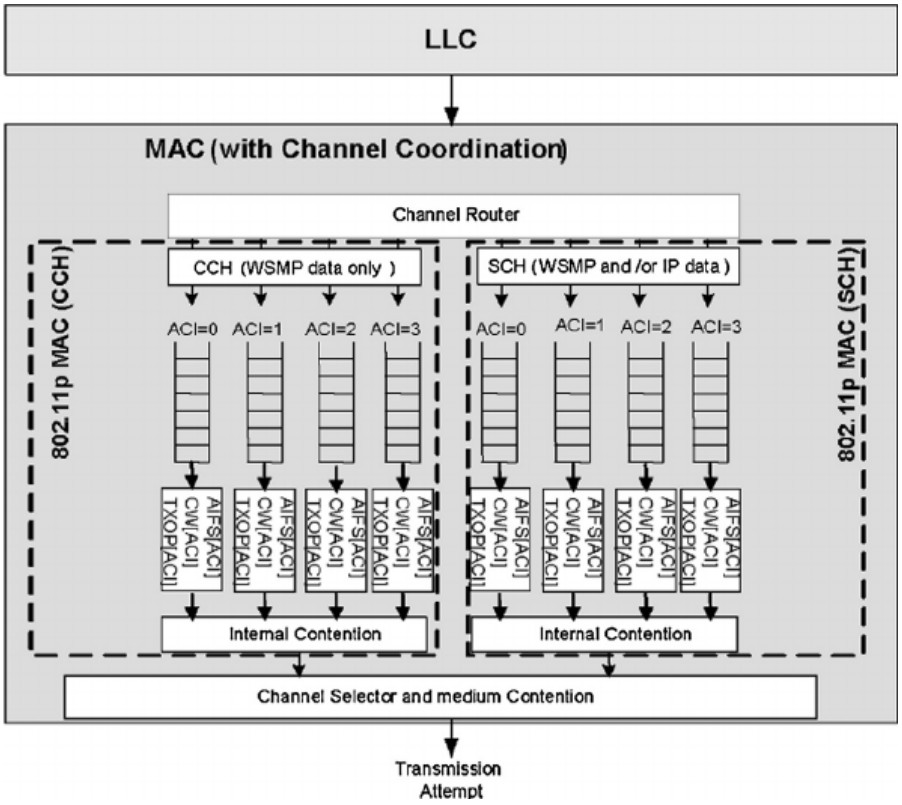

Figure 2.4: IEEE 802.11p MAC architecture

including EDCA and state variables, for each channel on which it operates [5].

WAVE defines three types of devices: single transceiver (i.e., can only be on one channel at a time), dual transceivers (i.e., one is dedicated to CCH while the other switches between SCHs), and multi-transceivers (i.e., having a transceiver for each channel). The goal of IEEE 1609.4 is to specify a mechanism that allows all WAVE devices to communicate. In this regard, IEEE 1609.4 defines two channel access modes: 1) continuous, where CCH and SCHs are constantly monitored (i.e., the case of dual and multi-transceiver devices); and 2) alternating, which uses Coordinated Universal Time (UTC), obtained from GPS signals, to define a time division concept as illustrated in Figure 2.5 [5]. Indeed, each second is divided into ten Synchronization Intervals (SIs). Each SI consists of one Control Channel Interval (CCI) followed by one Service Channel Interval (SCI). Guard Intervals (GIs) are inserted at the end of each CCI/SCI to account for synchronization imprecisions [49]. When using the alternating mode, vehicles shall

monitor CCH during CCI to not miss safety messages, and can switch to one of SCHs during SCI.

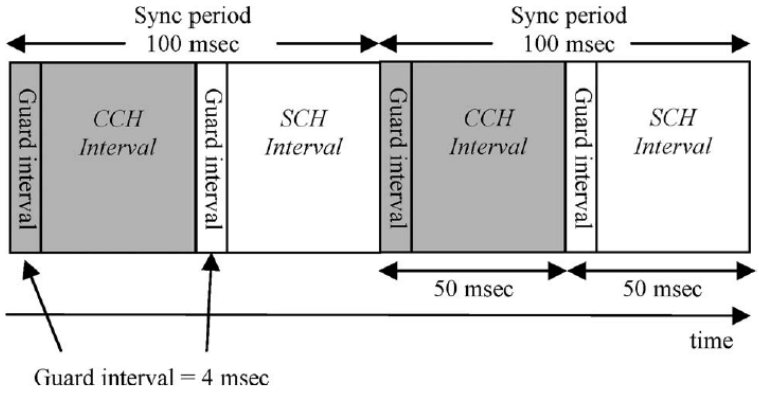

Figure 2.5: Alternating access mode: CCI followed by SCI

2.2.4 IEEE 1609.3

IEEE 1609.3 defines a new protocol, called WAVE Short Message Protocol (WSMP), considered efficient for 1-hop transmission of safety messages since it avoids the packet overhead associated with conventional internet protocols. Packets sent using WSMP are called WAVE Short Messages (WSMs). The minimum WSM overhead is 5 bytes, and will rarely exceed 20 bytes, options and extensions included. This makes WSMP of great value given WAVE's pivotal concern (i.e., channel congestion).

2.2.4.1 Wave Short Message

WSM format is depicted in Figure 2.6 [5]. It consists of variable-length header followed by variable-length payload and includes both mandatory and optional fields.

The *WSM Version* field indicates the version number associated with the current 1609.3 standard, which is 3 [50].The *Provider Service Identifier* (PSID) field plays a similar role as a TCP/UDP port. It identifies the service that WSM payload is associated with. For bandwidth efficiency, PSID is defined in variable-length format. Leading bits are used to indicate the number of bytes in PSID. For instance, a leading bit of 0

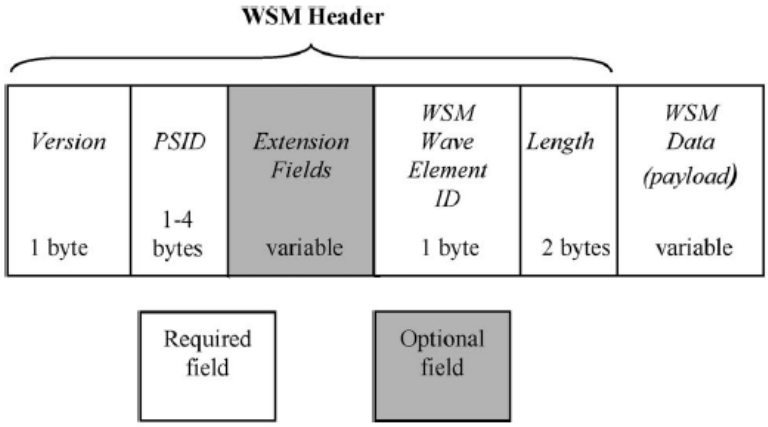

Figure 2.6: WSM format

indicates that PSID is 1-byte long while a leading bit of 01, 011, and 0111 indicate that PSID is 2-bytes, 3-bytes, and 4-bytes long, respectively.

The *Extension Fields* are optional fields used for future extensibility. IEEE 1609.3 defines 4 extension fields: channel number, data rate, transmit power used, and channel load. Each one of these extensions has three attributes: identifier (1-byte), length (1-bytes), and content (1-byte) [50]. The *WSM WAVE Element ID* field is used to identify extensions contained in WSM header [50] while the *Length* field indicates the length of the payload. The range of values for WSM length is 1 to $WsmMaxLength - h$, where h is the length of WSM header. Finally, *WSM Data* field contains the higher layer information being transferred.

2.2.4.2 Wave Service Advertisement (WSA)

IEEE 1609.3 defines another type of messages, labeled WSA. It contains information regarding services to be offered by WAVE devices. A service can be almost any exchange of information that provides value to a vehicle's occupants [5]. Traffic alerts, tolling, navigation, parking availability, and Internet access are few examples among many. Most services are provided by RSUs, but vehicles could also cater services. Keep in mind that safety messages are not considered as a service and therefore are not announced via WSA.

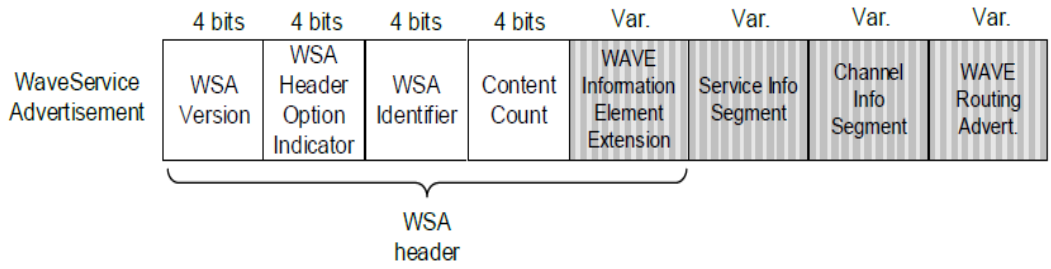

Figure 2.7: WSA format

WSAs are broadcasted over CCH. This is to make all vehicles in an area aware of the existing services. These services can be offered on one or more SCHs. Indeed, a WSA-sender, labeled *provider*, may offer up to 32 services, which can all be advertised with a single WSA. These services can be supported by IPv6 or WSMP. When hearing WSAs, vehicles interested in the advertised services, labeled *users*, switch to the appropriate SCHs at the beginning of SCI.

The format of WSA message is shown in Figure 2.7 [47]. The *WSA Version* field shall be 3 for the current 1609.3 standard [50]. The *Header Option Indicator* field indicates which optional fields (i.e., the shaded fields) are present in WSA. A value of 1 in the i^{th} bit implies that the i^{th} optional field is present. The *WSA Identifier* field is an unsigned integer, between 0 and 15, used to uniquely identify each WSA. The *Content Count* field is used by the recipient to determine whether the received WSA is a repeat of a previously received WSA (i.e., case of persistent WBSS, defined in Chapter 5). The *WAVE Information Element Extension* field has the same format as extension fields in WSM (i.e., identifier, length, and content). It defines five extensions: Repeat Rate, indicating the number of times WSA is transmitted per 5s; transmit power used, indicating the power with which the WSA frame was transmitted; 2DLocation; 3DLocation, considering elevation; and Advertiser Identifier.

The *Service Info Segment* field describes the services being offered (up to 32 instances). Each service instance has ten fields: 1) PSID; 2) Channel Index: indicates SCH where the advertised service will be offered; 3) Service Info Option Indicator: indicates the presence of Service Info WAVE Information Element Extension field if set to 1; 4)

Service Info WAVE Information Element Extension: provides supplementary information about the service; 5) IPv6 Address; 6) Service Port; 7) Provider MAC Address; 8) Received Channel Power Indicator (RCPI) Threshold: indicates the recommended minimum received WSA signal value below which the service should be ignored; 9) WSA Count Threshold: indicates the recommended minimum number of received WSAs below which the service should be ignored; and 10) WSA Count Threshold interval: indicated the time interval over which received WSAs are counted. It is optionally used with WSA count threshold.

The *Channel Info Segment* field provides information regarding channels on which services are being offered. There can be up to 32 instances of channel info, each having seven fields: 1) Operating Class: allows the channel number to uniquely identify a specific channel in the context of a country; 2) Channel Number; 3) Transmit Power Level; 4) Adaptable: indicates whether *Data Rate* is a boundary or fixed value; 5) Data Rate; 6) Channel Info Option Indicator: indicates the presence of Channel Info WAVE Information Element Extension field if set to 1; and 7) Channel Info WAVE Information Element Extension, which has two fields: a) EDCA Parameter Set; and b) Channel Access, indicating the time slots during which the provider will be on the associated channel.

Finally, the *WAVE Routing Advertisement* (WRA) field is used when the provider offers a service that utilizes IPv6. It provides information to users about how to connect to the Internet. Each WSA includes one WRA at most. WRA has the following fields: 1) Router Lifetime: indicates the duration during which the Default Gateway is valid; 2) IP Prefix: indicates the IPv6 subnet prefix; 3) Prefix Length; 4) Default Gateway; 5) Primary Domain Name System (DNS); and 6) WRA optional WAVE Information Element Extension, which contains secondary DNS and Gateway MAC Address fields.

2.2.5 IEEE 1609.2

IEEE 1609.2 uses certificates to authenticate messages. These certificates include information such as the public key of the sender, the permissions associated with that public key, the identifier of the issuer, information to determine whether or not the cer-

tificate has been revoked, the region within which the certificate is valid (i.e., mainly for RSUs), the validity period, and the services that the certificate holder is allowed to provide [51]. Vehicles will typically be reloaded with new certificates infrequently (i.e., each year). These certificates can be used for a limited time (e.g., 5 to 10 minutes) [5], so that vehicles' movements cannot be easily tracked using their safety messages broadcast over long intervals [5]. For bandwidth efficiency purposes, once certificates are exchanged between vehicles, only certificate digests can be appended to WSMs.

Besides, IEEE 1609.2 defines an encryption algorithm that uses a combination of symmetric and asymmetric cryptography. The symmetric algorithm is Advanced Encryption Standard (AES) with 128-bit keys in Counter CBC-MIC mode while Elliptic Curve Integrated Encryption Scheme (ECIES) is the asymmetric algorithm [52]. The sender will encrypt the message with a symmetric key, and then will encrypt the symmetric key using the asymmetric algorithm [5]. The receiver will decrypt the symmetric key first then the message.

2.2.6 SAE J2735

This SAE standard specifies a list of message types that are to be used by VANET applications [53]. Each message is defined as a collection of data structures, called *data elements* and *data frames*. A data element is the most basic structure in SAE J2735 standard. A data frame, on the other hand, is a complex data structure, composed of one or more data elements or other data frames [53]. SAE J2735 standard defines the syntax (i.e., length and format) and semantics of each data element and data frame.

One of the most important messages in SAE J2735 standard is the Basic Safety Message (BSM). It conveys vehicle state information necessary to support V2V safety applications. It has also the flexibility to convey additional information, as required by the application [5]. BSM has two parts. Part I includes critical state information that must be sent in every BSM (e.g., position, dynamics, direction, system status, and size). Part II is optional and can be tailored to applications' needs.

2.3 Chapter Summary

WAVE has the capacity to support various types of applications, including infotainment applications that offer new business opportunities. WAVE relies on several standards (e.g. DSRC, IEEE 802.11p, IEEE 1609.4, IEEE 1609.3, and IEEE 1609.2), and basic interoperability tests among independent WAVE implementations are encouraging [54]. Still, a number of challenges remain. Among them, an efficient mechanism to select the best service channel to be used by service providers (i.e., mainly vehicles) is needed. This is addressed in chapter 5. In addition, the fact that IEEE 802.11p EDCA sets TXOP of all ACs to 0 deprives infotainment applications, especially those using high priority ACs (i.e., AC_VO, AC_VI), from efficiently using service channels. This problem is tackled in chapter 6. Finally, the harmonization of standards between the United States and other regions of the world shall be performed to promote fast market penetration.

CHAPTER 3

RELATED WORK

Many schemes have been proposed to address the problem of QoS assurance in the context of vehicular ad hoc networks. They are divided into networking layer approaches and MAC layer techniques. The first part of this chapter describes the routing challenges facing VANET in urban settings and presents the different routing protocols that have been designed to tackle those issues. Afterwards, we describe how data packets of V2V infotainment applications are transmitted following the WAVE framework and review existing mechanisms that enable providers selecting the least congested service channels. Finally, we outline the distinctive factors that shall be considered when analyzing the performance of the IEEE 802.11p EDCA mechanism and surveys the different models proposed in this regard.

3.1 Routing in Urban VANET

The urban environment poses a series of technical challenges to VANET's routing. Estimating the exact number of vehicles on road segments is complicated since traffic density fluctuates considerably from downtown to suburbs and from day to night. In addition, vehicles' spatial distribution over road segments can be uneven as vehicles tend to pile up at intersections, leading to sporadic connectivity. Furthermore, the presence of obstacles (e.g., buildings, trees, and large vehicles) blocks signal propagation between neighboring vehicles, making of intersections the ultimate point for routing decisions. To address these issues, extensive research has been carried out. The following subsection reviews some of the well known routing protocols in the literature designed for VANET in urban settings.

3.1.1 Node-Centric Routing Protocols

The first attempt to solve the issue of routing in urban VANET was the deployment of node-centric routing protocols designed mainly for mobile ad hoc networks (MANETs). MANET is a self-configuring type of wireless networks in which communication between mobile nodes (i.e., low to moderate mobility) can be carried out without reliance on centralized resources or fixed infrastructure. A well known MANET routing protocol is Ad-hoc On Demand Distance Vector (AODV) [55]. AODV creates routes between nodes only when they are requested by source nodes. Indeed, Route Request (RREQ) packets are flooded through the network in order to create routing paths to destination nodes. RREQ contains the source IP address, the source node's sequence number, the destination IP address, and the destination node's sequence number. Sequence numbers are used to maintain the consistency of the routing information (i.e., routing tables). Routes remain active as long as source nodes transmit periodic "Hello" messages. In case "Hello" messages are no more received, routes time out and are deleted from the routing tables.

Still, due to nodes' high mobility, MANET protocols seem to be unsuitable for VANET. In fact, the experimental study presented in [56] showed that AODV was unable to maintain long routes in VANET and suffered large packet losses along with high end-to-end delay. Consequently, MANET protocols had to be customized to become VANET-compliant. Namboodiri et al. [57] proposed PRAODV, which uses vehicles' speed and location information to predict links' lifetime and constructs alternative routes before links expire. Since PRAODV selects the shortest alternative path, which may not always be the best solution, a modified version called PRAODV-M was also presented in [57] in order to select the path with the maximum predicted lifetime. Ooi et al. [58], on the other hand, studied AODV's RREQ flooding and concluded that it can definitely cause network congestion in VANET. Subsequently, they proposed that RREQ messages can only be forwarded within a limited zone, called Zone of Relevance (ZOR) (i.e., an example of ZOR is the vicinity of a car crash).

Despite these modifications, several studies (e.g. [11, 59]) have shown that node-

centric schemes still have poor performance in various VANET settings. As a result, they are no longer used. Several routing strategies have been developed specifically for the adverse environment of VANET. Among them, position-based routing (PBR) [9] ought to be the most convenient routing approach for urban VANET as it exhibits great resilience to network topology. It requires each vehicle to periodically broadcast its position via beacon messages. This is feasible nowadays as most vehicles are equipped with GPS devices. To attest for PBR convenience, projects such as CarTALK2000 [60] and NOW [8] have already deployed it.

3.1.2 Position-based Routing Protocols

Various position-based routing protocols have been designed to address the routing issues in urban VANET. One of the well-known schemes is Greedy Perimeter Stateless Routing (GPSR) [10]. It combines greedy forwarding, by sending packets to the closest neighbor to the destination, with perimeter routing, a sequence of edges traversed using the right hand rule in order to go around void regions. Despite its good performance in highway scenarios, studies such as [12] and [13] have shown that GPSR suffers from sever performance degradation in urban environments. This is because: 1) direct communication between nodes may not be possible due to obstacles (e.g., buildings); and 2) frequent topology changes may induce routing loops. This implies that packets might get forwarded in the wrong direction, yielding high delivery delay.

To address these shortcomings, several anchor-based protocols have been proposed. Lochert et al. proposed Geographic Source Routing (GSR) [11] and Greedy Perimeter Coordinator Routing (GPCR) [12]. GSR combines static street maps with Dijkstra's algorithm to compute the shortest distance path, expressed as a list of intersections, between source and destination. Like GSR, GPCR also computes the shortest distance path between source and destination. However, instead of using static street maps like GSR, GPCR only exploits local information obtained via beacon messages. Indeed, GPCR always forwards packets to nodes at intersections, called coordinators, responsible for making routing decisions (i.e., shortest path to destination) since they have better network visibility. Still, due to their lack of traffic-awareness, both GSR and GPCR are

highly susceptible to network fragmentation as the distribution of vehicles on road segments is uneven.

Subsequently, traffic-aware routing schemes have emerged. Lui et al. [13] proposed Anchor-based Street and Traffic Aware Routing (A-STAR) protocol. It combines street maps with statically or dynamically rated maps. These maps show the number of city buses going through each street statically or based on the current traffic state, and are used to identify the sequence of intersections, labeled anchors, through which packets might be forwarded. In case an anchor gets disconnected, A-STAR marks it as *out of service* and computes a new anchor path. Naumov et al. [14] proposed Connectivity-Aware Routing (CAR) which seeks to find connected paths between source and destination nodes. CAR uses beacon messages to adapt to changes in traffic conditions (e.g., number of neighbors, speed). These beacon messages include also *guards*, geographic markers, which are used to keep track of source and destination nodes' movements. A routing path, defined as a sequence of intersections received in RREQ packet, is selected by the destination considering real-time traffic information. Similarly, Jerbi et al. [15] proposed Greedy Traffic Aware Routing Protocol (GyTAR), a greedy-based protocol that uses real time traffic, collected via beacons and control packets, to select the routing path between source and destination. Instead of computing the entire routing path, GyTAR makes a routing decision whenever a data packet reaches an intersection. The road segment that has the best balance between road density and distance to destination is selected to forward data packets.

Mobility-centric data dissemination for VANET (MDDV) [16] and Vehicle-assisted data delivery in VANET (VADD) [17] use opportunistic forwarding to transport data packets from source to destination. MDDV considers road traffic conditions as well as the number of lanes on each road segment to select the best road-based trajectory to forward data. VADD uses historic traffic flow data to forward data packets over road segments with the lowest delivery delay. Both protocols use carry-and-forward when no vehicle can be found along the forwarding trajectory. This implies that data packets are stored until a forwarding opportunity is possible (i.e., finding a suitable forwarder). Intersection-based Geographical Routing Protocol (IGRP) [18] deploys location servers

to store local topology information and construct routes with high connectivity probability and satisfactory QoS constraints (i.e., delay, number of hops, and Bit Error Rate (BER)). Likewise, Intersection-based Connectivity Aware Routing (iCAR) [19] combines connectivity information with average communication delay to enable better routing decisions. It avoids road segments with high vehicular density and high data volume and uses carry-and-forward in low vehicular density. Finally, Backbone-Assisted Hop Greedy Routing (BAHG) [20] relies on connectivity information, collected via backbone nodes located at road segments and intersections, to select routing paths with minimum number of hops, i.e., intermediate junctions, in order to reduce the end-to-end delay. An update procedure was also proposed to deal efficiently with destination mobility.

3.1.3 Limitation of Existing Routing Protocols

Most of the aforementioned protocols only acquire local network topology via beacon messages. Thus, they are exposed to two main issues: 1) local maximum problem: a situation where no other connected road segment is closer to the destination than the current one; and 2) data congestion: forwarding data packets, originated from different source-destination pairs, over the same routing path.

Figure 3.1 illustrates the local maximum problem. *A, B, C, G, E,* and *F* are junctions and data packets are to be sent from source node *S* to destination node *D*. Most existing schemes will forward data packets through the path $A-B-C$ since road segments $S_{A,B}$ and $S_{B,C}$ are highly connected. But once at intersection *C*, packets encounter the local maximum problem since *C* and *F* are disconnected. This implies that packets will be either carried to junction *F* or forwarded back to intersection *B* in order to select another road segment, escalating therefore the end-to-end delay. With an up-to-date knowledge of network topology, packets would have been forwarded over the path *A-G-E-F* instead.

Figure 3.2 shows a scenario where the path *F-C-B-A* is exploited by pairs (S_1, D_1) and (S_2, D_2). This incurs large queuing delay at intermediate nodes, thus further increasing the end-to-end delay. With the load balancing capability, (S_2, D_2) packets can be transmitted over the path *F-E-G-A* while (S_1, D_1) packets are forwarded over the path *F-C-B-A*.

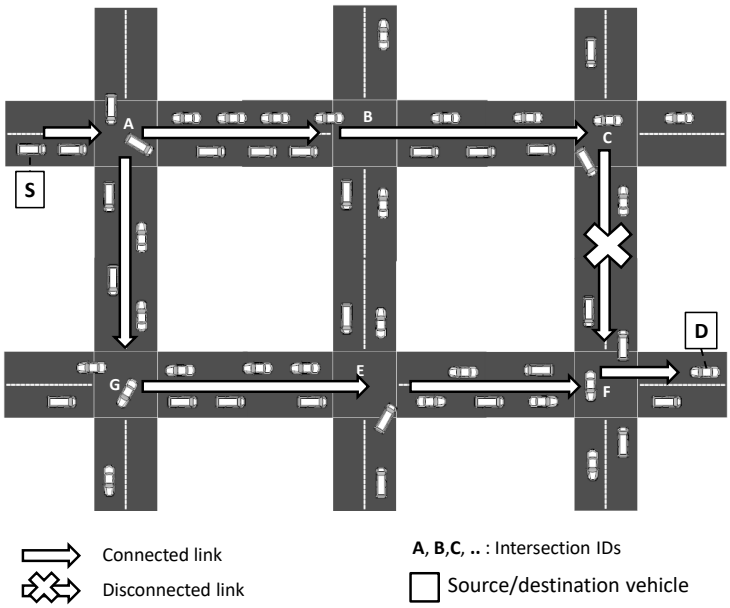

Figure 3.1: Local maximum problem

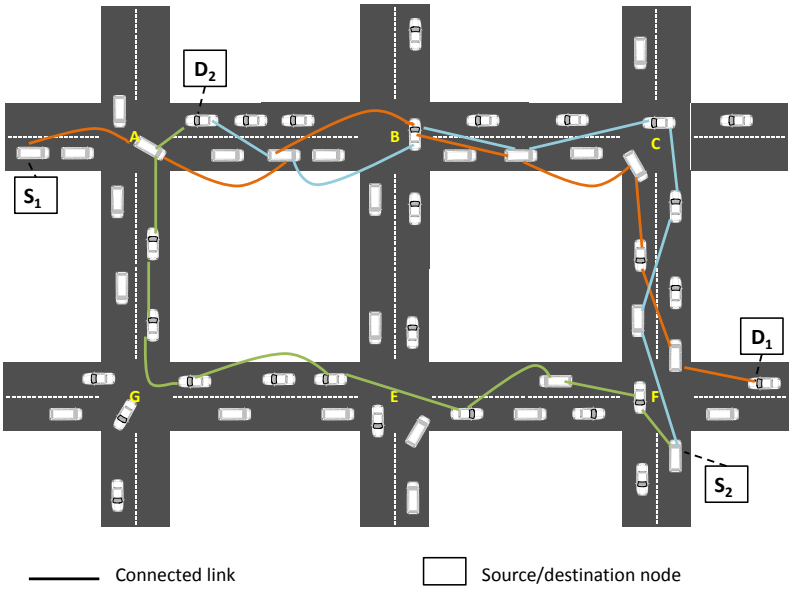

Figure 3.2: Data congestion problem

Given these shortcomings, we propose SCRP (see Chapter 4) that provides a solution to the aforementioned problems through:

1. Creating backbones over road segments and connecting them via bridge nodes at intersections. These nodes collect connectivity and delay information and assign weights to road segments. Packets are forwarded over road segments with low end-to-end delay, avoiding therefore the local maximum problem.
2. Identifying various routing paths between source and destination to be used for load balancing, reducing therefore data congestion.

3.2 DSRC Service Channel Selection

WAVE allows for data packets of infotainment applications to be transmitted within WAVE Basic Service Set (WBSS). It mandates that vehicles shall monitor received WSA messages to keep track of used SCHs in their 1-hop range. This way, they can select the least congested (i.e., used) SCH to establish their WBSS. Yet, this mechanism suffers from two major shortcomings: 1) vehicles might end-up using obsolete SCHs information due to WSA collisions; and 2) vehicles lack SCHs information within 2-hop range, yielding poor service quality as two providers within carrier sense range may select the same SCH to setup their WBSS. Several schemes have been proposed to help mitigating these issues. They are of two types: allocation-based and prediction-based.

3.2.1 Allocation-based Schemes

Allocation-based schemes require vehicles to maintain channel occupancy tables (OCTs), where the state of each SCH (i.e., free or busy) is stored. To disseminate SCH state information, OCTs are piggybacked into control messages (i.e., WSA [22, 23] or RTS/CTS [24, 25]) or data packets (i.e., [26, 27]).

Campolo et al [22] proposed CRaSCH, a cooperative reservation scheme for service channels. It requires providers to maintain SCH status vectors, containing information about SCHs status occupancy. Indeed, CRaSCH appends a new field to WSA, called *ChannelGossip*, indicating the current occupancy status of every SCH (i.e., 2-hop status

information). Whenever WSA messages are received, CRaSCH performs the "OR" operation between the values contained in the *ChannelGossip* field of the received WSAs and the SCH status vectors. This way, each provider is able to build its personal view of the reserved SCHs in both 1-hop and 2-hop ranges, and can select the least used SCH. In case a vehicle receives two different WSAs reserving the same SCH, a channel collision warning (CCW) frame is broadcasted, urging the provider of the last received WSA to choose another SCH.

Similarly, Wang et al. [23] proposed Minimum Duration Counter (MDC), a scheme that maintains SCH status tables containing two fields: SCH number and duration counter. The latter designates the corresponding SCH usage duration (i.e., estimated time for each data transmission). Providers make use of these tables to select the least used service channels. Once selected, providers update their respective tables and piggyback them into WSAs in order to disseminate updated SCH information.

Asynchronous Multi-Channel Protocol (AMCP) [24] and Asynchronous Multi-Channel MAC (AMCMAC) [25] use the RTS/CTS mechanism to negotiate the use of a common available data channel. They also inform neighboring nodes to set these channels as unavailable for the entire data transmission duration. Indeed, in AMCP, a provider chooses a free channel from its OCT and includes it into RTS. When receiving RTS, a user checks if that channel is marked as free in its own OCT. If so, it broadcasts a CTS containing the received SCH; otherwise, it broadcasts a rejecting CTS and the whole process is repeated. To make the handshake process shorter, each provider in AMCMAC appends the list of all available channels to RTS. A user compares the list of received available channels with its own OCT. If a match is found, the user replies with CTS containing the SCH in common.

Distributed Reliable Multi-channel MAC (DRMMAC) [26] and Dedicated Multi-channel MAC (DMMAC) [27] were designed to give every vehicle in the network the chance to conduct collision-free and delay bounded transmission for safety messages. In fact, CCI is divided into an Adaptive Broadcast Frame (ABF) and a Contention-based Reservation Period (CRP). ABF consists of time slots that can be dynamically reserved for collision-free delivery of safety and control messages. During CRP, vehicles nego-

tiate and reserve SCHs to transmit non-safety messages. To enable vehicles to reserve a slot in ABF, both schemes use a Time Division Multiple Access (TDMA) approach. Indeed, Frame Information (FI) is attached to every transmitted packet over CCH, including safety messages. FI consists of vehicle's identifier as well as the states of all slots in its 1-hop range. Providers use FI in order to select free slots (i.e., not used by any other vehicle in their vicinities) to transmit their frames.

Finally, Su et al. [28] proposed a TDMA cluster-based multichannel MAC that is made of three protocols: cluster configuration, intercluster communication and intracluster communication. In the cluster configuration protocol, vehicles moving in the same direction are grouped into clusters and Cluster Heads (CHs) are elected among them. The intercluster communication protocol governs the exchange of safety and non-safety messages between different clusters over separate channels. Lastly, the intracluster communication protocol uses a TDMA scheme to enable CHs to collect/deliver safety messages from/to cluster members. These CHs are also responsible for assigning data channels to their respective cluster members, allowing them to transmit non-safety messages.

3.2.2 Prediction-based Schemes

Prediction-based schemes require vehicles to be equipped with multiple transceivers, i.e., one for each channel, to monitor all channels continuously. They deploy prediction mechanisms to identify channels that are likely to be available in the near future.

Inage et al. [29] created databases to store and provide information regarding geographical and temporal channels availability. Based on this information, the best channel, defined as the channel to be available the longest possible in the movement direction of the vehicle, is selected. Similarly, Chen et al. [30] created a spectrum utilization database that keeps track of channels' usage (i.e., DSRC channels, WiFi, and TV white space) according to their temporal and spatial accessibility. The spectrum utilization database takes cloud-sourced channel measurement (i.e., congestion level) from users as input and computes the average values of channel utilization mapped to all combinations of discretized time of day and location. The least congested channel is then selected to be

used. Bozidar et al. [31] also created a database to dynamically select the best channel along with the best transmission rate. The database has two parameters: 1) the number of time periods during which packets were transmitted to a user on a specific channel using a specific rate; and 2) the number of successfully transmitted packets to the same user over the same channel and using the same data rate. The best (channel, rate) pair is then selected.

Brahmi et al. [32] proposed a cluster-based approach for channel selection. Cluster members listen to all channels and report observations to their respective CHs. After aggregating all the observations, CHs decide on the state of each channel (i.e., free or busy) in the current time slot and estimate their state in the subsequent time slot using a hidden markov model (HMM). Available channels are assigned by CHs to cluster members based on the type of messages, i.e., safety or non-safety, to be transmitted. Likewise, Mapar et al. [33] proposed a framework that enables vehicles, labeled Secondary Users (SUs), to access TV white space in an opportunistic manner without causing interferences to stationary roadside TV users, labeled Primary Users (PUs). It monitors the fluctuation of Received Signal Strength (RSS) in order to determine whether a channel is currently free or occupied by either PU or SU. It then uses a hidden Markov model to figure out the channels that are likely to be available in the near future. The least congested SCH is selected to be used. Finally, Boyaci et al. [34] proposed a cross-layer predictive approach to select the least congested service channel. It consists of collecting energy data at the physical layer and feeding them to the MAC layer. This latter combines the received data with information retrieved from a database containing channel usage history in order to predict the state of SCHs in the future. The least used channel among the ones to be available is chosen.

3.2.3 Limitation of Existing SCH Selection Schemes

Despite their adequate performance, both allocation-based and prediction-based schemes have different limitations. On the one hand, only one busy state is considered, implying that service differentiation between various traffic classes is not supported. Besides, relying only on control messages (i.e., WSA, RTS/CTS) to disseminate SCHs informa-

tion may lead to inaccurate decisions, especially in a dense vehicular network, where control messages may suffer from multiple collisions. This will make the information in OCTs obsolete, rendering therefore the allocation-based schemes of limited value. On the other hand, the use of multiple transceivers implies that prediction-based schemes are cost-ineffective (i.e., according to the US Department of Transportation, one transceiver in 2017 costs $335 for new cars and $233 as aftermarket equipment [**?**]) and can suffer from cross-channel interferences [35].

These observations have motivated us to propose ASSCH (see Chapter 5), a novel channel selection mechanism that compels vehicles to cooperate in order to identify the least congested service channel to be used. It is WAVE-compliant and it requires vehicles to be equipped with single transceivers. It is based on a stochastic modeling to capture the different features impacting the service channel's choice (e.g. number of providers, service priority, and channel occupancy time) and exploits beacon messages to exchange SCHs state information. The rational behind choosing beacon messages is twofold: 1) they are transmitted periodically, allowing for SCHs state information to be updated regularly instead of event-driven (i.e., receipt of WSA); and 2) they do not generate any additional overhead as they are a key component of VANET.

3.3 IEEE 802.11p EDCA Performance Analysis

To accurately analyze the performance of the IEEE 802.11p EDCA mechanism for infotainment applications, we need to consider six factors: 1) Number of Access Categories considered (NAC): a model is considered pertinent if all the access categories (ACs) of the EDCA mechanism (i.e., AC_BK, AC_BE, AC_VI, and AC_VO) are taken into consideration; 2) AC queue condition (QC): an AC queue can be either saturated or non-saturated. The former implies that AC has always data frames to send while the latter indicates otherwise; 3) The backoff procedure (BP): defined as the mechanism used by ACs to timely differ their transmissions when sensing a busy channel. It largely depends on the parameters of each AC (see Section 2.2.2); 4) The backoff counter freezing (BCF): when the channel is sensed busy, ACs freeze their backoff countdown, and

resume decrementing it once the channel is sensed idle; 5) The busy channel at zero (BCZ): when the countdown reaches 0, ACs can transmit their frames only if the channel is sensed idle. Otherwise, ACs invoke the backoff procedure once again; and 6) Internal collisions (IC): occur when two or more ACs within the same station initiate simultaneous packet transmissions. This is solved by doubling the contention window for all involved ACs and then invoking the backoff procedure. This way, ACs with high priority are always the first to access the channel.

In the literature, few models were proposed to analyze the performance of IEEE 802.11p EDCA. While most of them were designed for safety applications [36–38], only two (i.e., [39, 40]) can be applied to non-safety applications. Eichler et al. [36] evaluated the performance of the EDCA mechanism through simulations while considering the collision probability, throughput, and delay. However, no mathematical analysis was provided for the backoff phase. Gallardo et al. [37], proposed a Markovian model to analyze the performance of EDCA over CCH. The model is made of three Markov chains, each representing one AC, which are used to compute throughput, frame error rate, and delay. Still, the proposed model does not consider the busy channel at zero and was not verified through simulations. Likewise, Kaabi et al. [38] presented an analytical model to examine the performance of EDCA over CCH. The model contains one Markov chain representing the backoff procedure and is used to compute the probability of transmission as well as the throughput. Nevertheless, the model lacks the busy channel at zero and only one AC was simulated.

Han et al.[39] proposed a Markovian analytical model for EDCA that is suitable for both basic access and the RTS/CST access mode. It can be applied to all ACs and was validated through simulations. It has two Markov chains: one modeling the backoff procedure and the other modeling the contention phase after a busy period. Yet, the proposed model lacks the backoff counter freezing as well as the busy channel at zero; in addition, they only simulated two ACs and did not use the same values of the EDCA parameters as defined by the IEEE 802.11p standard (i.e., see Table 2.II). Similarly, Jun et al. [40] studied the access performance of the IEEE 802.11p EDCA mechanism using Markov chains. Indeed, a 2-D Markov chain is first constructed to model the backoff

procedure and to establish a relationship between the transmission probability and the collision probability of each AC. Then, a 1-D Markov chain is proposed to model the contention period of each AC and establish another relationship between the probability of transmission and the probability of collision. Based on the two Markov chains, models for normalized throughput and access delay are derived. Both Markov chains consider all the aforementioned factors, except the busy channel at zero.

These observations have motivated us to propose a Markovian model that considers all the aforementioned factors. The model describes two Markov chains that are used to compute the transmission probability and the probability of collision of each AC, from which an accurate throughput model is derived. Table 3.I shows the comparative review of the discussed models for the IEEE 802.11p EDCA performance analysis.

Table 3.I: Comparison of IEEE 802.11p EDCA Performance Analysis Models

Model	App. Type	NAC	QC	BP	BCF	BCZ	IC
Eichler [36]	safety	4	✓	×	×	×	×
Gallardo [37]	safety	3	×	✓	✓	×	×
Kaabi [38]	safety	1	×	✓	✓	×	×
Han [39]	non-safety	2	×	✓	×	×	✓
Jun [40]	non-safety	4	✓	✓	✓	×	✓
Our Approach	non-safety	4	✓	✓	✓	✓	✓

3.3.1 EDCA Performance Analysis Considering TXOP

Since IEEE 802.11p allows each AC to transmit only one packet per channel access ($TXOP = 0$), service channels are not efficiently used. We believe that by enabling high priority ACs (i.e., AC _VO and AC _VO) to transmit more than one frame per channel access ($TXOP \neq 0$), we can enhance the throughput of infotainment applications. In the literature, the model proposed by Harigovindan et al. [41] is the only one to consider TXOP when analyzing the performance of IEEE 802.11p EDCA. It focuses on tuning $TXOP$ limits in order to provide bit-based fairness for vehicles with different

velocities when accessing the Internet via RSUs; yet, no mathematical analysis for the backoff procedure was presented nor was the busy channel at zero taken into consideration. Therefore, we propose a second model that extends the one mentioned above by taking into account TXOP, unexploited in the IEEE 802.11p standard.

3.4 Chapter Summary

In this chapter, we started by reviewing the different schemes proposed to address the issue of routing in urban VANET. Most of these routing protocols rely on local topology information, obtained via beacon messages, to make routing decisions that depend on the routing metrics used. However, almost all of them endure the local maximum and/or data congestion problems, increasing therefore the end-to-end delay. We then described the various mechanisms proposed in the literature to allow service providers to select the least congested/used service channels. These mechanisms are of two types: allocation-based and prediction-based, and both have different limitations. Finally, we discussed multiple models that were designed to assess the performance of IEEE 802.11p EDCA and have shown that they do not consider all the factors mentioned earlier.

We will devote the rest of this thesis to our contributions that aim at enhancing infotainment applications QoS. In Chapter 4, we detail the proposed routing algorithm, labeled SCRP, which selects low end-to-end delay routing paths to forward data packets. In Chapter 5, we describe the proposed service channel selection scheme, labeled ASSCH, that couples SCH state information with a stochastic model, predicting SCHs state in the near future, in order to select the least congested service channels. Finally, Chapter 6 outlines the proposed models for analyzing the performance of the IEEE 802.11p EDCA mechanism considering all the above-mentioned factors along with TXOP. Figure 3.3 depicts the system level description of our solutions for QoS support of infotainment applications in VANET.

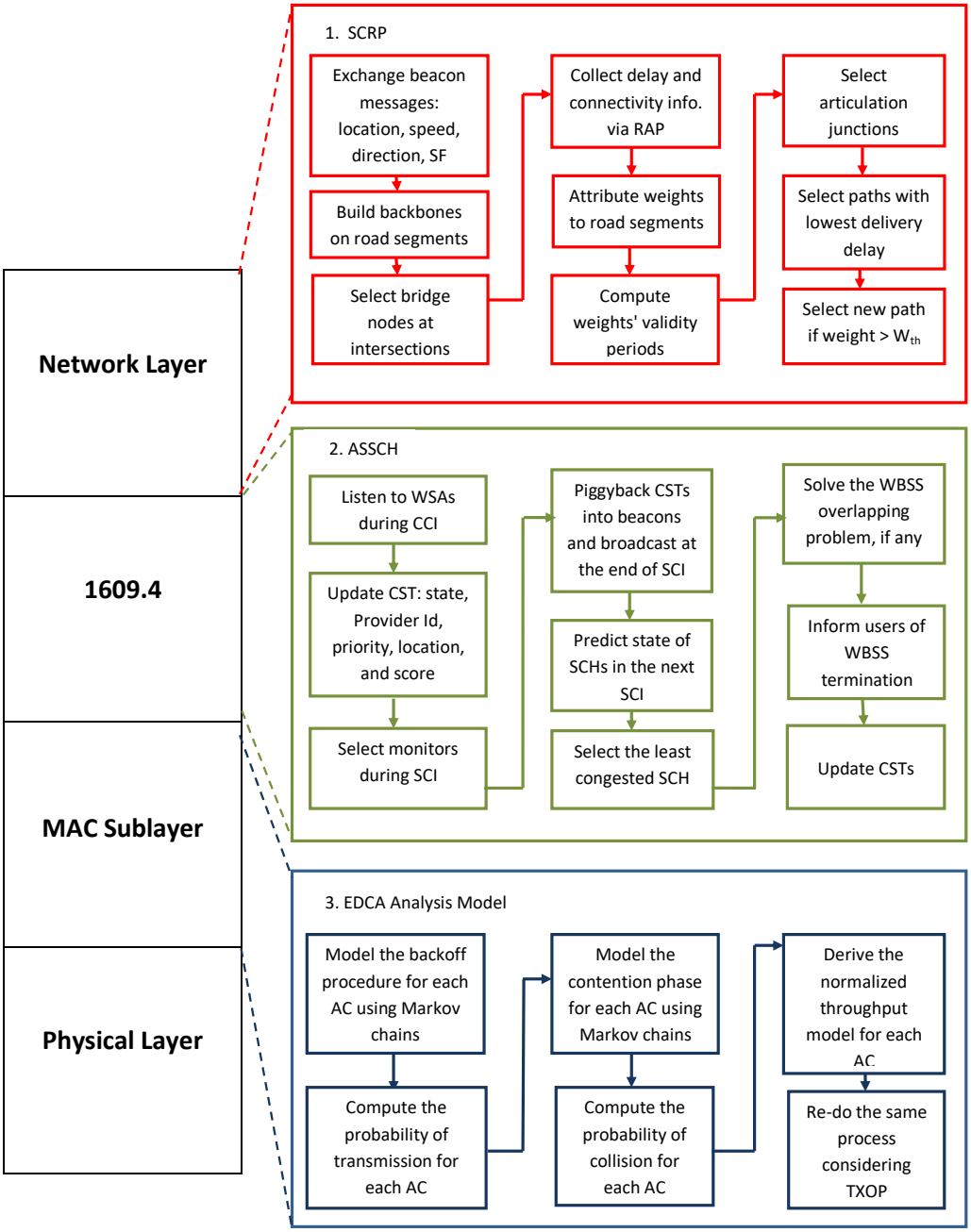

Figure 3.3: Our solution for QoS support of infotainment applications in VANET

CHAPTER 4

SCRP: STABLE CDS-BASED ROUTING PROTOCOL FOR URBAN VEHICULAR AD HOC NETWORKS

This chapter addresses the issue of selecting routing paths with minimum end-to-end delay (E2ED) for non-safety applications in urban vehicular ad hoc networks. Most existing schemes aim at reducing E2ED via greedy-based techniques (i.e. shortest path, connectivity, or number of hops), which make them prone to the *local maximum* and/or data congestion problems, yielding high E2ED. As a solution, we propose SCRP, a distributed routing protocol that computes end-to-end delay for the entire routing path before sending data messages. To do so, SCRP builds stable backbones on road segments and connects them at intersections via bridge nodes. These nodes assign weights to road segments based on collected information of delay and connectivity. Routes with the lowest aggregated weights are selected to forward data packets. Simulations results show that SCRP outperforms some of the well-known protocols in the literature.

The rest of the chapter is organized as follows. Section 4.1 presents the motivation behind SCRP design. Section 4.2 describes the network model while Section 4.3 presents the different components of SCRP. Section 4.4 outlines SCRP sensitivity analysis while Section 4.5 portrays the simulations results. Finally, Section 4.6 concludes the chapter.

4.1 Problem Statement

The fact that VANET accommodates two types of communications, Vehicle-to-Vehicle (V2V) and Vehicle-to-Infrastructure (V2I), has opened the door for a plethora of interesting applications to thrive. While some focus on enhancing road safety via assisting drivers in avoiding hazardous events (e.g., car crashes, slippery roads, etc.), others aim at making passengers' journey comfortable and entertaining. For example, traffic statistics can be acquired in real-time to compute alternative routes in case of congestions.

Moreover, speed and density information can be collected on the fly to allow for better traffic light management. Finally, businesses such as malls, restaurants, gas stations, and parking lots can promote their services using Road Side Units (RSUs). These RSUs can also provide passengers with internet access to check their emails, download music, and play online games [2].

Most of these infotainment applications have rigid requirements in terms of delivery delay and throughput; yet, meeting them in urban VANET is not straightforward. Numerous routing schemes have been proposed in the literature. Almost all of them are greedy-based, where a routing decision is to be made whenever an intersection is reached. This decision hinges on the routing metric used. For instance, GPSR [10], GSR [11], and GPCR [12] select the shortest distance path between source and destination, while GyTAR [15], A-STAR [13], RBVT [1], and IGRP [18] forward packets through well connected road segments. Nevertheless, these protocols and several others suffer two major problems: local maximum and data congestion.

To overcome these limitations, we propose SCRP. It is a distributed geographic source routing scheme that takes advantage of the network topology information to select routing paths with low E2ED. To achieve this goal, SCRP builds stable backbones over road segments by considering vehicles' speed and spatial distribution. These backbones are connected at intersections via bridge nodes that keep up-to-date network topology and monitor the delay to incur for transmitting data packets over road segments. Based on this information, SCRP assigns weights to road segments; the ones with the lowest weights are selected to construct routing paths. This way, SCRP avoids the local maximum problem and balances data traffic over all possible routing paths.

4.2 Network Model

Our network model consists of roads and intersections to mimic a typical urban environment. We define $S_{i,j}$ as the road segment between intersections I_i and I_j. Each road segment has distinctive characteristics such as length, width, number of lanes, and traffic density. Vehicles have unique IDs and are equipped with GPS and other gadgets

that provide information about their location, speed, and direction. They also have access to digital maps (e.g., [61, 62]) that include precise information about road segments and intersections. When forwarding data packets, source nodes inquiry location services (e.g., RLSMP [63]) to acquire the location of the destination nodes.

4.3 Stable CDS-based Routing Protocol

SCRP has 6 procedures: backbone creation, link lifetime estimation, bridge node selection, road segment assessment, articulation junction selection, and route construction. The following subsections describe each one of them in more details.

4.3.1 Backbone Creation

This procedure is performed in each road segment. We assume that the creation process starts at the beginning of each road segment and continues onward until an intersection is reached. To build virtual backbones, we used the concept of *connected dominating sets (CDS)*, which we define as follows:

Definition. *Given an undirected graph $G(V,E)$ where V is the set of vertices and E is the set of edges (i.e., wireless links existing at time t), a dominating set (DS) is a subset $V' \subseteq V$, where every node in V is either in V' or adjacent to at least one node in V'. V' is called a CDS if there exists a path $e_i, e_a, e_b, ..., e_n, e_j$ between any two nodes $i, j \in V'$ such that $a, b, ..., n \in V'$.*

We do not aim at finding Minimum-CDS (MCDS) since finding one is NP-hard [64] and produces unstable backbones [65]. We describe stability in terms of the backbone's lifetime, defined as the time to elapse before the first disconnection between any pair of backbone nodes occurs. Therefore, the longer the backbone's lifetime, the more stable it is. Figure 4.1 illustrates the way backbone creation procedure is carried out. First, vehicles exchange beacons of the form: $< ID, x, y, v, d, b, SF >$, where *ID* is the vehicle's identifier, *(x, y)* are its Euclidian coordinates, v is its speed, and d is its direction. b is a 1-bit flag to indicate the state of the vehicle. If *Normal Vehicle* (*NV*), b is set to 0; if

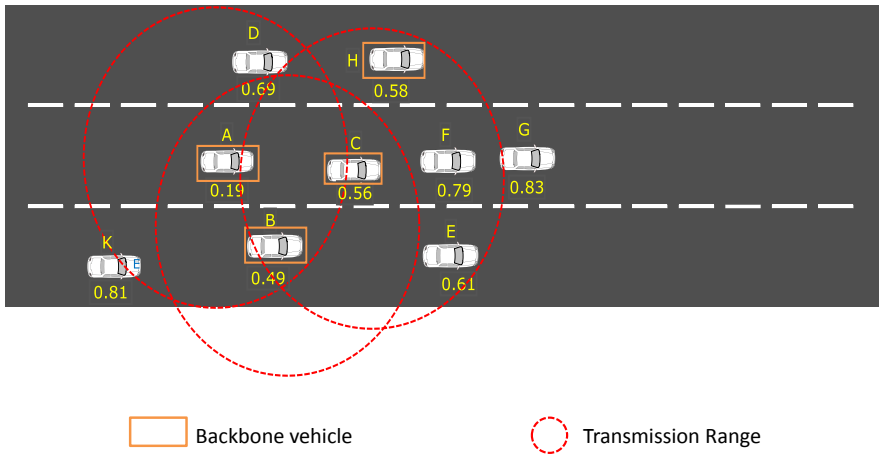

Figure 4.1: Backbone creation mechanism.

Backbone Vehicle (*BV*), b is set to 1. *SF* denotes the vehicle's stability factor, indicating the vehicle's suitability to be a backbone vehicle. It is computed as follows:

$$SF_i = \alpha \left[max \left(\frac{1}{3}, \frac{R - d_{nb}}{R} \right) \right] + \beta \left(\frac{V_{nb}^t}{v_i^t} \right) \quad \alpha, \beta \in [0,1] \tag{4.1}$$

where R is the transmission range while V_{nb} and d_{nb} are the average speed of i's neighbors and the average distance between vehicle i and its neighbors, respectively. α and β are weighting coefficients. d_{nb} is computed by predicting the future positions of neighboring vehicles using information included in beacons, avoiding situations where vehicles might change positions during inter-beacon intervals.

Observe that the first part of the stability factor penalizes vehicles that have most of their neighbors located far away. This is because the higher the distance between two vehicles, the lower is their link's quality [21]. We chose $\frac{1}{3}$, set using simulations, as an upper bound for $(R - d_{nb})$ in order to reduce the effect of obstructing vehicles, discussed in [66], which degrades links' quality. The second part, however, reflects the speed rela-

tionship between a vehicle and its neighbors. Indeed, vehicles moving with low relative speeds can be considered as moving in a platoon; therefore, they have high probability of staying connected for a long time, unlike vehicles moving with high relative speeds which shall endure rapid link disconnections, jeopardizing our backbone's stability.

When receiving beacon messages, each node constructs its neighboring list. Each entry in this list includes information extracted from beacons. Whenever a new neighbor is discovered, a new entry is added and a timer is set. Each vehicle waits for two consecutive beacon intervals to hear from its neighbor. If no beacon is received, the neighbor's entry is deleted. Once the neighboring list is established, every node compares its *SF* to the ones received from its neighbors. The vehicle with the lowest *SF*, vehicle *A* in Figure 4.1, is added to the backbone. It sets its *b*-flag to 1 and chooses the neighbor with the lowest *SF*, vehicle *B* in Figure 4.1, as the next forwarder. Then, *A* sends a *DESIG* message to *B*, informing it that it has been selected as a backbone vehicle. Once received, *B* sets the *b*-flag to 1 and picks up the next vehicle to be included in the backbone, vehicle *C*. This mechanism is repeated till the whole road segment is covered.

4.3.2 Link Lifetime Estimation (LLT)

Let BV_i and BV_j be two backbone vehicles. The time that they will stay connected depends on their speed and direction. For instance, when they move in the same direction, a disconnection occurs when BV_j moves out of BV_i's transmission range. Hence:

$$LLT = \frac{R - d_{i,j}}{|v_i - v_j|} \tag{4.2}$$

where $d_{i,j}$ denotes the distance between BV_i and BV_j.

In case BV_i and BV_j move in opposite directions, two scenarios are to be considered:

- BV_i and BV_j are approaching each other. In this case, a link disconnection occurs when both vehicles cross each other and be R meters apart.

$$LLT = \frac{R + d_{i,j}}{|v_i + v_j|} \tag{4.3}$$

- BV_i and BV_j are moving away from each other. A disconnection happens when both vehicles are R meters apart.

$$LLT = \frac{R - d_{i,j}}{|v_i + v_j|} \tag{4.4}$$

Note that LLT is stored in the neighboring list. It is computed and updated after each beacon interval. It is used to compute the weight validity period, described in Section 4.2.4.

4.3.3 Bridge Nodes Selection

With backbones spanning only over road segments, SCRP nominates *bridge nodes* to connect them at intersections. Figure 4.2 illustrates the bridge node selection mechanism.

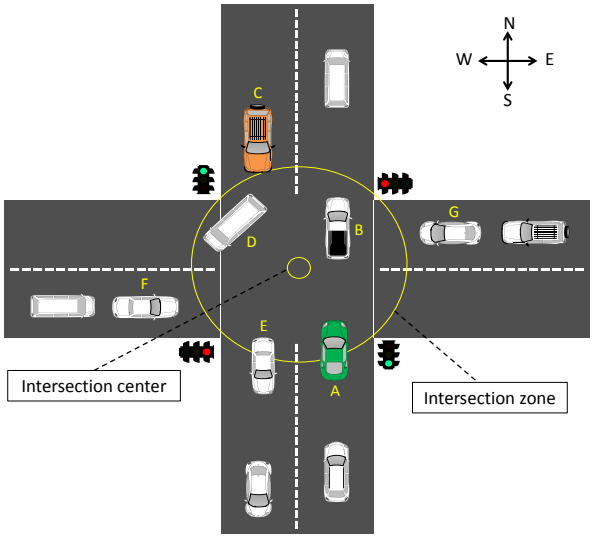

Figure 4.2: Bridge node selection mechanism

Originally, all vehicles within the intersection zone are candidates (i.e., *A, B, C, D,* and *E*). We discard vehicles that went past the intersection's center (i.e., *B*, *D*, and *E*) since they are in their way to leave the junction. From the remaining candidates, we look for vehicles that are close to the intersection zone's boundary (i.e., *A* and *C*) and check

whether they were *BVs*. In case there is only one, say *C*, we select it as the bridge node; otherwise, the slowest vehicle among the former *BVs* is chosen as the bridge node. This way, we guarantee that bridge nodes stay longer at intersections. For further insight, Figure 4.3 depicts the flowchart of the bridge node selection mechanism.

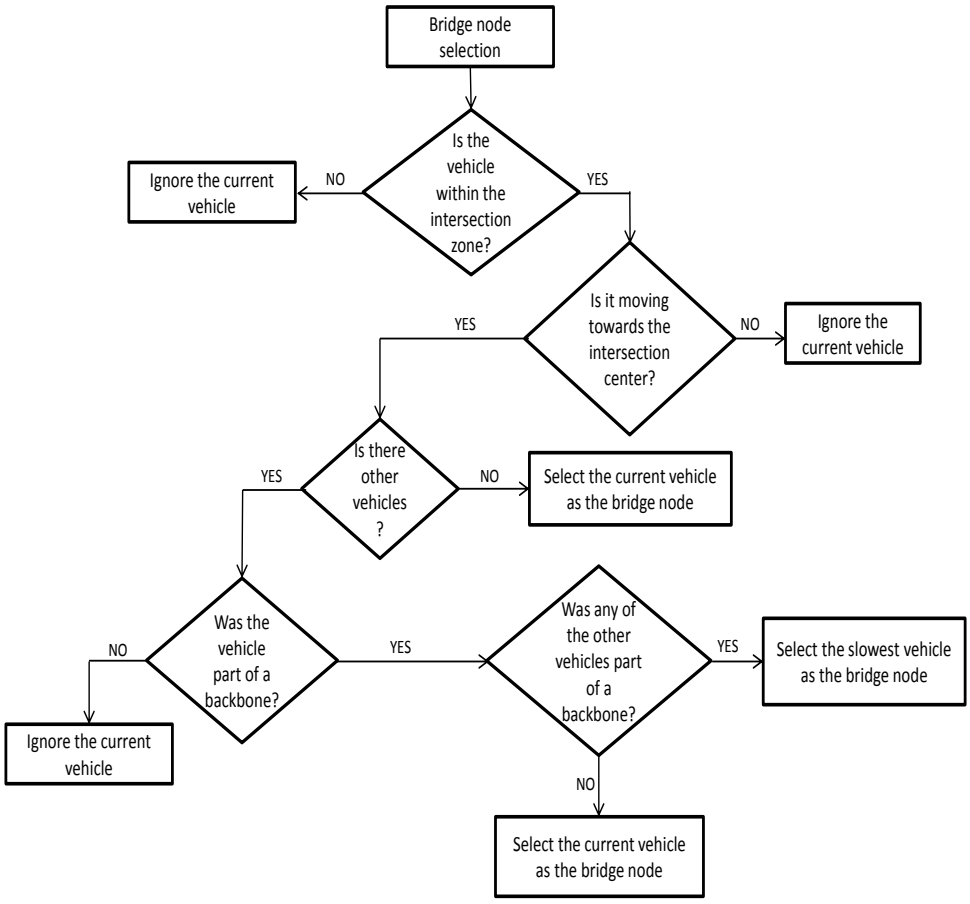

Figure 4.3: Bridge node selection flowchart

When a bridge node is about to leave the intersection zone, it looks for a substitute. It computes t_{cross} for each *BV* neighbor, defined as the time needed to cross the intersection zone. t_{cross} is then compared to the remaining time of the green light phase t_{rem}, computed as follows:

$$t_{rem} = t_g - [(t_a \bmod t_C) - (t_C - t_g)] \tag{4.5}$$

where t_g is the green light phase, t_a is the time to reach the traffic light, and t_C is the light cycle. t_g and t_C are assumed constants as in [67]. In case $t_{rem} > t_{cross}$, the bridge node selects the BV with the highest t_{cross}; otherwise, it chooses a backbone vehicle from the vehicles stopped by the red light. Ideally, the selected BV should be close to the boundary of the intersection zone (i.e, F and G in Figure 4.2).

4.3.4 Road Segment Assessment (RSA)

RSA is a distributed procedure that focuses on assessing the convenience of a road segment to be part of a routing path. It sets up routing tables at bridge nodes to facilitate packet forwarding. Whenever a bridge node is selected at an intersection, SCRP triggers RSA. The bridge node starts by generating a Road Assessment Packet (RAP) and broadcasting it over road segments. RAP collects information regarding connectivity, delay, and hop count. Its format is depicted in Figure 4.4, where *timestamp* designates RAP generation time, *cells* denotes the number of cells traveled when using carry-and-forward, and *options* holds additional routing information.

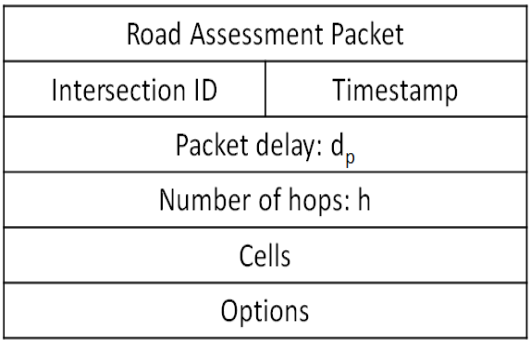

Figure 4.4: RAP format

d_p represents the average delay to incur for transmitting a new data packet over a road segment. It is defined as the sum of delays to incur at each backbone vehicle, d_{h_i}.

$$d_p = \sum_{i=1}^{h} d_{h_i} \tag{4.6}$$

According to [68], d_{h_i} has two components: T_q and T_{tx}. The former denotes the queuing

delay and is defined as the time elapsed between the moment a packet enters the queue until it becomes the head of it. The latter represents the transmission delay and is defined as the time from the moment the packet becomes the queue's head until it is successfully transmitted or dropped. T_{tx} also incorporates the time when the channel is busy as well as the backoff time when the channel is idle. Therefore, d_{h_i} can be expressed as follows:

$$d_{h_i} = E[T_{tx} + T_q] \tag{4.7}$$

T_q and T_{tx} are correlated. Indeed, the queuing delay of a packet corresponds to the time needed for all packets queued ahead of it to be transmitted. Thus, when a new packet arrives to a queue containing k packets, d_{h_i} can be written as:

$$d_{h_i} = (k+1)E[T_{tx}] \tag{4.8}$$

Observing Equation. 4.8, we can infer that d_{h_i} implies the memoryless property and is, therefore, exponentially distributed. This is compatible with the finding in [69] which demonstrates that the MAC service time for the IEEE 802.11 DCF can be approximated by an exponential random variable. This is still valid for EDCA when access categories are individually examined since they are considered as independent DCF stations [70].

Figure 4.5 illustrates the dissemination of RAP over road segments. When the green car located at I_A is elected as the bridge node, it generates and broadcasts RAP over $S_{A,B}$ and $S_{A,C}$. When receiving RAP, each BV over $S_{A,B}$ increments h to include itself, computes d_h using Equation 4.8 and adds it to the value of d_p. It then forwards RAP to the next BV. This process continues until RAP reaches I_B. Since $S_{A,C}$ does not hold a backbone, RAP will be carried until reaching I_C. Bridge nodes at I_B and I_C compute RAP's delivery delay, d_{rap}, as follows:

$$d_{rap} = t_{rx} - Timestamp \tag{4.9}$$

where t_{rx} designates RAP's received time.

d_{rap} is then compared to two thresholds: T_{bc} and T_{cf}. T_{bc} represents the upper bound

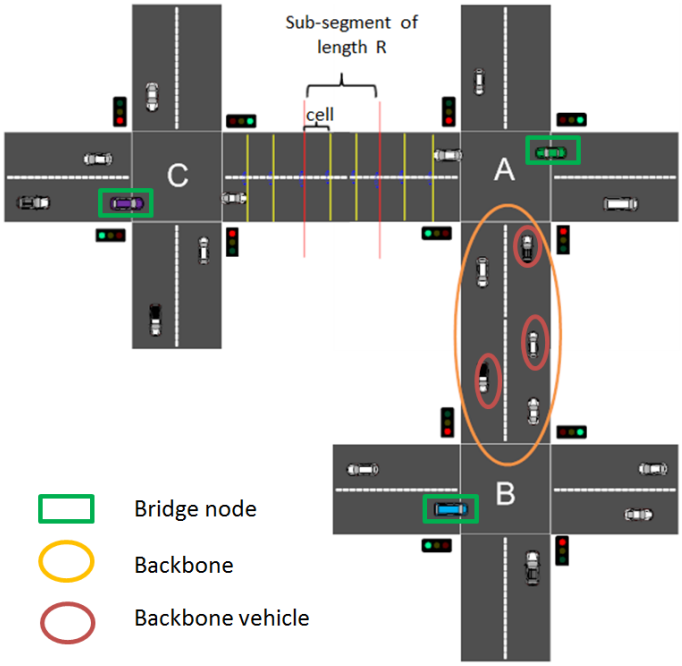

Figure 4.5: Connectivity and delay information collected via RAP

for the time needed by RAP to travel a road segment in the presence of a backbone. It is computed as follows:

$$T_{bc} = \sum_{i=1}^{h_{max}} T_{tx} \tag{4.10}$$

where h_{max} represents the maximum number of BVs a road segment can hold. It is given by:

$$h_{max} = \lceil \frac{3L}{2R} \rceil \tag{4.11}$$

with L denoting the length of the road segment. T_{cf}, on the other hand, describes the maximum tolerable time to wait for RAP when using carry-and-forward. It should not exceed t_{cross} in order to allow bridge nodes to have the desired information before leaving their respective intersections. Hence, T_{cf} is expressed as follows:

$$T_{cf} = t_{cross} - T_{bc} \tag{4.12}$$

Note that T_{bc} was subtracted from t_{cross} in order to give bridge nodes enough time to process received RAPs.

When $d_{rap} < T_{bc}$, bridge nodes infer that road segments hold backbones. In case $T_{bc} < d_{rap} < T_{cf}$, bridge nodes assume that road segments are partially disconnected and that carry-and-forward is to be used moderately. Otherwise, bridge nodes deduce that road segments are completely disconnected. Based on this information, bridge nodes assign weights to road segments.

$$w_{S_{(i,j)}} = \begin{cases} d_p, & d_{rap} < T_{bc} \\ d_p + p_{cf} d_{cf}, & T_{bc} < d_{rap} < T_{cf} \\ \infty, & \text{otherwise} \end{cases} \tag{4.13}$$

d_{cf} is the delay to incur when using carry-and-forward. To compute it, we divide the road segment into n sub-segments of length R (i.e., $S_{A,C}$ in Figure 4.5). Each sub-segment is further partitioned into m cells of length l, defined as the sum of the vehicle's average length l_{av} and the average safety distance d_s. Each cell can contain at most two vehicles with opposite directions. Hence, we obtain:

$$d_{cf} = \frac{cells * l}{v_{av}} \tag{4.14}$$

where v_{av} is the vehicles' average speed on the road segment.

p_{cf} is the probability of using the carry-and-forward mechanism. To estimate it, we first derive the probability of having at least one vehicle in a cell. We model the vehicles arrival to road segments as a Poisson process. Let λ_i be the vehicles' arrival rate at road segment $S_{i,j}$. The probability of having at least one vehicle in a cell is:

$$p_{cell} = 1 - \exp^{-(\frac{\lambda_i}{nm})} \tag{4.15}$$

Assume two vehicles u_1 and u_2 are moving from I_i to I_j. u_1 and u_2 are disconnected if they are m cells apart. Let p_{dis} be the probability of disconnection. p_{dis} can be written

as:

$$p_{dis} = (1 - p_{cell})^{m-1} \tag{4.16}$$

Now, if u_1 is the only vehicle in $S_{i,j}$, p_{cf} in this case can be expressed as

$$p_{cf} = \prod_{k=1}^{\lfloor \frac{d_{u_1,I_j}}{R} \rfloor} p_{disc} \tag{4.17}$$

where d_{u_1,I_j} is the distance between vehicle u_1 and intersection I_j.

As weights are dependent on connectivity and delay information, they need to have validity periods. In case a road segment $S_{i,j}$ is holding a backbone, the validity period is the time till a disconnection occurs (see Section 4.2.2). Otherwise, the validity period is the time until the bridge node crosses the intersection (i.e., t_{cross}). Therefore, we express the weight validity period (WVP) of $S_{i,j}$ as:

$$WVP_{S_{i,j}} = \begin{cases} min(B_{S_{i,j}}), & \text{if backbone} \\ t_{cross}, & otherwise \end{cases} \tag{4.18}$$

where $B_{S_{i,j}} = \{LLT_1, LLT_2, ..., LLT_k\}$ is the set of the estimated link lifetimes for BVs over $S_{i,j}$.

After computing the weights of road segments as well as their validity periods, each bridge node constructs a routing table. These tables contain the list of road segments, reachable from their respective junctions along with their weights and their validity periods. These tables are used by SCRP to construct routing paths. The weight of a routing path, made of q road segments, can thus be expressed as:

$$w_{pth} = \sum_{i=1}^{q} w_i \tag{4.19}$$

Consequently, the weight validity period of a routing path can be expressed as:

$$WVP_{pth} = min(R_{pth}) \tag{4.20}$$

where $R_{pth} = \{WVP_{S_{i,j}}, WVP_{S_{j,a}}, ..., WVP_{S_{p,z}}\}$ is the set of WVPs of the road segments forming the routing path.

4.3.5 Articulation Junction Selection

Having a global knowledge of the network topology is extremely difficult given the considerable size of modern cities. In this regard, we divide the city into zones and elect articulation junctions in each one of them. The size of each zone is set, using simulations, to 3×3 blocks in order to limit RAP flooding and control its size.

An articulation junction is the intersection that is connected to most of the junctions in its respective zone. It has up-to-date view of the zone's network topology. Electing an articulation junction is done in a distributed and dynamic fashion, as illustrated in Figure 4.6. At first, each bridge node appoints its respective intersection as the articulation junction, and sets ρ, the number of junctions to which it is connected, to 0. After exchanging the first round of RAPs, bridge nodes update their respective ρ according to the number of RAPs received (Figure 4.6(a)). In the second round, bridge nodes append their routing tables to RAPs, using the *options* field, before broadcasting them. When received, bridge nodes compare the routing tables received with their own. The intersection with the largest ρ is set as the articulation junction. To illustrate, bridge nodes at junctions C, G, and I designate B, H, and F as the articulation junction, respectively while D, F, and H set E as the articulation junction (see Figure 4.6(b)). For A and B, since both have the same ρ, the intersection with the lowest total aggregated weight is chosen as the articulation junction (i.e., A in this case). The same process will be repeated in the subsequent rounds (Figure 4.6(c)), but only new or updated entries are appended to RAPs instead of the whole routing tables. Eventually, E is nominated as the articulation junction (Figure 4.6(d)).

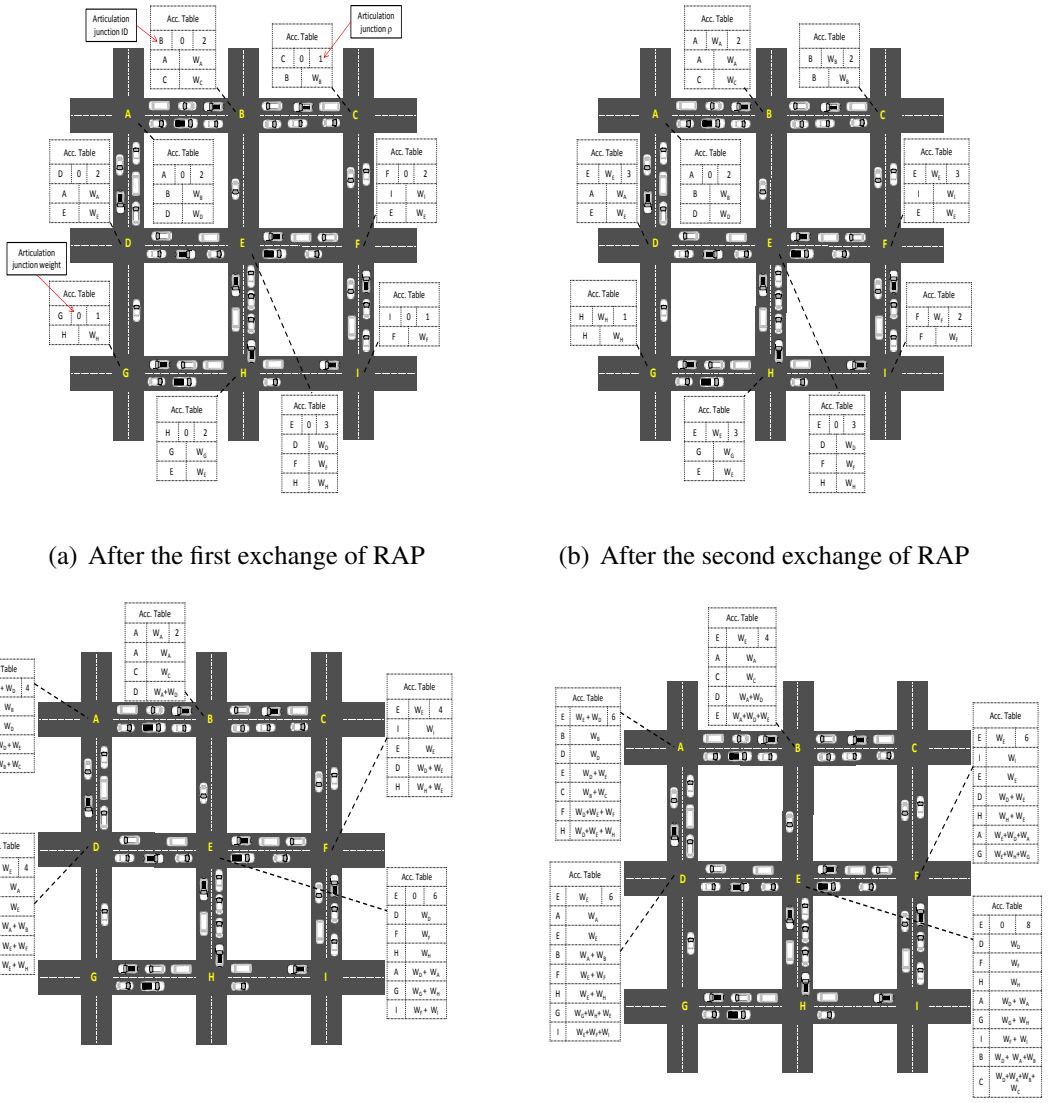

(a) After the first exchange of RAP

(b) After the second exchange of RAP

(c) After the third exchange of RAP

(d) After the forth exchange of RAP

Figure 4.6: Articulation junction selection procedure

4.3.6 Route Construction

When a source node wants to send data packets to a destination, it generates a *"Route Query"* (*RQ*) containing the source node's ID, the destination ID, and the location of the destination. The source node forwards *RQ* to the closest bridge node. Once received, the bridge node checks its routing table to see whether it can reach the destination. If

yes, it generates a *"Route Result"* (*RR*) and forwards it to the source node. Otherwise, the bridge node transfers *RQ* to the zone's articulation junction. The bridge node at the articulation junction checks first whether the destination is within the zone. If yes, it computes the route with the lowest weight to the destination, using its routing table, and includes it into *RR*'s header. Otherwise, it computes the sub-path with the lowest weight between the source node and itself and includes it into *RQ*; then, it forwards *RQ* to its neighboring articulation junctions. This procedure continues till the destination is reached.

It is possible that the destination receives multiple *RQs*, implying the existence of several routing paths. In this case, the destination stores all paths in its routing table along with their validity periods. It selects the path with the lowest weight, includes it into *RR* header, and forwards it back to the source node. When received, the source node starts sending data packets. These data packets are also used by bridge nodes as a means to refresh the weights attributed to road segments along with their validity periods. When the weight of the current path exceeds a threshold w_{th}, the destination reselects the path with the lowest weight from the list, includes it in a *"Route Update"* (*RU*), and sends it to the source node. When received, the source node starts forwarding data packets on the new routing path.

4.4 SCRP Sensitivity Study

In this section, we analyze the key parameters that might impact the performance of SCRP if set inappropriately. This includes β, h_{max}, and w_{th}.

4.4.1 Determining β

To determine the best value of β to be used, we simulated a road segment of 1500 meters while varying the number of vehicles (i.e., from 15 to 30) to depict low and medium densities. Speed ranges between 30 and 80 Km/h for low density, and between 30 and 60 Km/h for medium density.

A backbone is built over the road segment and the stability index, defined as the ratio

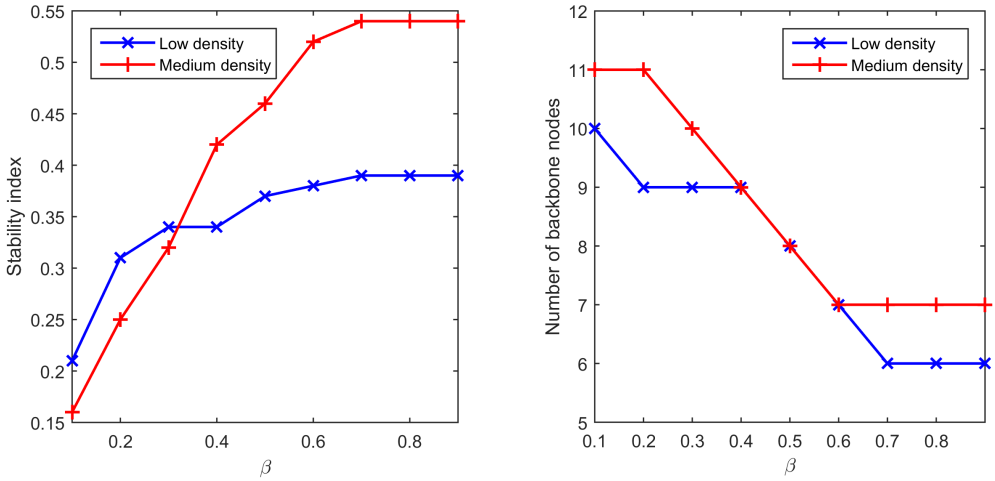

(a) β vs. stability index (b) β vs. number of backbone nodes

Figure 4.7: Determining the value of β

between WVP and the average backbone lifetime, is computed. Clearly, the higher the stability index, the more stable is the backbone. Figure 4.9(a) shows β as a function of the stability index. We observe that as β increases, the stability index increases. The reason is that backbone vehicles stay connected much longer, yielding more stable backbones. This implies that SF is upper-bounded by the second term, particularly by β. When $\beta \geq 0.7$, the stability index becomes steady. Figure 4.9(b) plots β as a function of the number of backbone nodes. We observe that when β increases, the number of backbone nodes for both densities drops. Furthermore, when $\beta \geq 0.6$, the number of backbone nodes remains constant. The reason is twofold: 1) the number of BVs cannot be reduced anymore in order to preserve the backbone connectivity; and 2) selected BVs yield the most stable backbone. Therefore, in the subsequent simulations, we set the value of β to 0.7 and that of α to 0.3.

4.4.2 Determining h_{max}

T_{bc} is used to tell whether a backbone exists on a road segment. Hence, T_{bc} depends on the road segment's length and the vehicles' density.

Figure 4.8 plots different T_{bc} values along with d_{rap} obtained via simulations. We

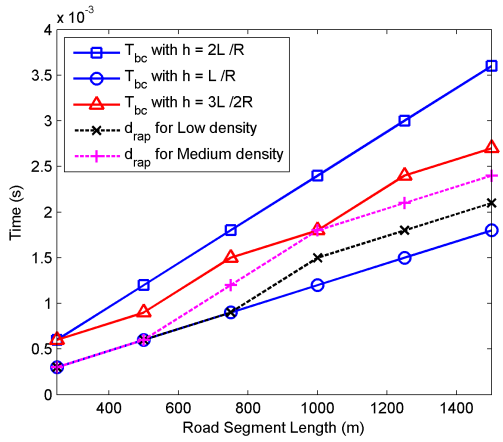

Figure 4.8: Determining the value of h_{max}

observe that both small and large values of h_{max} result in T_{bc} not confining d_{rap} adequately. This is because: 1) small values of h_max penalize larger road segments by considering them as partially disconnected even if they hold backbones; and 2) large values of h_{max} may consider partially disconnected road segments as segments with built backbones, leading to inaccurate routing decisions. To illustrate, when $L = 1500$ meters and $h = 2L/R$, T_{bc} is 50% higher than d_{rap}. The best approximation of T_{bc} occurs when $h = 3L/2R$ as there is a slight difference between T_{bc} and d_{rap} for both low and medium densities (i.e., $2T_{tx}$ and T_{tx}, respectively). Therefore, we set h_{max} to $3L/2R$ in our simulations.

4.4.3 Determining w_{th}

Identifying a convenient value for w_{th} is crucial for the proper functioning of SCRP as it adjusts the tradeoff between performance and overhead. To demonstrate the impact of w_{th}, we considered a grid of 2500×2500 meters, consisting of 2 zones. We, then, setup four traffic flows, F_i $(i = 1,2,3,4)$ where $F1$ and $F2$ are active during the whole simulation, while $F3$ and $F4$ are activated and deactivated at different time intervals. Activation/deactivation periods follow an exponential distribution with mean of 100 seconds. The packets generation rate is fixed to 20 packets/second.

Figure 4.9 plots w_{th} as a function of E2ED and throughput. Both small and large

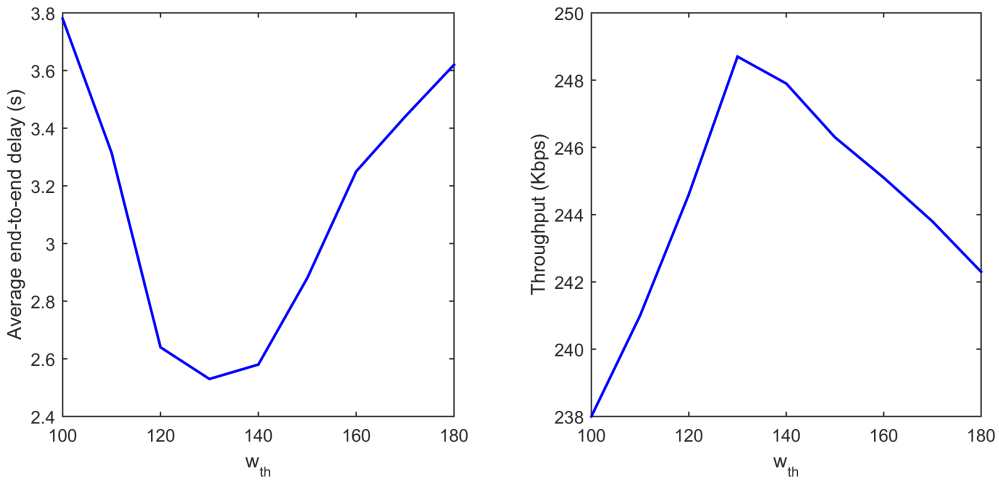

(a) Average E2ED vs. w_{th} (b) Throughput vs. w_{th}

Figure 4.9: Determining the value of w_{th}

values of w_{th} yield low throughput and longer E2ED. This is because: 1) a small value of w_{th} might trigger the rerouting process so often, which incurs needless overhead; and 2) a large value of w_{th} prevents SCRP from timely responding to a congested path, degrading therefore its performance. Figure 4.9 also shows that $w_{th} = 130$ ms allows for an optimal performance of our routing protocol. Hence, we set w_{th} to 130 ms in our simulations.

4.5 Performance evaluation

In this section, we present a simulation-based evaluation of SCRP and three other urban routing protocols: GPSR [10], GyTAR [15], and iCAR [19]. These protocols were chosen since they use different metrics to make routing decisions: GPSR [10] uses shortest path, GyTAR [15] uses connectivity and distance to destination, and iCAR [19] uses connectivity and delay.

4.5.1 Simulation settings

We have implemented our protocol using ns-2 [71] and we deployed SUMO [72] and MOVE [73] to generate realistic mobility traces for VANET. Vehicular flows were created with specified origins and destinations. Each flow has a different inter-arrival time and Dijkstra's shortest path is used to compute routes from starting points to destination positions. The city map is a grid area of 7500×7500 m with bidirectional roads. There are 165 intersections, 45 of them are unsignalized. The number of nodes is varied between 150 and 600 to portray the network state at different time periods. Their speed fluctuates between 30 and 80 Km/h, which is common for an ordinary city environment. We setup ten multihop UDP flows; they start at different time instants and continue throughout the simulation.

To model the impact of obstacles, we deploy the free space with urban area path loss exponent model proposed in [74]. In addition, we set 5 dB attenuation rate to count for shadow fading caused by obstructing vehicles. The schemes are evaluated in terms of average E2ED, packet delivery ratio (PDR), and routing overhead (RO). Results are presented in the following subsections. Other system parameters are described in Table 4.I.

Table 4.I: Simulation Parameter Settings

Parameter	Value
R	250 m
l_{av}	5 m
d_s	3 m
ω	8 m
Data rate	2Mbps
Beacon interval	1 second
Packet generation rate	1 - 50 packets/second
Packet size	512 byte

4.5.2 Simulation Results and Analysis

4.5.2.1 Probability of Connectivity

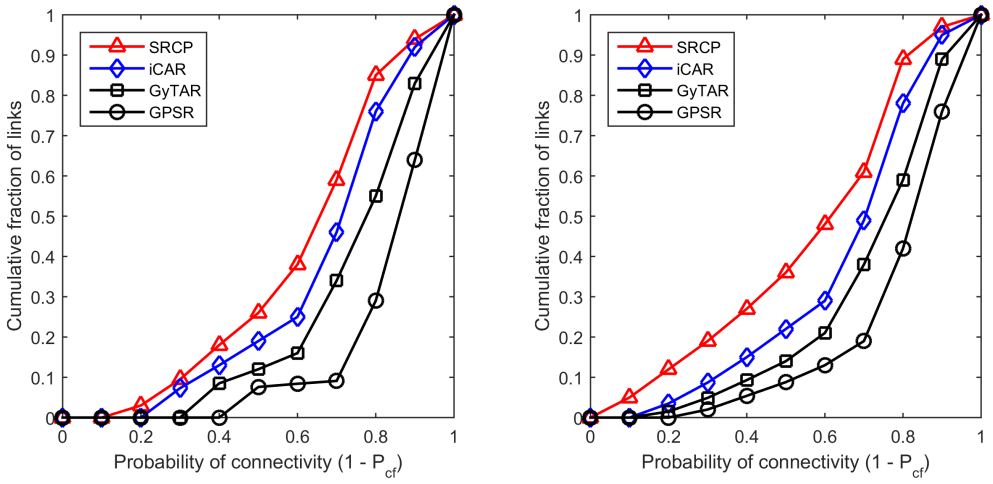

(a) (b)

Figure 4.10: CDF of the links connectivity for (a) $N = 200$ and (b) $N = 400$

Figure 4.10 compares the cumulative distributed function (CDF) of links connectivity used by the simulated protocols with respect to p_{cf} for 200 and 400 vehicles. As expected, SCRP, iCAR and GyTAR choose routes that have high connectivity to relay messages while GPSR selects the shortest routing paths without considering link connectivity. Figure 4.10 also shows that SCRP outperforms the other schemes as it prioritizes segments with built backbones when forwarding data packets, thus taking advantage of the up-to-date knowledge of the network topology. For example, when the connectivity probability is set to 0.7, SCRP uses carry-and-forward over 38% of the links when the network density is 400, against 50% for iCAR, and 60% for GyTAR.

4.5.2.2 End-to-End Delay

Figure 4.11(a) shows the average E2ED as a function of the network density. We observe that all protocols have the tendency of decreasing E2ED as the network density increases. The reason is that, increasing the density of the urban network reduces the

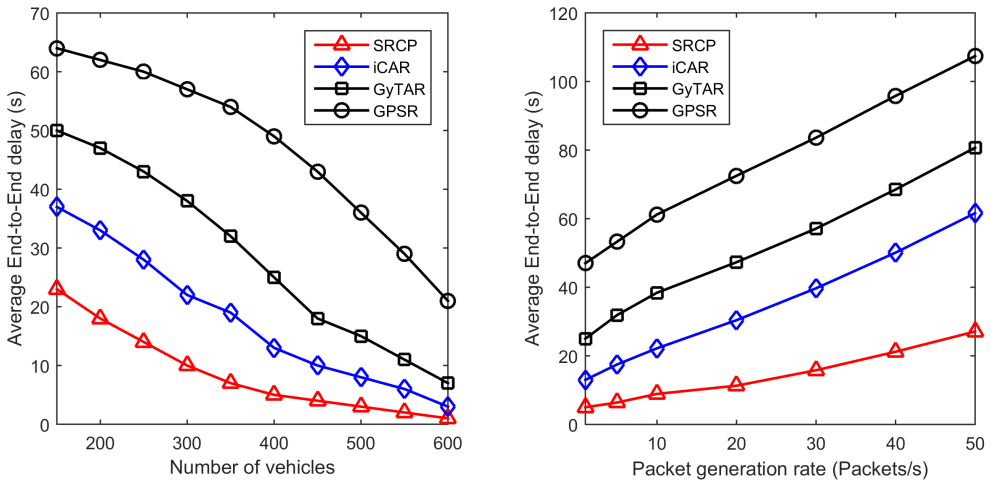

(a) (b)

Figure 4.11: Average E2ED vs. network density and packet generation rate

number of disconnected road segments, lowering therefore p_{cf}. We also observe that SCRP incurs the lowest E2ED as it eliminates the local maximum problem, because of the use of bridge nodes and articulation junctions. Unlike SCRP, iCAR and GyTAR rely only on local information to make routing decisions whenever an intersection is reached, making them prone to the local maximum problem. As for GPSR, the high E2ED can be explained by the excessive use of the carry-and-forward mechanism.

Figure 4.11(b) shows E2ED variation with respect to packet generation rate. We observe that the average E2ED for all protocols increases with the increase of data load. As GPSR and GyTAR do not allow for load balancing, they both experience data congestion, which escalates E2ED. SCRP and iCAR provide lower E2ED due to the use of alternative routes. Still, SCRP outperforms iCAR (e.g., by 43% when traffic load is set to 50 packets/s). This is because iCAR uses the delay induced by Control Packets (CPs) to estimate the delay to incur for data packets; this leads to inaccurate results as CPs and data packets may not belong to the same Access Category (AC) of the EDCA mechanism.

4.5.2.3 Packet Delivery Ratio

Figure 4.12(a) exhibits PDR as a function of the network density. We observe that PDR for all schemes increases with the increase of the network density. We also observe that SCRP outperforms all the other routing schemes. This is because SCRP forwards packets over roads with built backbones, incurring lower queuing delay. Likewise, iCAR achieves good PDR compared to GyTAR and GPSR thanks to its prediction method, which checks the existence of a neighbor before forwarding data packets. As GyTAR forwards packets over roads with high vehicular traffic, it suffers multiple collisions, leading to transmissions failure. Furthermore, its road connectivity evaluation procedure may give inaccurate results since it does not consider traffic lights. Finally, due to its long delivery delays, packets in GPSR are dropped before reaching the destination.

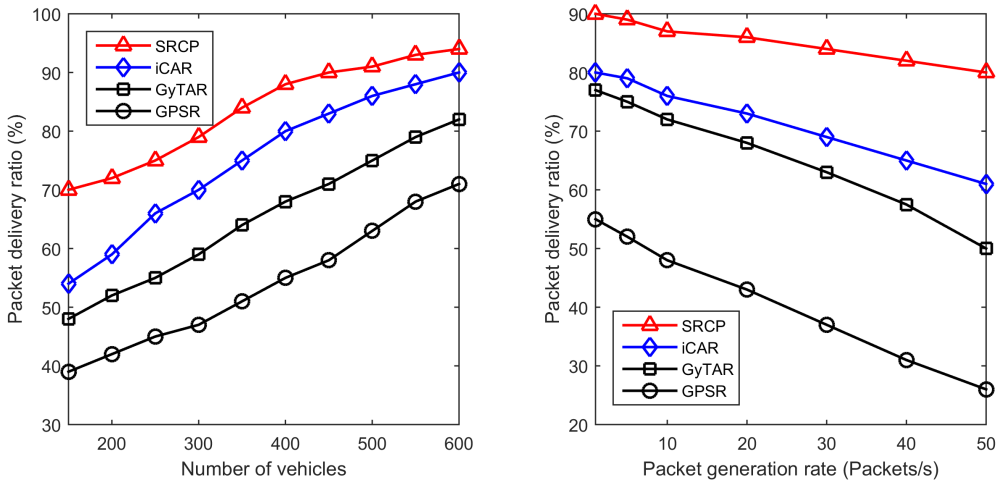

(a) (b)

Figure 4.12: PDR vs. network density and packet generation rate

Figure 4.12(b) shows PDR as a function of the packet generation rate. We observe that PDR of all schemes decreases with the increase of packet rate. GPSR has the worst PDR as many packets get dropped due to the excessive use of carry-and-forward. GyTAR's PDR is lower than iCAR's because it lacks the load balancing capability, inducing therefore multiple retransmissions. Even though iCAR allows for load balancing, its

PDR is still low compared to SCRP. This is due to the inaccurate estimation of the data packet delay that impacts its routing decisions, leading to packet losses.

4.5.2.4 Routing Overhead

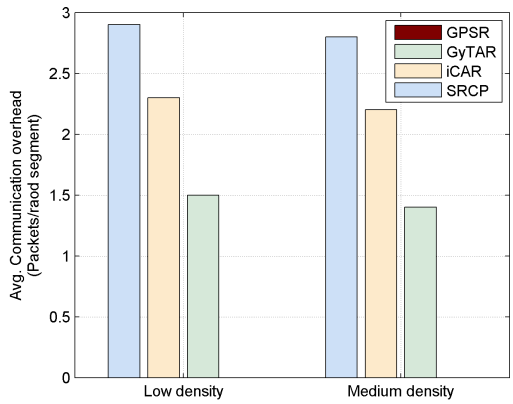

Figure 4.13: Average routing overhead vs. network density

Figure 4.13 depicts the average RO for the simulated routing schemes. We consider all control packets used in the routing process, except beacon messages since they are a key component of VANET. GPSR is the only protocol to not generate any routing overhead as it relies on the Euclidian distances to make its routing decisions. SCRP, iCAR, and GyTAR incur additional routing overhead since they use discovery packets to collect density and delay information over road segments. SCRP incurs the highest routing overhead due to the creation of backbones over road segments as well as the use of *RQ*s, *RR*s, and *UR*s when establishing and updating routes. We also observe that as the network density increases, the routing overhead decreases. In fact, the higher the density, the lower are the changes in the network topology, thus reducing the number of triggered control packets. Note that SCRP generates few extra control packets per road segment compared to iCAR. This is a small price to pay given the gains obtained in terms of E2ED and PDR.

4.6 Chapter Summary

In this chapter, we proposed a novel routing protocol for VANET in urban scenarios, called SCRP. SCRP exploits up-to-date topology information to enhance the QoS of non-safety applications for low to moderate network densities. It thrives to find the most stable paths between source and destination that incur low E2ED. To do so, it starts by building backbones on road segments and connecting them via bridge nodes at intersections. Then, it assigns weights to the different road segments based on information collected through RAPs. Simulation results show that SCRP achieves better performance compared to existing greedy-based schemes, making it a good candidate for non-safety VANET applications. Still, before forwarding data packets of non safety applications, a mechanism is needed to decide on the service channel to be used. This will be covered in the next chapter.

CHAPTER 5

ALTRUISTIC SERVICE CHANNEL SELECTION SCHEME (ASSCH) FOR V2V INFOTAINMENT APPLICATIONS

The Wireless Access for Vehicular Environment (WAVE) specifies that data packets of infotainment applications are to be sent within WAVE basic service sets (WBSS). These WBSS are to be established on the least congested service channels. WAVE proposes a mechanism to select such channels. Nevertheless, owing to high mobility in VANET, there is a high chance of having overlapped WBSS, yielding unsatisfactory performance. Several approaches have been proposed to avoid such a scenario. Yet, they are either inefficient or cost-ineffective. In this chapter, we propose ASSCH, an altruistic mechanism that impels vehicles to collaborate in order to select the least congested (i.e., used) service channel. ASSCH also includes a mechanism for WBSS termination, which is not specified in WAVE. To the best of our knowledge, none of the existing schemes have proposed something similar. Simulation results demonstrate that our mechanism allows for quicker access to service channels, handles the overlapping problem better, and incurs high channel efficiency.

The rest of the chapter is organized as follows. Section 5.1 presents the motivation behind the design of ASSCH. Section 5.2 describes the system model. Section 5.3 details the proposed service channel selection scheme. Section 5.4 presents the simulation results while Section 5.5 concludes the chapter.

5.1 Problem Statement

WAVE [75] was proposed to cope with VANET challenges. It operates on the DSRC spectrum that is partitioned into seven channels. One of them is referred to as the control channel (CCH) and is exclusively dedicated to transmitting safety and control messages. The remaining six are used for transferring data packets of non-safety applications and are referred to as service channels (SCHs). To enable vehicles to switch between these

channels, WAVE uses the coordinated universal time (UTC), where each second is subdivided into ten synchronization intervals (SI). Each SI consists of one CCH interval (CCI) followed by one SCH interval (SCI). A guard interval (GI) is inserted at the end of each CCI/SCI to account for synchronization imprecisions [47].

WAVE allows data packets of infotainment applications to be transmitted within WBSS, which can be established by any DSRC device (i.e., RSUs or OBUs) [5, 35]. A vehicle having packets to send, labeled *provider*, initiates WBSS by broadcasting WAVE Service Advertisement (WSA) message during CCI. WSA contains the identifier of the provider, a description of the service provided, and the service channel to be used [47]. When receiving WSA, vehicles may choose to join WBSS. If so, these vehicles, labeled *users*, along with the provider switch their transceivers to the advertised SCH at the beginning of SCI. The provider then starts sending its data frames and terminates WBSS once all of its packets are sent. There are two types of WBSS: persistent and non-persistent [76]. The former is announced at every CCI for the entire WBSS lifetime. The latter is announced only once, i.e., at the establishment phase. In this chapter, we focus on non-persistent WBSS. Note that WBSS does not require the association and authentication procedures, used by IEEE 802.11 BSS, in order to exchange data.

WAVE mandates that vehicles shall monitor received WSA messages in order to keep track of used SCHs in their 1-hop range. This way, they can establish their WBSS on the least congested SCH. Yet, this mechanism suffers from two major shortcomings: 1) vehicles might end-up using obsolete SCHs status information due to WSA collisions; and 2) vehicles lack SCHs status information within 2-hop range, yielding poor service quality as two providers within carrier sense range may select the same SCH to setup their WBSS. Besides, no mechanism was proposed to inform users of WBSS termination in case of non-persistent WBSS. The authors in [77] suggested that users can leave WBSS when an entire SCI elapses without receiving any data packet from their provider. Still, this approach sets SCHs state as busy for an entire SCI even if no communication is carried over them, leading to inefficient channel utilization.

These observations have motivated us to design ASSCH, a WAVE-compliant scheme that allows providers to select the least congested SCH when setting up their WBSS. It

has two objectives: 1) compel vehicles to cooperate in order to help providers select the least used SCHs. This is achieved by exchanging SCHs state information through beacon messages; and 2) notify users of their WBSS termination as quickly as possible in order to have up-to-date SCH status information.

5.2 Network Model

Our network mimics a real-life VANET scenario, where vehicles move along a multilane highway segment with obstacles (e.g., houses and trees) on both of its sides. Having unique IDs, vehicles arrive at the starting point of the highway following a Poisson process with an average rate of λ_a. Vehicles travel with different speeds, uniformly distributed between V_{min} and V_{max}. Beacon messages are generated at a rate of λ_b, enabling vehicles to transmit information regarding speed and location to neighboring vehicles. This information is provided by GPS devices. Vehicles are also equipped with single transceivers to enable Vehicle-to-Vehicle communication.

We adopt the alternating access mode (i.e., CCI followed by SCI) in order to allow for safety and infotainment applications to co-exist. Such a capability is considered especially attractive as an initial deployment strategy to push VANET market penetration. We make use of the FCC amendment [78] regarding DSRC, where only four SCHs (i.e., 174, 176, 180, and 182) are allocated for infotainment applications. The other two (i.e., 172 and 184) are reserved for future use. We set SCH 172 as the default service channel for vehicles that did not join any WBSS. A provider Pv_i, with $(i = 0,1,2,3)$ denoting its service priority, may request any SCH to establish its WBSS. Preference will always be given to providers with high priority services. Time is discretized into slots of length σ. At each slot, a channel can be either free or occupied. Let T_i be the *service time* of Pv_i, defined as the time period between WBSS establishment and termination, and is known only to Pv_i. To make it known to all vehicles, we alter its definition. Indeed, we consider T_i as the remaining time until SCH becomes free given that it is currently used by Pv_i. This way, we can model T_i as an exponential distribution with mean μ_i. The rational behind this modeling is that T_i is independent of the time the channel has been in use so

far, reflecting its memoryless nature.

5.3 ASSCH Components

ASSCH allows providers to select the least used SCHs when setting up their WBSS. It has three components: channel state information collection, future channel state prediction, and channel selection. The following subsections describe each one of them in more details.

5.3.1 SCHs State Information Collection

Vehicles maintain Channel State Tables (CSTs) to keep track of channel usage in their vicinities. CSTs have six fields: 1) SCH identifier; 2) state: indicating the current occupancy status of each SCH. A value of 1 implies that the channel is busy while a value of 0 indicates that the channel is free; 3) provider's identifier; 4) provider's position; 5) provider's priority (i.e., priority of the service it offers, with $i = 3$ as the highest); and 6) score: representing the utilization ratio of SCH, computed at the end of every SCI.

Before sending WSA to setup WBSS, Pv_i collects information about the current state of SCHs. This process is performed throughout an entire SI. During CCI, Pv_i listens for broadcasted WSAs in its vicinity and updates its CST accordingly. During SCI, Pv_i requires the cooperation of neighboring vehicles in order to monitor SCHs and collect updated state information. Indeed, when SCI starts, Pv_i switches to SCH 172 and broadcasts a *SCH Query* $(SCHQ)$ message to identify neighboring vehicles that have not joined any WBSS. $SCHQ$ includes Pv_i's identifier only. Let S_N be the set of vehicles on SCH 172. When receiving $SCHQ$, every element in S_N replies with a *SCH Response* $(SCHR)$ message, containing its identifier as well as the score of every SCH. When receiving $SCHR$, Pv_i chooses *monitors* (i.e., neighbors that will listen to SCHs during the current SCI) based on the following rules:

1. If the state of SCH_j is perceived to be free by all vehicles in S_N, monitoring SCH_j is delegated to the farthest neighbor. This helps detecting hidden terminals.

2. If otherwise, monitoring SCH_j is delegated to the neighbor with the maximum score for SCH_j.

Once monitors are identified, Pv_i creates and broadcasts a monitoring table (MT). Each entry in MT contains a monitor identifier as well as its assigned SCH. When receiving MT, monitors switch their transceivers to the assigned channels and start listening. At the end of SCI, monitors update their CSTs (i.e., state and score of the assigned SCH) and piggyback them into their beacon messages, which will be broadcasted in the subsequent CCI.

When receiving beacon messages, vehicles extract the encapsulated CSTs. For each occupied SCH, marked as free in their own CSTs, vehicles use the position field in the received CSTs to compute their distances to the provider currently using SCH. In case the distance is smaller than d_{th}, defined as the carrier sense range, they set the state of SCH to occupied; otherwise, they keep the state of SCH as free. This is to control the propagation of CSTs, allowing for SCHs spatial reuse without suffering co-channel interferences. According to [79], the average transmission range under the Nakagami propagation model can be expressed as:

$$R_{av} = \frac{1}{\alpha\Gamma(m)}\Sigma_{i=0}^{m-1}\frac{(m-1)!}{(m-1-i)!} \times \Gamma(m - 1 - i + \frac{1}{\alpha})\left(\frac{mP_{th}}{P_tK}\right)^{\frac{1}{\alpha}} \quad (5.1)$$

where m is the fading factor; $\Gamma(.)$ is the gamma function; α is the path loss exponent; $K = G_tG_r(c/(4\pi f_c))^2$; G_t and G_r are antenna gains of the transmitter and receiver, respectively; c is the speed of light; and $f_c = 5.9$ GHz is the carrier frequency. Hence, d_{th} can be expressed as:

$$d_{th} = \frac{R_{av}}{\rho}, \quad \rho \in (0,1] \quad (5.2)$$

Figure 5.1 shows an example of how CSTs are disseminated and updated. After collecting information about SCHs, Pv_A selects SCH_1 and broadcasts its WSA at $t = 120$ ms. When received, vehicles in zone 1 update SCH_1 entry in their CSTs by setting its state to occupied. They also set the provider identifier, position, and priority to Pv'_As. At $t = 200$ ms, these vehicles broadcast their beacon messages. For instance, all vehicles in

zone 2, including Pv_B and n_2, receive the beacon message from n_1 and update their CSTs (i.e., SCH_1 entry) accordingly. At $t = 220$ ms, Pv_B broadcasts its WSA with SCH_4 as its selected service channel. Here again, all vehicles in zone 2 update SCH_4 entry by setting its state to occupied; they also set the provider identifier, position, and priority to Pv'_Bs. Then, these vehicles broadcast their beacon messages at $t = 300$ ms. When received, vehicles in zone 3 compute the distance separating them from Pv_A. Since that distance is greater than d_{th}, they set the state of SCH_1 to free. When Pv_C wants to establish its own WBSS at $t = 320$ ms, it can use available SCHs, including SCH_1.

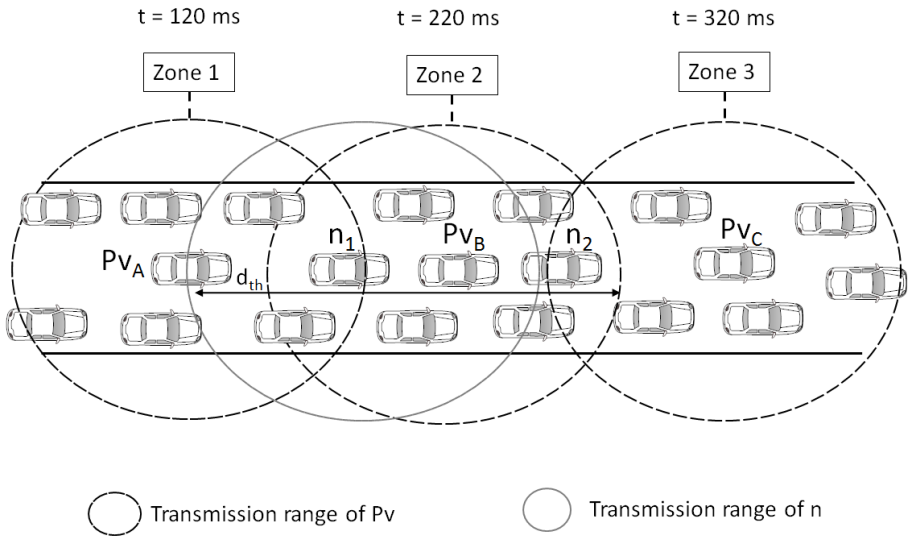

Figure 5.1: A sample scenario of how CSTs get disseminated and updated

Using this scheme, each vehicle is able to identify the state of SCHs in its 1-hop and 2-hop ranges as well as the priority of the providers using them. This information is then fed to a stochastic model to foresee the state of SCHs in the near future, as described in the next subsection.

5.3.1.1 Monitors Selection Problem

One might argue that two providers that are within transmission range may select the same vehicle to monitor two different SCHs. However, this is unlikely to happen. In

fact, whether they have the same or different priorities, either one of them will transmit its MT first; when hearing it, the other provider should proceed to select another vehicle, as monitor, before broadcasting its own MT.

Still, the real problem arises when providers are within $2-$hop range, as shown in Figure 5.2. Indeed, when the first MT is received, assume it is from Pv_A, M will immediately switch to the assigned SCH and starts listening. When Pv_B transmits its MT, M will miss it. This will deprive Pv_B from up-to-date information about the SCH assigned to M, leading to inaccurate channel selection decision. To mitigate this issue, we make each monitor broadcasts a small message, labeled *ASSIGNED*, before switching to the assigned SCH. *ASSIGNED* contains the monitor's identifier as well as the assigned SCH. It serves two purposes: $1)$ it acknowledges the receipt of MT by monitors; and $2)$ it allows providers to know whether the selected monitors are used by other providers. Keep in mind that $SCHQ$, $SCHR$, MT, and *ASSIGNED* are all transmitted over SCH 172 during SCI.

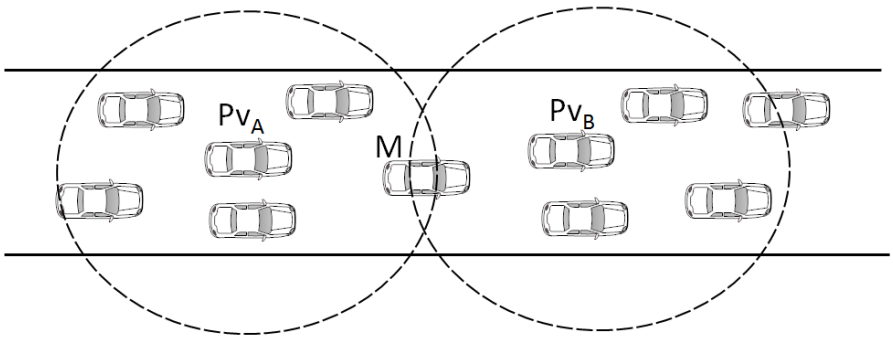

Figure 5.2: Monitors selection problem

5.3.2 SCHs Future State Prediction

In this subsection, we predict the state of each channel in the next SCI using the Markovian model shown in Figure 5.3. There are six states $\{S_f, S_h, S_0, S_1, S_2, S_3\}$ describing the channel status at the end of each SCI. A channel can be free (S_f), occupied by a provider with priority $(S_i, i = 0,1,2,3)$, or suffering a hidden terminal problem (S_h). Let p_q^i be the probability of Pv_i requesting a channel. The transition probabilities of the

Markov chain are viewed as conditional probabilities, where $P_{m,j}$ is the probability that the channel will be in state S_m in the next SCI given that it is in state S_j at the end of the current SCI. Before expressing these probabilities, we first present few elements that are essential to the derivation of the state transition matrix.

– Since vehicles only acquire local information via beacon messages, a provider cannot know the exact number of vehicles that are within its carrier sense range. Therefore, we estimate n using the fact that vehicles arrive to the highway following a Poisson process with rate λ_a. Indeed, the average number of vehicles in the carrier sense of a tagged vehicle can be expressed as:

$$n = \frac{4\lambda_a(d_{th} - R_{av})}{V_{min} + V_{max}} \tag{5.3}$$

– Given that the channel is used by Pv_i in the current SCI, the probability that Pv_i holds the same channel in the next SCI can be expressed as:

$$P^i_{hold} = P(t^i_s > 1) = e^{-\frac{1}{\mu_i}} \tag{5.4}$$

– Given that the channel is used by Pv_i in the current SCI, the probability that Pv_i releases the channel at the end of the current SCI is:

$$P^i_{release} = 1 - P^i_{hold} = 1 - e^{-\frac{1}{\mu_i}} \tag{5.5}$$

– The probability that no provider of priority i requests the channel can be computed as [33]:

$$P^i_{nrq} = e^{-np^i_q} \tag{5.6}$$

– The probability that at least one provider of priority i requests the channel is expressed as:

$$P^i_{rq\geq 1} = 1 - P_{nrq} = 1 - e^{-np^i_q} \tag{5.7}$$

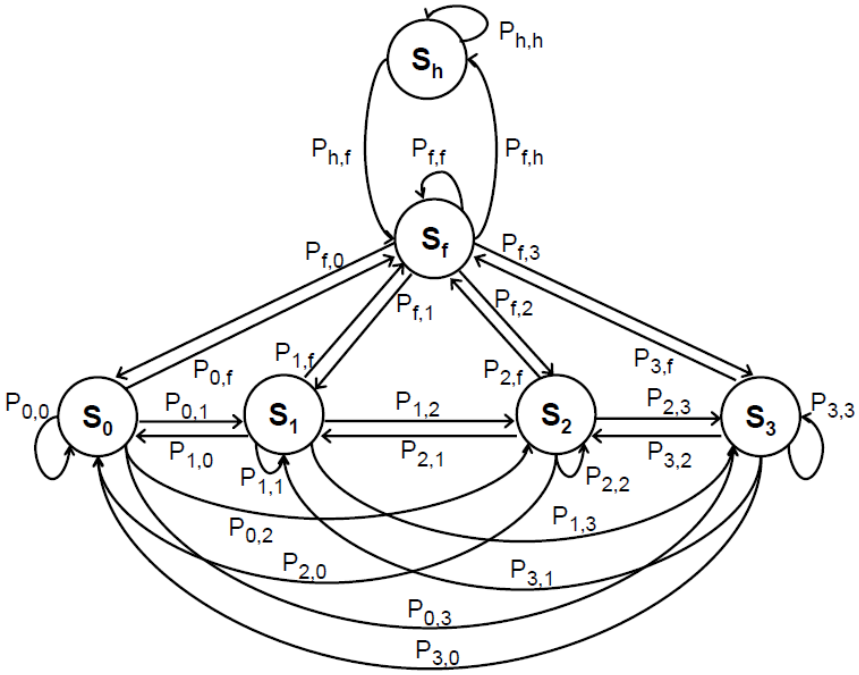

Figure 5.3: The Markov chain model for SCHs state prediction

The transition probabilities can therefore be expressed as follows:

$$P_{f,f} = e^{-n\Sigma_{i=0}^{3} p_q^i} \tag{5.8}$$

$$P_{f,0} = (1 - e^{-np_q^0}) e^{-n\Sigma_{i=1}^{3} p_q^i} \tag{5.9}$$

$$P_{f,1} = (1 - e^{-np_q^1}) e^{-n(p_q^2 + p_q^3)} \tag{5.10}$$

$$P_{f,2} = (1 - e^{-np_q^2}) e^{-np_q^3} \tag{5.11}$$

$$P_{f,3} = 1 - e^{-np_q^3} \tag{5.12}$$

$$P_{f,h} = 1 - e^{-n\Sigma_{i=1}^{3} p_q^i} \tag{5.13}$$

$$P_{0,f} = (1 - e^{-\frac{1}{\mu_0}}) e^{-n\Sigma_{i=0}^{3} p_q^i} \tag{5.14}$$

$$P_{0,0} = (1 - e^{-np_q^0} + e^{-(np_q^0 + \frac{1}{\mu_0})}) e^{-n\Sigma_{i=1}^{3} p_q^i} \tag{5.15}$$

$$P_{0,1} = (1 - e^{-\frac{1}{\mu_0}})(1 - e^{-np_q^1}) e^{-n(p_q^2 + p_q^3)} \tag{5.16}$$

$$P_{0,2} = (1-e^{-\frac{1}{\mu_0}})(1-e^{-np_q^2})e^{-np_q^3} \tag{5.17}$$

$$P_{0,3} = (1-e^{-\frac{1}{\mu_0}})(1-e^{-np_q^3}) \tag{5.18}$$

$$P_{1,f} = (1-e^{-\frac{1}{\mu_1}})e^{-n\Sigma_{i=1}^{3}p_q^i} \tag{5.19}$$

$$P_{1,0} = (1-e^{-\frac{1}{\mu_1}})(1-e^{-np_q^0})e^{-n\Sigma_{i=1}^{3}p_q^i} \tag{5.20}$$

$$P_{1,1} = (1-e^{-np_q^1}+e^{-(np_q^1+\frac{1}{\mu_1})})e^{-n(p_q^2+p_q^3)} \tag{5.21}$$

$$P_{1,2} = (1-e^{-\frac{1}{\mu_1}})(1-e^{-np_q^2})e^{-np_q^3} \tag{5.22}$$

$$P_{1,3} = (1-e^{-\frac{1}{\mu_1}})(1-e^{-np_q^3}) \tag{5.23}$$

$$P_{2,f} = (1-e^{-\frac{1}{\mu_2}})e^{-n\Sigma_{i=1}^{3}p_q^i} \tag{5.24}$$

$$P_{2,0} = (1-e^{-\frac{1}{\mu_2}})(1-e^{-np_q^0})e^{-n\Sigma_{i=1}^{3}p_q^i} \tag{5.25}$$

$$P_{2,1} = (1-e^{-\frac{1}{\mu_2}})(1-e^{-np_q^1})e^{-n(p_q^2+p_q^3)} \tag{5.26}$$

$$P_{2,2} = (1-e^{-np_q^2}+e^{-(np_q^2+\frac{1}{\mu_2})})e^{-np_q^3} \tag{5.27}$$

$$P_{2,3} = (1-e^{-\frac{1}{\mu_2}})(1-e^{-np_q^3}) \tag{5.28}$$

$$P_{3,f} = (1-e^{-\frac{1}{\mu_3}})e^{-n\Sigma_{i=1}^{3}p_q^i} \tag{5.29}$$

$$P_{3,0} = (1-e^{-\frac{1}{\mu_3}})(1-e^{-np_q^0})e^{-n\Sigma_{i=1}^{3}p_q^i} \tag{5.30}$$

$$P_{3,1} = (1-e^{-\frac{1}{\mu_3}})(1-e^{-np_q^1})e^{-n(p_q^2+p_q^3)} \tag{5.31}$$

$$P_{3,2} = (1-e^{-\frac{1}{\mu_3}})(1-e^{-np_q^2})e^{-np_q^3} \tag{5.32}$$

$$P_{3,3} = 1-e^{-np_q^3}+e^{-(np_q^3+\frac{1}{\mu_3})} \tag{5.33}$$

$$P_{h,h} = e^{-\frac{1}{\mu}}+(1-e^{-\frac{1}{\mu}})(1-e^{-n\Sigma_{i=0}^{3}p_q^i}) \tag{5.34}$$

$$P_{h,f} = (1-e^{-\frac{1}{\mu}})e^{-n\Sigma_{i=0}^{3}p_q^i} \tag{5.35}$$

$$\mu = \Sigma_{i=0}^{3}\mu_i \tag{5.36}$$

Given that SCH is free in the current SCI, it can be at one of the following states in the next SCI:

- S_f if no vehicle requested the channel (Equation 5.8).
- S_i if there is at least one Pv_i requesting the channel and no other provider with higher priority is requesting the same channel (Equations 5.9, 5.10, 5.11, 5.12).
- S_h if there is a transmission that cannot be decoded. This implies that there is at least one provider in 2-hop range using the channel, regardless of its priority (Equation 5.13).

Given that SCH is used by Pv_i in the current SCI, it can be at one of the following states in the next SCI:

- S_f if the current Pv_i releases the channel and no request is made by any provider (Equations 5.14, 5.19, 5.24, 5.29).
- S_i in case:
    1. the current Pv_i holds the channel while there are no requests from other providers or Pv_i releases the channel and there is at least another provider, having similar priority as Pv_i, requesting the channel while there are no requests from other providers with higher priorities (Equations 5.15, 5.21, 5.27, 5.33).
    2. the current Pv_i releases the channel and there is at least another provider requesting the channel:
        - having lower priority than Pv_i while there are no requests from other providers with higher priority (Equations 5.20, 5.25, 5.26, 6.20, 5.31, 5.32).
        - having higher priority than Pv_i (Equations 5.16, 5.17, 5.18, 5.22, 5.23, 5.28).

Given that SCH is at state S_h in the current SCI, it can be at one of the following states in the next SCI:

- S_h if the current provider keeps using the channel OR the current provider releases the channel and another provider in 2-hop range is using it (Equation 5.34).
- S_f if the current provider releases the channel and no other provider in 2-hop range is using it (Equation 5.35).

After computing the transition probabilities of all possible states based on SCHs current state, Pv_i predicts the state of each channel in the next SCI as follows:

$$\begin{aligned} S_{m,j} &= argmax \quad P_{m,j} \\ m, j &\in \{f, h, 0, 1, 2, 3\} \end{aligned} \tag{5.37}$$

5.3.3 SCH Selection

The final step is to select the least used service channel on which Pv_i can setup its WBSS. For that, Pv_i classifies SCHs, based on their predicted states, into six sets: S'_f, S'_h, S'_0, S'_1, S'_2, and S'_3. The subscript of each set denotes the predicted state. When selecting SCH, preference is always given to channels in S'_f. If $S'_f = \{\emptyset\}$, channels in S'_j, with $j < i$, are considered. In case $S'_{j<i} = \{\emptyset\}$, we make providers wait till a service channel becomes available. Note that instead of randomly choosing a channel in a set $S'_{j<i}$, we select the channel with the lowest score. This is rational since a low score can imply that the provider using SCH has fewer data packets to send. As a result, Pv_i has higher chances of transmitting its data packets, lowering therefore the delay to setup its WBSS. Observe that we did not solicit SCHs in S'_j with $j = i$ and $j > i$ in order to avoid causing collisions to providers with same or higher priority. Observe also that SCHs in S'_h are not considered in order to reduce the possibilities of enduring the hidden terminal problem, thus enhancing the service quality of Pv_i.

5.3.3.1 WBSS Overlapping Problem

It might happen that two providers (Pv_A and Pv_B in Figure 5.4), located within 2-hop range, select the same SCH to establish their WBSS. This will result in overlapping WBSS, with Pv_A and Pv_B unaware of this situation, leading to data collisions.

To tackle this problem, ASSCH uses a mechanism similar to the Channel Collision Warning (CCW) described in [22]. Indeed, when vehicles U_1 and U_2 in Figure 5.4 receive WSAs from Pv_A and Pv_B reserving the same SCH, they broadcast a warning message, labeled *Overlapping SCH Notification* $(OSCHN)$. OSCHN contains the SCH

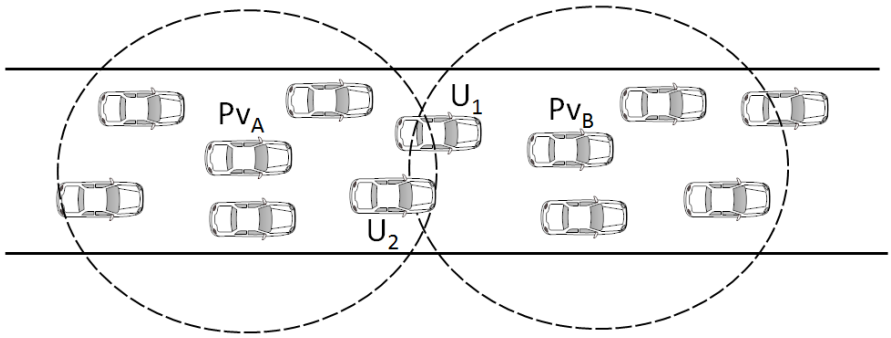

Figure 5.4: WBSS overlapping problem

in question along with the identifier and the priority of the provider which will keep the channel, selected based on the following rules:

1. In case Pv_A and Pv_B have different priorities, the provider with the highest priority will keep the channel.
2. In case Pv_A and Pv_B have the same priority, the first provider to broadcast WSA will keep the channel.

Assume that Pv_A is the one to keep SCH as it has higher priority. Since both U_1 and U_2 detect the overlapping problem, both will try to send *OSCHN*, leading probably to collision. To avoid such a scenario, both vehicles wait for a time interval before transmitting OSCHN, computed as follows:

$$t_i = \left(\frac{|d - d'|}{max(d, d')} \right) + \gamma \tag{5.38}$$

where d and d' are distances between the current vehicle and Pv_B and Pv_A, respectively. γ is a randomly generated time offset to break the tie when Pv_B and Pv_A are of equal distance to the current vehicle. Equation 5.38 indicates that the closest vehicle to the provider to select a new SCH (i.e., Pv_B) will be the first to transmit OSCHN, increasing therefore the probability of OSCHN successful delivery. Since U_1 is the closest vehicle to Pv_B, it will be the first to send OSCHN. When receiving $U_1's$ OSCHN, U_2, Pv_A, and Pv_B will react as follows:

– U_2 cancels its OSCHN transmission since it learns that it is not the closest vehicle

to Pv_B.

- Pv_A determines that its WSA was successfully transmitted and that it is entitled to use the selected SCH.
- Pv_B learns that the selected SCH is already reserved by Pv_A. Thus, it updates its CST (i.e., setting the state of the perviously selected SCH to occupied and the provider using it to Pv_A) and selects a new SCH.

To quickly handle WBSS overlapping problem, ASSCH assigns OSCHN messages higher priority than WSA messages. Bear in mind that our overlapping SCH notification mechanism is different from CCW [22] in two ways. First, ASSCH considers providers' priority and WSA generation time when deciding about which provider should keep SCH. Second, unlike CCW that relies only on providers to send warning messages, ASSCH impels all vehicles that detect an overlapping problem to get involved in notifying concerned providers. This makes ASSCH more immune against OSCHN message loss.

5.3.4 WBSS Termination

Amadeo et al. proposed a mechanism in [77] that enables users to detect non-persistent WBSS termination. Indeed, if no data frame is received during an entire SCI (see Fig. 5.5), users consider that WBSS has been terminated. Yet, this mechanism causes inefficient channel utilization as users keep the state of the channel as occupied for one additional SCI. To expedite the notification process, we add a *T-bit* flag to beacon messages to indicate WBSS termination (see Fig. 5.6). When a provider ends its WBSS, it sets *T-bit* flag to 1. When receiving the provider's beacon message, users check the *T-bit* value. If set to 1, it implies that WBSS was terminated. Hence, they leave it immediately and update their CSTs. If set to 0, users know that WBSS is still alive, keeping the state of the reserved SCH as occupied. Note that only beacons originated from providers are checked for *T-bit* since the same flag is always set to 0 for all other vehicles. To make the termination scheme more efficient, ASSCH gives higher priority to providers' beacon messages, allowing them to be transmitted first. This way, users as well as neighboring vehicles can quickly get notified, enabling them to update their

CSTs instantly, which will help reducing the waiting time to establish other WBSS.

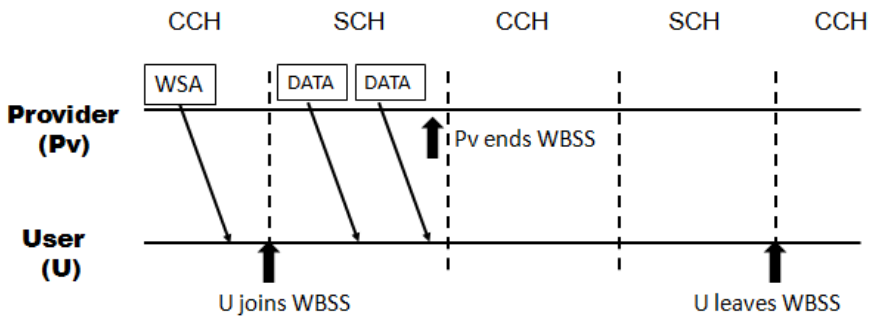

Figure 5.5: WBSS setup and termination according to Amadeo et al.

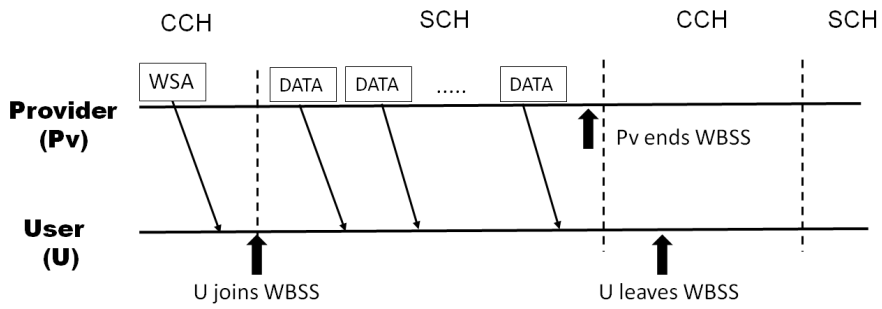

Figure 5.6: WBSS setup and termination according to ASSCH

5.4 Performance Evaluation

In this section, we present a simulation-based evaluation of ASSCH and compares it to CRaSCH [22], an allocation-based scheme that is closely related to our service channel selection mechanism. We also implemented a multi-transceiver ASSCH, called MASSCH, to simulate a prediction-based scheme in order to demonstrate the high performance of ASSCH. The IEEE 802.11p [47] standard is used as a basis for comparison.

5.4.1 Simulation Settings

We used OMNET++ [80] along with Veins [81] to implement the different schemes and deployed SUMO [72] to generate realistic traces for our VANET. The simulation setup is a one directional highway segment of 4000 meters with two lanes. Vehicle speed is uniformly distributed between 80 and 120 km/h, which is typical for a highway scenario. The Nakagami-m propagation model is used with the fading factor m set to 1.5 for short distance ($\leq$80 meters) between transmitters and receivers and decreases to $m = 0.5$ for longer distances ($>$80 meters) [81]. Other parameters are listed in Table 5.I.

Table 5.I: Simulation Parameter Settings

Parameter	Value
Data rate	6 Mbps
λ_a	1 vehicle/s
λ_b	10 beacons/s
α	2
P_t	20 mW
P_{th}	3.162e-13 W
ρ	0.5
Antenna height	1.5 m
$G_t = G_r$	1
μ_2, μ_3 (in seconds)	7, 6
p_q^2, p_q^3	0.01, 0.02

We simulated an application that allows local sharing of two types of files: 1) a 5 seconds video file at 20 fps, where each frame is 320×240 with 16.7 million colors; and 2) a 30 seconds audio file with 2 channels, 16-bit bit depth, and a sample rate of 44.1 KHz. Once providers reach a specific point on the highway, they randomly choose the type of service to offer (i.e., audio or video), and then trigger the SCH selection scheme to choose the least used SCHs. When receiving WSA, interested vehicles join WBSS. Once SCI begins, providers start transmitting their data packets. Four metrics were used to assess the performance of the simulated schemes:

– Prediction accuracy rate: the rate of successfully estimating SCHs state by a

provider over its time travel on the highway segment.

– Average capture delay (ACD): the delay experienced by providers to establish WBSS. It is defined as the elapsed time between the moment providers send WSA messages and the moment their first data packet is transmitted. It indicates how well the different schemes handle service differentiation.
– Overlapping SCI (OSCI): the number of SCIs during which two or more providers initiate WBSS over the same SCH. This metric evaluates how the different schemes cope with the WBSS overlapping problem.
– Average throughput: the amount of data bits transmitted over a time period.

5.4.2 Simulation Results

5.4.2.1 Prediction Accuracy Rate

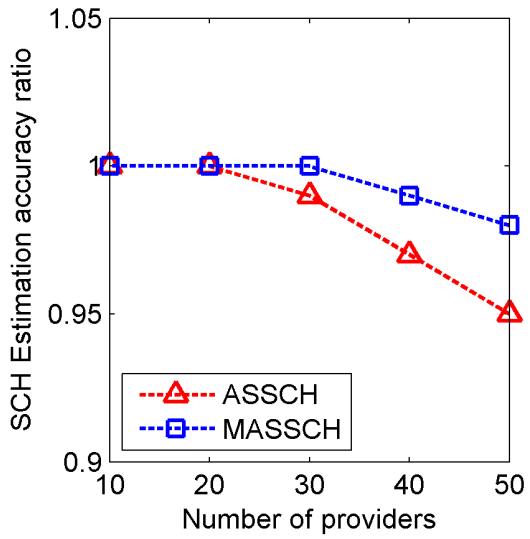

Figure 5.7: Prediction accuracy rate vs. Number of providers

Figure 5.7 shows the prediction accuracy rate for ASSCH and MASSCH (i.e. they are the only simulated schemes to predict the state of SCHs in the future). We observe that as the number of providers increases, the prediction accuracy slightly decreases. MASSCH marginally outperforms ASSCH thanks to the use of multiple transceivers

(i.e., 1 for CCH and five for SCHs), allowing it to continuously monitor SCHs. This offers a better estimation of channels state, making its SCH selection mechanism more accurate. Even though ASSCH only uses one transceiver, its accuracy estimation of SCHs state matches that of MASSCH (i.e., only 3% less than MASSCH when the number of providers in the network is set to 50 and only 1.4% less on average). The reason is twofold: 1) ASSCH not only uses CSTs, but also compels providers to acquire real-time SCHs state information during SCI, using monitors; and 2) ASSCH disseminates SCHs state information using beacon messages, allowing CSTs to be updates periodically, therefore reducing the impact of WSA collisions.

5.4.2.2 Average Capture Delay

Figure 5.8 shows ACD variation with the number of providers. We observe that ACD of all schemes increases with the increase of providers' density. IEEE 802.11p generates the lowest delay for both audio and video services. This is because vehicles lack 2-hop visibility (i.e., they only keep track of used SCHs in 1-hop range), relaxing therefore the spatial SCH reuse policy (i.e., even if providers are within carrier sense range, they can still use the same SCH, regardless of their priority). MASSCH outperformed ASSCH and CRaSCH since it uses multiple transceivers. ASSCH experiences lower ACD compared to CRaSCH (e.g., when the number of providers is set to 50, ASSCH incurs ACD that is 11% and 89% lower than CRaSCH for video and audio services, respectively). The reason is threefold: 1) ASSCH gives preference to providers with high priority when selecting SCHs as well as when solving WBSS overlapping problem (i.e., the provider with the highest priority is always the one to keep SCH). Unlike ASSCH, CRaSCH does not differentiate between traffic flows, which explains why the video service incurred lower ACD compared to the audio service; 2) ASSCH uses beacon messages, instead of WSA, to disseminate CSTs. This helps vehicles maintain up-to-date CSTs even when collisions involving WSA messages occur, allowing for better selection decisions; and 3) ASSCH uses the WBSS termination mechanism, allowing vehicles to get notified rapidly. This way, more SCHs can be made available for new providers to choose from. Observe that when the number of providers is set to 50, ASSCH provides ACD that is

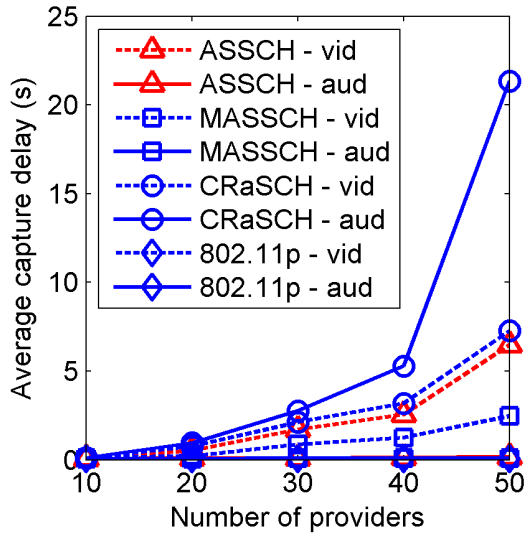

Figure 5.8: Average capture delay vs. providers' density

62% and 34% higher than the one incurred by MASSCH for video and audio services, respectively. This is a tiny price to pay given the cost savings that can be achieved.

5.4.2.3 Overlapping SCIs

Figure 5.9 shows the number of overlapping SCI with respect to the number of providers in the network. We observe that OSCI for all schemes increases with the increase in the number of providers. As expected, MASSCH outperforms all the schemes due to its ability to quickly detect hidden terminals. ASSCH deals better with the overlapping WBSS problem compared to CRaSCH. For instance, in a network with 50 providers, ASSCH experiences OSCI that is 44% and 84% lower than that experienced by CRaSCH for video and audio services, respectively. The reason is that ASSCH compels all vehicles that detect SCH overlapping problem to get involved in notifying the conflicting providers. This gives ASSCH a better network visibility, allowing it to closely match the performance of MASSCH (i.e, 17% and 41% higher than MASSCH for video and audio services, respectively, when the number of providers is set to 50). IEEE 802.11p generates the highest OSCI as it lacks a mechanism to address the overlapping WBSS problem and relies only on received WSAs to keep track of used SCHs.

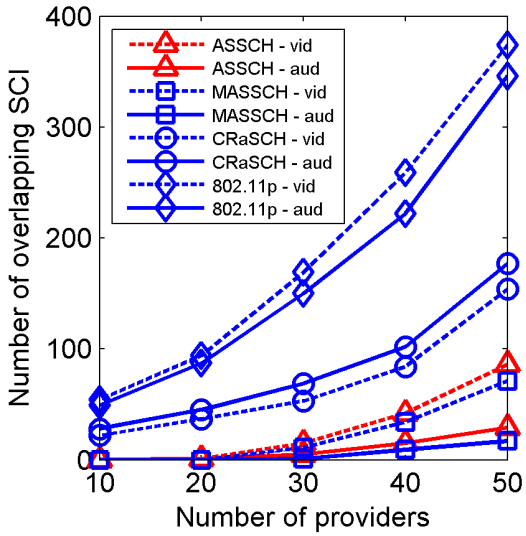

Figure 5.9: Overlapping SCIs vs. number of providers

5.4.2.4 Average Throughput

Figures 5.10(a) and 5.10(b) depict the average throughput and the collision rate (CR) of all schemes as a function of the number of providers. We observe that CR increases as the providers' density increases, implying throughput's drop. Here again, MASSCH outperforms all the schemes thanks to its ability to quickly detect hidden terminals, making it resilient to packet losses. Also, IEEE 802.11p has the worst performance as it lacks 2-hop visibility, making it prone to the hidden terminal problem. ASSCH incurs CR that is 81% and 7% lower than that of CRaSCH for audio and video services, respectively. This is because: 1) like MASSCH, ASSCH can avoid selecting SCHs suffering the hidden terminal problem thanks to the use of monitors during SCI; 2) giving preference to high priority providers (i.e., audio service) to establish their WBSS first implies efficient SCH utilization. Indeed, SCHs used by high priority providers are not solicited during SCH selection, avoiding therefore unnecessary contention. This yields higher throughput (i.e., data packets are transmitted in a short period of time) and lower packet loss (i.e., low collision probability). Low priority providers, however, might share SCHs with high priority providers (i.e., when the remaining SCHs are occupied by high priority providers). Consequently, they endure frequent contention phases, which might

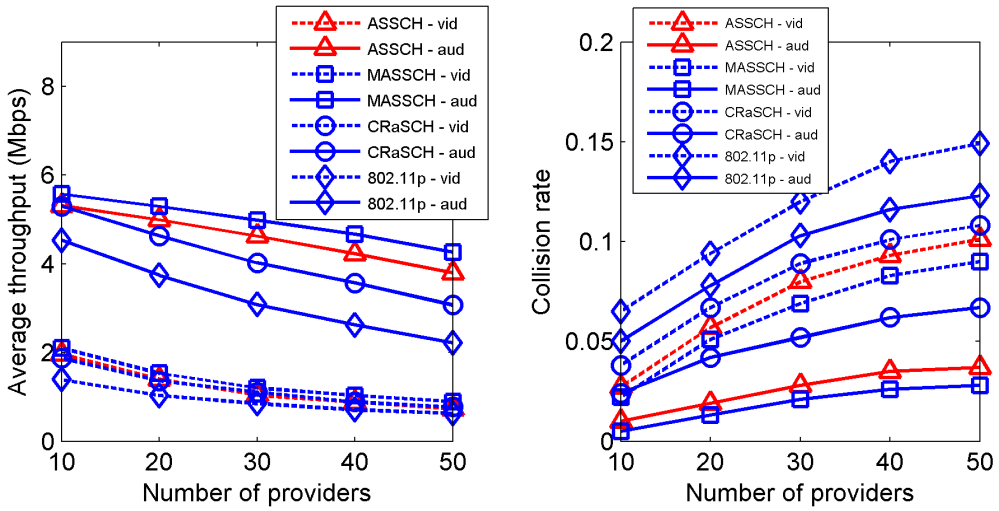

(a) (b)

Figure 5.10: Average throughput and collision rate vs. providers' density

increase their collision probability. This explains the low throughput of ASSCH-vid compared to CRaSCH-vid (i.e., CRaSCH allows one WBSS per SCH); and 3) updating CSTs periodically makes freshly released SCHs quickly available to be exploited by new providers. Observe again that ASSCH performed nearly as good as MASSCH since this latter incurs CR that is only 14.5% and 3.6% lower than that of ASSCH for audio and video services, respectively, when the number of providers is set to 50.

5.5 Chapter Summary

In this chapter, we proposed ASSCH, a hybrid single-transceiver SCH selection mechanism that seeks to enhance the service quality of V2V infotainment applications. ASSCH makes use of WSA and beacon messages as well as cooperation among vehicles in order to update CSTs. These CSTs allow providers to select the least used SCHs to establish WBSS. Furthermore, using the WBSS termination mechanism, ASSCH informs users immediately to leave terminated WBSS and update their CSTs accordingly. Simulation results show that ASSCH outperforms existing allocation-based schemes and performs as good as prediction-based schemes since it allows for quicker access to service channels, handles the overlapping WBSS problem better, and incurs high through-

put. Therefore, ASSCH can be a good candidate for service channel selection for V2V infotainment applications (e.g., media sharing, weather forecast, traffic statistics dissemination), particularly during the initial deployment of VANET, as multi-transceiver vehicles might not be widely popular [35].

CHAPTER 6

IEEE 802.11P EDCA PERFORMANCE ANALYSIS FOR INFOTAINMENT APPLICATIONS

This chapter tackles the issue of accurately modeling the IEEE 802.11p EDCA mechanism for infotainment applications. Most existing schemes were designed for safety applications and do not consider all the factors that can affect EDCA performance (i.e., queue saturation condition, backoff procedure, and internal/external collisions). It this regard, two stochastic models are proposed which take into account all EDCA major factors. The first model describes two Markov chains that are used to compute the transmission probability and the probability of collision of each AC, from which an accurate throughput model is derived. The second model extends the first one by taking into account the transmission opportunity (TXOP), unexploited in IEEE 802.11p, in order to enhance the performance of infotainment applications, throughput in particular. Simulation results are provided to demonstrate the accuracy of the proposed analytical models.

The remainder of this chapter is organized as follows. Section 6.1 gives an overview of the IEEE 802.11p EDCA mechanism. Section 6.2 presents the assumptions made as well as the notations used for both models. Section 6.3 describes the first proposed model along with simulation results. The same goes with Section 6.4 which describes the second proposed model. Finally, Section 6.5 concludes the paper.

6.1 IEEE 802.11p EDCA Overview

Like IEEE 802.11e [82], IEEE 802.11p uses the EDCA mechanism to support different levels of quality of service. Indeed, four access categories (ACs) are defined, each having its own parameters, i.e., minimum contention window (CW_{min}), maximum contention window (CW_{max}), and arbitration inter-frame space number ($AIFSN$). Yet, unlike IEEE 802.11e, IEEE 802.11p sets TXOP to 0 for all ACs, implying that ACs shall send only one packet per channel access.

When AC_i ($i = 0, 1, 2, 3$, with 0 as the highest priority) has a packet to send, it senses the channel first. If the channel is sensed idle for at least an Arbitrary Inter-Frame Spacing ($AIFS_i$), the packet can be transmitted.

$$AIFS_i = AIFSN_i \times T_s + SIFS \tag{6.1}$$

T_s designates the duration of a time slot while $SIFS$ represents the length of the Short Inter-Frame Space. If the channel is sensed busy, AC_i continues sensing the channel. When it becomes idle and stays idle for $AIFS_i$, AC_i invokes the backoff procedure. To this end, AC_i selects a backoff counter k between 0 and CW_i, where CW_i is set to CW_{min_i} at the beginning. Whenever the channel is sensed idle, k is decremented. Otherwise, k is stopped at its current value. AC_i resumes decrementing k only when it senses that the channel has been idle for at least $AIFS_i$. When k reaches 0 and the channel is sensed busy, AC_i invokes the backoff procedure without changing the value of CW_i. Otherwise (i.e., channel is idle), AC_i transmits its packet.

Upon failing to receive an acknowledgment frame (ACK) on time, AC_i concludes that its previous transmission was unsuccessful and will attempt to retransmit the packet. At each retransmission, CW_i is doubled and a new backoff procedure is invoked. When CW_i reaches CW_{max_i}, AC_i uses CW_{max_i} for the upcoming retransmissions. When the retransmission limit r_i is reached, the packet is dropped and CW_i is reset to CW_{min_i}.

To accurately analyze the performance of IEEE 802.11p EDCA, we will consider all the factors described in Section 3.3. This includes the number of ACs considered, the AC queue condition, the backoff procedure, the backoff counter freezing, the busy channel at zero, and the internal and external collisions. To the best of our knowledge, none of the proposed models [36–40] have considered all of these factors.

6.2 Assumptions and Notations

Like most related work, i.e., [37–41, 83], we assume that ACs have the same collision probability for different transmissions. We also assume that packets are dropped only due to collisions. The notations used in both models are summarized in Table 6.I.

Table 6.I: Notations' definition

Notation	Definition
CW_j^i	Contention window size of AC_i at backoff stage j
m_i	The backoff stage where $CW_m^i = CW_{max}^i$
p_b	Probability of a busy channel in a slot
p_{c_i}	Collision probability of AC_i in a slot
τ_i	Transmission probability of AC_i
p_{s_i}	Probability of successful transmission for AC_i
p_{f_i}	Probability of $TXOP_i$ not yet expired
T_L	Transmission time of a packet of size L
$\overline{T_i}$	Average expected time spent at all states by AC_i

Each state in the Markov chain, modeling the backoff procedure, is represented by a pair of integers (j,k), where j denotes the backoff stage while k designates the backoff counter. j is initiated to 0 and is incremented by 1 whenever a collision occurs. When j reaches r_i, the packet is dropped if a collision happens, and j is reset to 0. k is initialized to a value uniformly distributed between $[0, CW_j^i]$ and is decremented by 1 whenever the channel is sensed idle in a slot. CW_j^i is computed as follows:

$$CW_j^i = \begin{cases} CW_{min}^i + 1, & \text{if } j = 0 \\ 2^j CW_0^i, & \text{if } 1 \leq j \leq m_i - 1 \\ CW_{max}^i + 1, & \text{if } m_i \leq j \leq r_i \end{cases} \tag{6.2}$$

After each successful transmission or packet drop, AC_i shall invoke the backoff procedure with backoff stage $j = 0$ [47]. We label this as post-backoff procedure. In case no packets were queued at the end of the post-backoff phase, AC_i keeps silent. It will contend for the channel again once it has packets to be transmitted.

6.3 IEEE 802.11p EDCA Performance Analysis Model

6.3.1 Probability of Transmission

Figure 6.1 illustrates the 2-D Markov chain describing the backoff procedure of AC_i.

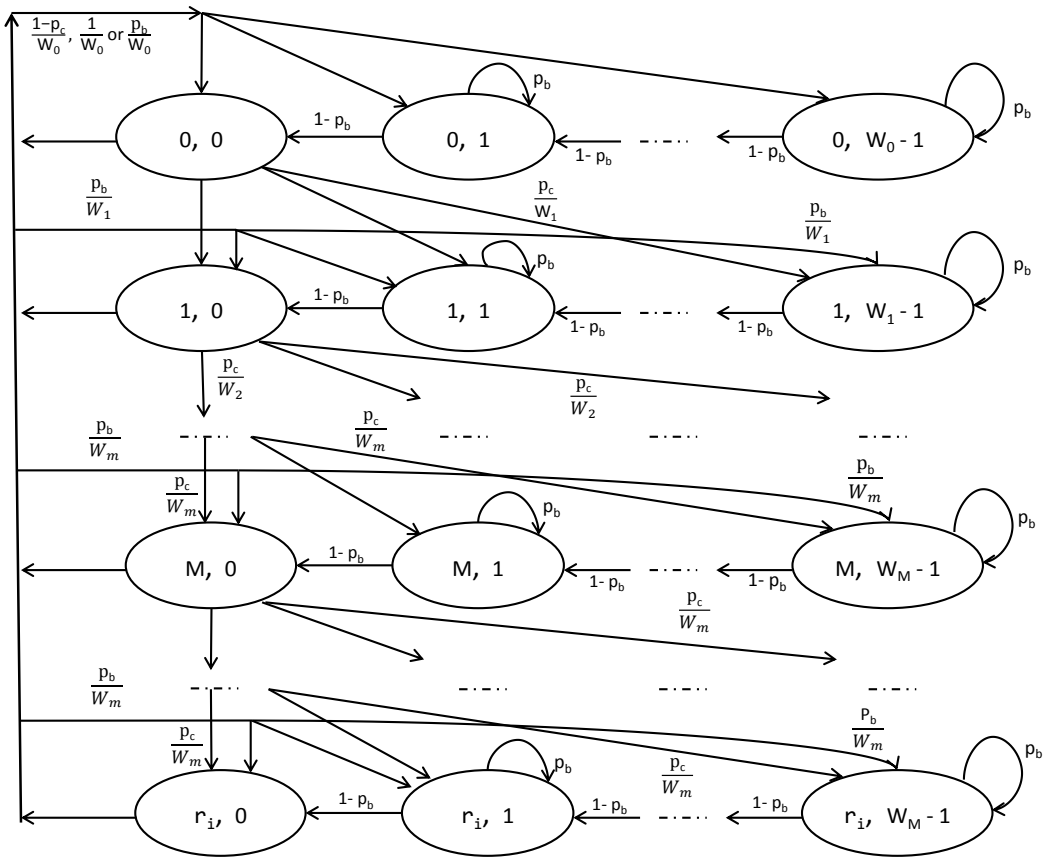

Figure 6.1: The Markov chain modeling the backoff procedure of AC_i

The transition probabilities of the Markov chain are expressed as follows:
For $0 < k \leq CW_j^i - 1$ and $0 \leq j \leq r_i$

$$P(j,k|j,k) = p_b \tag{6.3}$$

$$P(j,k-1|j,k) = 1 - p_b \tag{6.4}$$

For $0 \leq k \leq CW_j^i - 1$ and $0 \leq j \leq r_i$

$$P(0,k|j,0) = \frac{1-p_{c_i}}{W_0^i} \tag{6.5}$$

$$P(0,k|r_i,0) = \frac{1}{W_0^i} \tag{6.6}$$

$$P(j,k|j-1,0) = \frac{p_{c_i}}{W_j^i} \tag{6.7}$$

$$P(j,k|j,0) = \frac{p_b}{W_j^i} \tag{6.8}$$

During the backoff process, k is stopped at its current value whenever the channel is sensed busy, as indicated by Equation 6.3. Otherwise, k is decremented by 1 according to Equation 6.4. Equation 6.5 accounts for the situation where the previous packet is successfully transmitted and the post-backoff procedure is invoked. Equation 6.6 implies that the post-backoff procedure is invoked after r_i is reached, regardless of the status of the previous packet (i.e., either successfully transmitted or dropped). Equation 6.7 reveals that whenever a collision occurs, the backoff procedure is invoked with the backoff stage j incremented by 1. Finally, Equation 6.8 specifies that when $k = 0$ and the medium is sensed busy, the backoff procedure is invoked while keeping the same value of j.

Using the Markov chain illustrated in Figure 6.1, a transmission occurs when $k = 0$ and the channel is sensed idle. Therefore, we have:

$$\tau_i = (1-p_b)\sum_{j=0}^{r_i} b(j,0) \tag{6.9}$$

where $b(j,0)$ denotes the stationary probability of state $(j,0)$. Using Equation 6.7, we can express $b(j,0)$ for $1 \leq j \leq r_i$ as follows:

$$b(j,0) = b(j-1,0)p_{c_i} \tag{6.10}$$

By recurring Equation 6.10, we have:

$$\sum_{j=0}^{r_i} b(j,0) = b(0,0) \sum_{j=0}^{r_i} p_{c_i}^j \tag{6.11}$$

Since the sum of all states in the Markov chain equals to one, we have:

$$\sum_{j=0}^{r_i} \sum_{k=0}^{W_j^i-1} b(j,k) = 1 \tag{6.12}$$

By recurring Equations 6.5- 6.8 and Equation 6.10 for $0 < j \leq r_i$, we obtain:

$$\sum_{k=0}^{W_1^i-1} b(j,k) = \frac{(W_j^i - 1) p_{c_i}^j (1+p_b) b(0,0)}{2(1-p_b)} + b(j,0) \tag{6.13}$$

For $j = 0$, and using Equations 6.5- 6.8 and Equation 6.10, we get:

$$\sum_{k=0}^{W_0^i-1} b(0,k) = \frac{(W_0^i - 1)(1+p_b) b(0,0)}{2(1-p_b)} + b(0,0) \tag{6.14}$$

Combining Equations 6.13 and 6.14, we can compute $b(0,0)$ as follows:

$$b(0,0) \;=\; \frac{2(1-p_b)}{1+p_b} \left[W_0^i \sum_{j=0}^{m-1} 2^j p_{c_i}^j \;+\; W_m^i \sum_{j=m}^{r_i} p_{c_i}^j \;-\; (1 \;-\; 2p_b) \sum_{j=0}^{r_i} p_{c_i}^j \right]^{-1} \tag{6.15}$$

Hence,

$$\tau_i \;=\; \frac{2(1-p_b)^2 \sum_{j=0}^{r_i} p_{c_i}^j}{1+p_b} \left[W_0^i \sum_{j=0}^{m-1} 2^j p_{c_i}^j + W_m^i \sum_{j=m}^{r_i} p_{c_i}^j - (1 - 2p_b) \sum_{j=0}^{r_i} p_{c_i}^j \right]^{-1} \tag{6.16}$$

6.3.2 Probability of Collision

Now, we need to compute the probability of collision p_{c_i} of AC_i. Equation 6.1 shows that $AIFS_i$ depends only on $AIFSN_i$ since $SIFS$ is similar for all ACs. According to [47], the default values of $AIFSN$ for AC_0, AC_1, AC_2 and AC_3 on SCHs are $2, 3, 6$, and

9, respectively (see Section 2.2.2). Given these values, four contention zones (z_j, $j = 1,2,3,4$) can be identified, as illustrated in Figure 6.2. Different ACs contend in different zones. For example, in z_1, only AC_0 is allowed to contend for the channel while in z_2, AC_0 and AC_1 can attempt to transmit. In z_4, all ACs can attempt to access the medium. Let N_s^j denotes the number of slots in the j^{th} contention zone. Based on Figure 6.2, the number of slots in each zone is $N_s^1 = 1$, $N_s^2 = 3$, $N_s^3 = 3$, and $N_s^4 = \infty$.

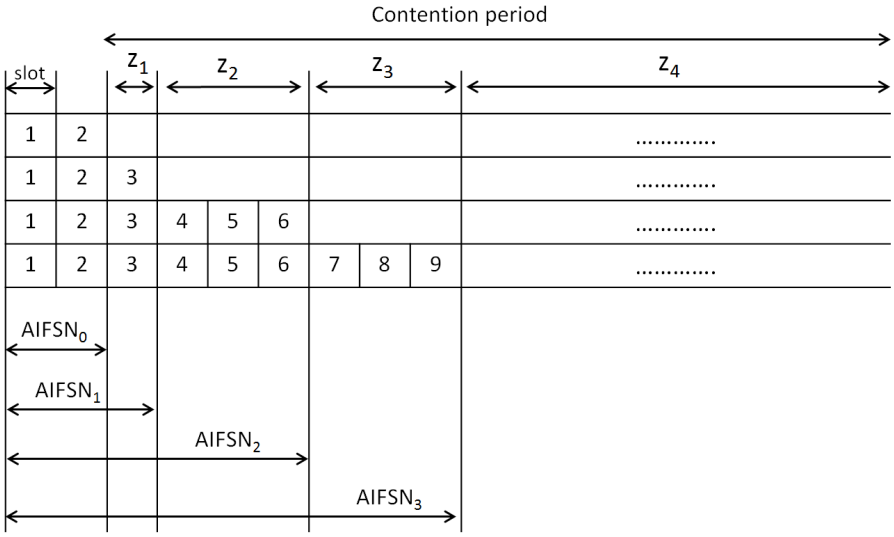

Figure 6.2: Contention zones for the different ACs

To describe the contention phase after a busy period, we adopt the model presented in [39, 40]. In this model, the slots involved in the contention phase (i.e., after $AFISN_0$) represent the states of the Markov chain (see Figure 6.3). The transition from the current state to the next is carried out when the channel is sensed idle. Otherwise, the current state transits to state 1. Therefore, the transition probabilities of the Markov chain illus-

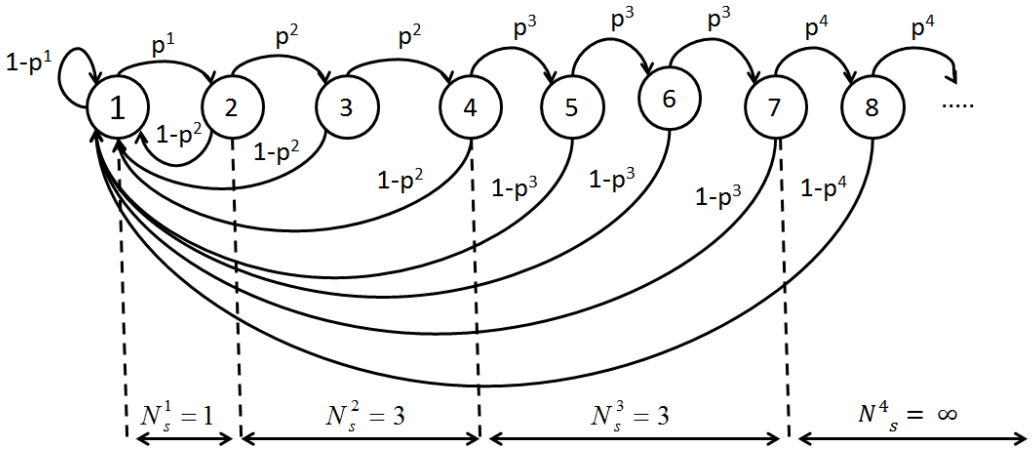

Figure 6.3: The Markov chain modeling the contention phase of AC_i

trated in Figure 6.3 are expressed as follows:

$$\begin{cases} P(s+1|s) = p^1,\ P(1|s) = 1-p^1 & 1 \le s \le N_s^1 \\ P(s+1|s) = p^2,\ P(1|s) = 1-p^2 & s \ge N_s^1 \\ P(s+1|s) = p^3,\ P(1|s) = 1-p^3 & x_1+1 \le s \le x_2 \\ P(s+1|s) = p^4,\ P(1|s) = 1-p^4 & s \ge x_2+1 \end{cases} \tag{6.17}$$

where $x_1 = N_s^1 + N_s^2$ and $x_2 = x_1 + N_s^3$. AC_i will transit from one state to another in a zone, i.e., from the current slot to the next one, if no transmission is carried over the current slot. Therefore, we have:

$$p^j = \prod_{i<j}(1-\tau_i)^{N_i} \quad j = 1,2,3,4 \tag{6.18}$$

where N_i designates the number of contending stations having AC_i.

Let p_s^s be the stationary probability of state s. Using the Markov chain in Figure 6.3,

we obtain:

$$p_s^{s+1} = \begin{cases} p_s^s.p^1, & 1 \leq s \leq N_s^1 \\ p_s^s.p^2, & N_s^1 + 1 \leq s \leq N_s^2 \\ p_s^s.p^3, & x_1 + 1 \leq s \leq x_2 \\ p_s^s.p^4, & s \geq x_2 \end{cases} \tag{6.19}$$

Since the sum of the stationary probabilities in a Markov chain equals 1, we get:

$$p_s^1 = \left[\frac{1-(p^1)^{N_s^1}}{1-p^1} + (p^1)^{N_s^1} \frac{1-(p^2)^{N_s^2}}{1-p^2} + (p^1)^{N_s^1}(p^2)^{N_s^2} \frac{1}{1-(p^3)^{N_s^3}} + (p^1)^{N_s^1}(p^2)^{N_s^2}(p^3)^{N_s^3} \frac{1}{1-p^4} \right]^{-1} \tag{6.20}$$

The stationary probability of a zone can be defined as the sum of the stationary probabilities of all states in the zone [39, 40]. Therefore:

$$p_z^1 = \sum_{s=1}^{N_s^1} p_s^s, \quad p_z^2 = \sum_{s=N_s^1+1}^{N_s^2} p_s^s, \quad p_z^3 = \sum_{s=x_1+1}^{x} p_s^s, \quad p_z^4 = \sum_{s=x_2+1}^{\infty} p_s^s \tag{6.21}$$

The collision probability of AC_i in zone z_j (i.e., $p_{c_i}^{z_j}$) is equivalent to the probability that when AC_i has a packet to transmit in a slot, there is at least another $AC_{i'}$ that has a packet to transmit in the same slot. $AC_{i'}$ can be of the same or different priority than AC_i. Thus, $p_{c_i}^{z_j}$ can be expressed as:

$$p_{c_i}^{z_j} = \begin{cases} 1 - \prod_{i'<i}(1-\tau_{i'})^{N_{i'}}.\prod_{i\leq i'<j}(1-\tau_{i'})^{N_{i'}-1}, & i < j \\ 0, & i \geq j \end{cases} \tag{6.22}$$

Hence, the collision probability of each AC_i can be computed as:

$$p_{c_i} = \frac{\sum_{i\leq j} p_z^j p_{c_i}^{z_i}}{\sum_{i\leq j} p_z^j} \tag{6.23}$$

Now we need to quantify p_b. Since p_b is the probability that the channel is busy in a slot, it is simply the probability that at least one station is using the channel in that slot.

$$p_b = 1 - \sum_{j=1}^{4} p_z^j p^j \tag{6.24}$$

By solving equations 6.16, 6.22, and 6.23, we obtain the probabilities of transmission and collision of each AC. These quantities are then used to derive the normalized throughput for each AC.

6.3.3 Normalized Throughput

Let D_i designates the normalized throughput of AC_i. We define D_i as the fraction of time used by AC_i to successfully transmit a packet from the average expected time that it spends in all the states. Therefore, we have:

$$D_i = \frac{p_{s_i} T_L}{\overline{T_i}} \tag{6.25}$$

Let $p_{s_i}^{z_j}$ designates the probability of successful transmission of AC_i in zone z_j. $p_{s_i}^{z_j}$ is equivalent to the probability that when AC_i is transmitting in a slot in z_j, no other $AC_{i'}$ has packets to transmit. Again, $AC_{i'}$ can have the same or different priority than AC_i. Therefore, $p_{s_i}^{z_j}$ can be expressed as:

$$p_{s_i}^{z_j} = \begin{cases} N_i \tau_i \prod_{i \le i' < j} (1-\tau_{i'})^{N_{i'}-1} \prod_{i' < i} (1-\tau_{i'})^{N_{i'}}, & i < j \\ 0, & i \ge j \end{cases} \tag{6.26}$$

Hence,

$$p_{s_i} = \sum_{j=1}^{4} p_z^j p_{s_i}^{z_j} \tag{6.27}$$

The Markov chain in Figure 6.1 shows that $\overline{T_i}$ is not fixed as it depends on the channel's state (i.e., idle or busy). The channel is idle in a slot when no transmission is carried out; therefore, the duration of the idle state is T_s. A busy channel in a slot, however, can

be interpreted in two ways: successful transmission or collision. Thus, we have:

$$\overline{T_i} = (1 - p_b)T_s + p_{s_i}T_{suc} + (p_b - p_{s_i})T_c \tag{6.28}$$

where T_{suc} and T_c are the durations of a successful transmission and a collision, respectively, and are expressed as follows:

$$\begin{cases} T_{suc} = AIFS_i + T_h + T_d + SIFS + T_{ACK} + 2\delta \\ T_c = AIFS_i + T_h + T'_d + \delta \end{cases} \tag{6.29}$$

where T_h, T_d, and T_{ACK} are the transmission times of the header, the payload, and the ACK frame, respectively; T'_d denotes the transmission time of the largest packet involved in the collision; and δ represents the propagation delay.

6.3.4 Performance Evaluation

To validate the accuracy of our model, we used OMNET++ [80] along with Veins [81] to simulate the IEEE 802.11p standard and we generated the mobility traces using SUMO [72]. Our simulation scenario represents a one-directional highway segment of length $4000m$ with 2 lanes. The vehicles' speed is uniformly distributed between 80 and 120 km/h. We use SCH 174 as the default service channel. Vehicles having packets to be transmitted are labeled as providers while vehicles receiving packets are labeled as users. When a Service Channel Interval (SCI) starts, providers contend for the channel to transmit fixed size UDP packets ($L = 512$ $bytes$). We used the Nakagami-m propagation model with $m = 1.5$ for short distance ($\leq$80 meters) between transmitters and receivers and $m = 0.5$ for longer distances ($>$80 meters) [81]. Other simulation parameters are listed in Table 6.II.

Table 6.II: 1^{st} Model Simulation Parameters

CW_{min}^0	3	CW_{max}^0	7
CW_{min}^1	3	CW_{max}^1	7
CW_{min}^2	7	CW_{max}^2	15
CW_{min}^3	15	CW_{max}^3	1023
r_i	7	T_s	13 μs
$SIFS$	32μs	Data rate	3 Mbps
Trans. power	20 mW	Sensitivity	-89 dBm

6.3.4.1 Simulation Results and Analysis

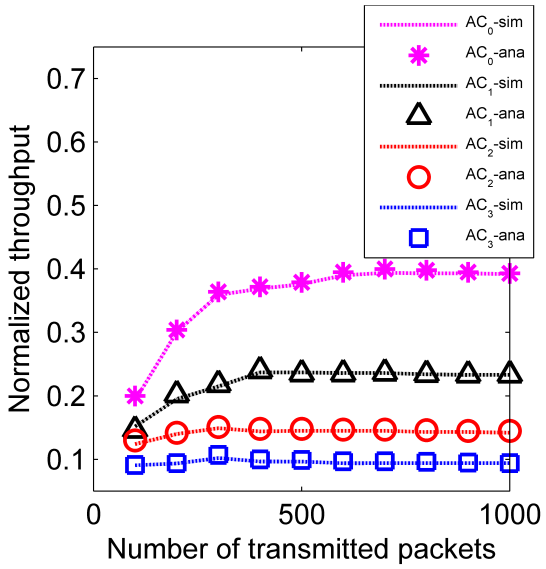

Figure 6.4: Normalized throughput vs. traffic load

Fig. 6.4 shows the normalized throughput for the different ACs as a function of traffic load. There are 4 providers, each having packets for a particular *AC*. All providers are within 1 hop-range, contending to transmit their packets. We observe that the results from the analytical model closely match those of the simulation. We also observe that the normalized throughput has the tendency to stabilize for all ACs as the traffic load in-

creases. This is because ACs have more packets buffered in their queues (i.e., saturation condition), implying that they will continually contend for the channel.

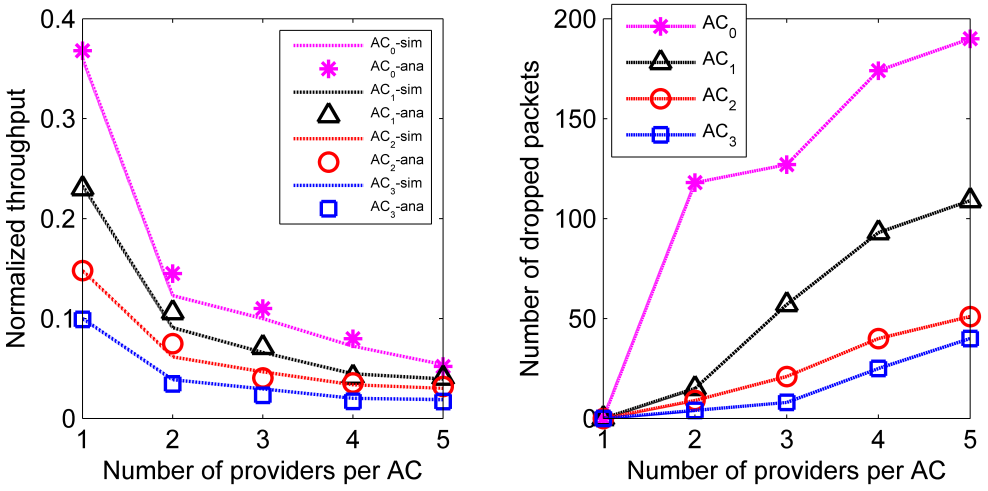

(a) (b)

Figure 6.5: Normalized throughput and success rate vs. number of providers

Fig. 6.5(a) shows the normalized throughput as a function of the number of providers in the network. In this scenario, providers have packets for all ACs and the number of packets to be transmitted is set to 500. Fig. 6.5(a) shows that simulation results are very close to the analytical results. Fig. 6.5(a) also shows that the normalized throughput quickly decreases, for AC_0 and AC_1 in particular, when the traffic load increases. The reason is twofold: 1) increasing the number of ACs in the network implies that more ACs will contend for the channel, leading to higher number of collisions (i.e., internal and external). Consequently, the probability of transmission τ_i decreases; and 2) increasing the number of ACs can lead to an increase in interferences originated from the hidden terminal areas, reducing therefore the normalized throughput.

To support our claim, we computed the number of dropped packets for all ACs; results are shown in Fig. 6.5(b). We observe that the number of dropped packets increases rapidly for AC_0 and AC_1 as the number of contending ACs increases. For instance, when only one provider has packets for AC_0, no packet is dropped; however, when five providers have packets for AC_0, the number of dropped packets reaches 190 (i.e., 38%

packet loss).

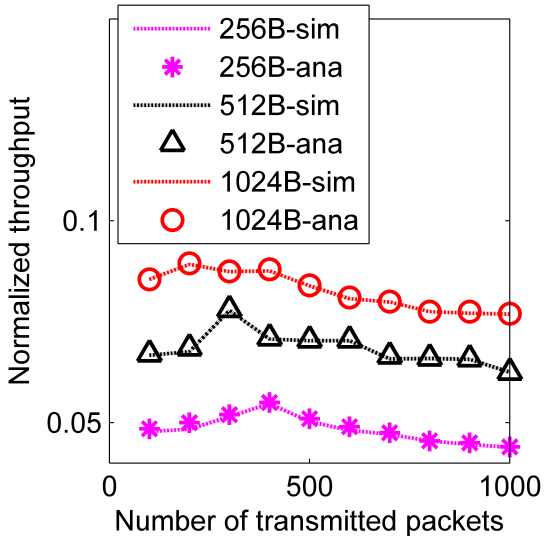

Figure 6.6: Normalized throughput vs. packet size

Finally, Fig. 6.6 depicts the impact of packet size on normalized throughput for AC_0. Results of the remaining ACs were not shown for the sake of clarity. Four providers contend for the channel. Each one of them has packets for all ACs. Here again, we observe that simulation results are very close to analytical results. Moreover, as traffic load increases, the normalized throughput of all packet sizes reaches a maximum value and starts decreasing. This is due to the increase of interfering traffic from hidden nodes as well as the increase in the number of collisions. Fig. 6.6 also demonstrates that the larger the packet size, the higher is the normalized throughput. This is because large packet sizes allow for the transmission of a high number of data bits compared to low packet sizes (e.g., 256 *bytes*), reducing therefore the time the channel is perceived as idle.

6.4 IEEE 802.11p EDCA Performance Model Considering TXOP

In this model, we study the impact of transmission opportunity (TXOP) on the performance of the IEEE 802.11p EDCA mechanism. We define TXOP as the time interval

during which ACs can send one or multiple frames when accessing the channel. It can be regarded as the maximum time ACs are allowed to hold the channel after winning a contention. We believe that by enabling high priority ACs (i.e., AC_0 and AC_1) to transmit more than one frame per channel access, we can enhance the throughput of infotainment applications.

The model proposed by Harigovindan et al. [41] is the only model in the literature that considers TXOP when analyzing the performance of IEEE 802.11p EDCA. However, a mathematical analysis of the backoff procedure was not presented and the busy channel at zero was not considered. Thus, in this section, we propose a Markovian model, which is an extension to the first proposed model, that takes TXOP into account. While the probability of collision will remain unchanged (i.e., as it is mainly dependent on AIFS), the probability of transmission as well as the normalized throughput will be modified to accommodate TXOP.

6.4.1 Probability of Transmission

Figure 6.7 illustrates the 2-D Markov chain describing the backoff procedure of AC_i when considering TXOP.

The state S_M represents the state where AC_i can send frames without contending for the channel as long as its TXOP is not yet expired. The transition probabilities of the Markov chain, other than the ones already stated in Section 6.3.1, are expressed as follows:

$$P(S_m|j,0) = p_{f_i}(1-p_{c_i}) \tag{6.30}$$

$$P(S_m|S_m) = p_{f_i} \tag{6.31}$$

$$P(0,k|S_m) = \frac{p_{f_i}p_{c_i}}{W_0} + \frac{1-p_{f_i}}{W_0} \tag{6.32}$$

If AC_i successfully transmits the first frame, it is allowed to transmit other frames, as long as $TXOP_i$ is not yet expired (Equation 6.30). Equation 6.31 accounts for the situation where AC_i stays at S_M as long as $TXOP_i$ holds, regardless of wether AC_i has frames to send or not. Finally, Equation 6.32 specifies that a backoff procedure is invoked when

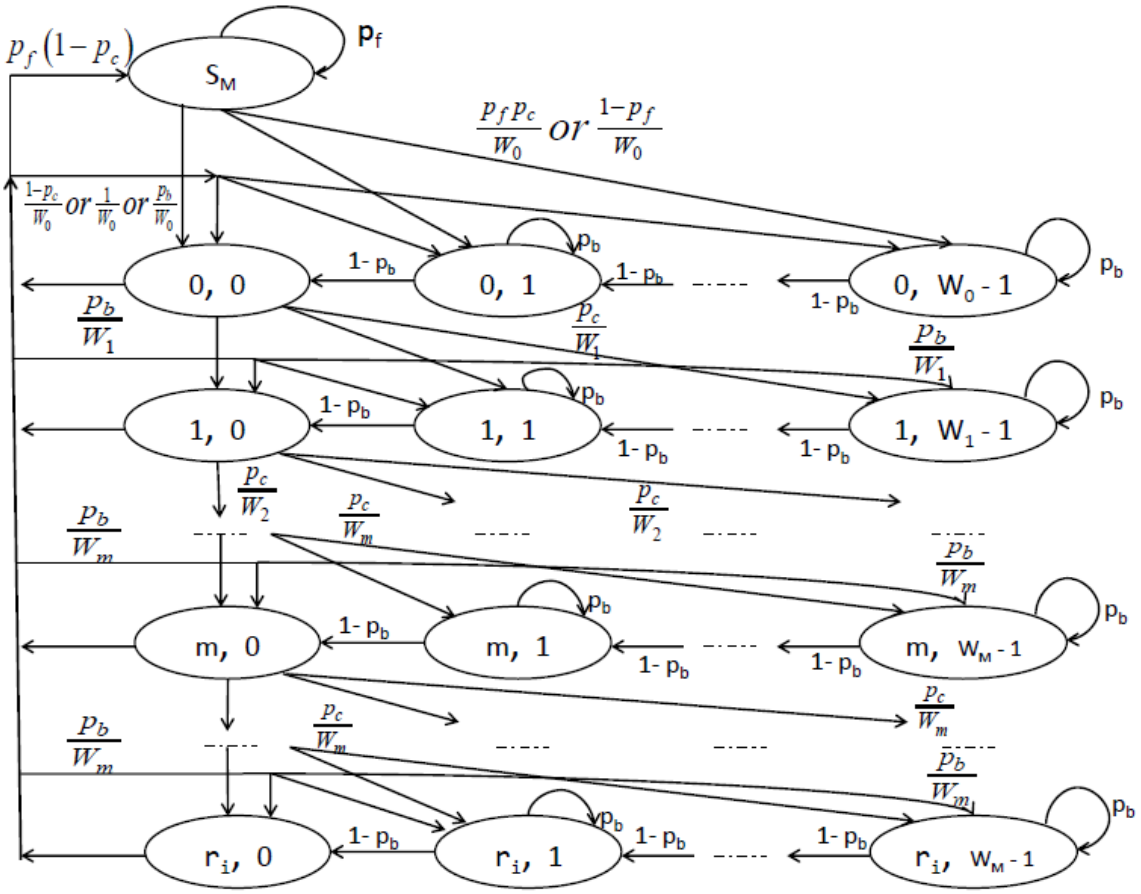

Figure 6.7: The Markov chain modeling the backoff procedure considering TXOP

AC_i is at S_M if: 1) a collision occurred while transmitting the current frame and $TXOP_i$ is not yet expired; or 2) $TXOP_i$ has expired (i.e., post-backoff procedure).

Using the Markov chain, illustrated in Figure 6.7, a transmission occurs when:

- $k = 0$ and the channel is sensed idle.
- AC_i is at state S_M and $TXOP_i$ is not yet expired.

Hence, we have:

$$\tau_i = b_{S_M} p_{f_i} + (1 - p_b) \sum_{j=0}^{r_i} b(j,0) \tag{6.33}$$

where b_{S_M} designates the stationary probability of state S_M and can be expressed as:

$$b_{S_M} = \frac{p_{f_i}}{1 - p_{f_i}} b(0,0) \tag{6.34}$$

We know that the sum of all states in the Markov chain equals to 1. Thus, we have:

$$b_{S_M} + \sum_{j=0}^{r_i} \sum_{k=0}^{W_j^i - 1} b(j,k) = 1 \tag{6.35}$$

For $j = 0$, and using Equations 6.5- 6.8, Equation 6.10 and Equation 6.32, we get:

$$\sum_{k=0}^{W_0^i - 1} b(0,k) = \frac{(W_0^i - 1)(1 + p_b) b(0,0)}{2(1 - p_b)} + \frac{(W_0^i - 1) p_{f_i} (1 - p_{f_i} + p_{f_i} p_{c_i}) b(0,0)}{2(1 - p_b)(1 - p_{f_i})} + b(0,0) \tag{6.36}$$

Combining Equations 6.13 and 6.36, we get:

$$\sum_{j=0}^{r_i} \sum_{k=0}^{W_j^i - 1} b(j,k) = \left[\sum_{j=0}^{r_i} (p_{c_i})^j + \frac{1 + p_b}{2(1 - p_b)} \left(W_0 \sum_{j=0}^{m-1} (2p_{c_i})^j + W_m \sum_{j=0}^{r_i} (p_{c_i})^j - \sum_{j=0}^{r_i} (p_{c_i})^j \right) + \frac{(W_0^i - 1) p_{f_i} (1 - p_{f_i} + p_{f_i} p_{c_i})}{2(1 - p_b)(1 - p_{f_i})} \right] b(0,0) \tag{6.37}$$

Using Equation 6.34 and Equations 6.35- 6.37, we have:

$$b(0,0) = \left[\sum_{j=0}^{r_i} (p_{c_i})^j + \frac{1 + p_b}{2(1 - p_b)} \left(W_0 \sum_{j=0}^{m-1} (2p_{c_i})^j + W_m \sum_{j=0}^{r_i} (p_{c_i})^j - \sum_{j=0}^{r_i} (p_{c_i})^j \right) + \frac{p_{f_i}}{1 - p_{f_i}} \left(1 + \frac{(W_0^i - 1)(1 - p_{f_i} + p_{f_i} p_{c_i})}{2(1 - p_b)} \right) \right]^{-1} \tag{6.38}$$

Thus,

$$\tau_i = \left[\sum_{j=0}^{r_i} (p_{c_i})^j + \frac{1 + p_b}{2(1 - p_b)} \left(W_0 \sum_{j=0}^{m-1} (2p_{c_i})^j + W_m \sum_{j=0}^{r_i} (p_{c_i})^j - \sum_{j=0}^{r_i} (p_{c_i})^j \right) + \frac{p_{f_i}}{1 - p_{f_i}} \left(1 + \frac{(W_0^i - 1)(1 - p_{f_i} + p_{f_i} p_{c_i})}{2(1 - p_b)} \right) \right]^{-1} \left[\frac{p_{f_i}}{1 - p_{f_i}} + \frac{(1 - p_b)(1 - (p_{c_i})^{r_i})}{1 - p_{c_i}} \right] \tag{6.39}$$

Now, we need to quantify p_{f_i}. p_{f_i} is the probability that AC_i with $TXOP_i$ has still

time to successfully transmit the current packet before $TXOP_i$ expires. $TXOP_i$ can be regarded as the time till the channel becomes free, given that it is used by AC_i. Clearly, $TXOP_i$ is independent of the time the channel has been used up to the current moment, implying the memoryless property. Therefore, p_{f_i} can be approximated by an exponential distribution with mean $TXOP_i$.

$$p_{f_i} = e^{-(\frac{1}{TXOP_i})} \tag{6.40}$$

6.4.2 Normalized Throughput

Let D_i designates the normalized throughput of an AC_i. We define D_i as the ratio of the payload transmitted by AC_i during its $TXOP_i$ and $\overline{T_i}$. Thus, we have:

$$D_i = \frac{\sum_{j=1}^{N_i} p_{s_i} T_L}{\overline{T_i}} \tag{6.41}$$

where $N_i = max(1, \lfloor \frac{TXOP_i}{T_L + SIFS} \rfloor)$. p_{s_i} is computed in the same way as in Section 6.3.3.

6.4.3 Performance Evaluation

In this section, we validate the accuracy of our model through simulations. We used ns-2 to simulate a highway scenario, where one RSU is placed at its center; vehicles passing by contend to transmit fixed-size UDP packets. AC parameter sets are kept the same as in Table 6.II. The other simulation parameters are listed in Table 6.III. We did not include results of AC_2 and AC_3 as we found that they are identical to the previously proposed model.

Table 6.III: 2^{nd} Model Simulation Parameters

Vehicles' speed	70 miles/h	Data rate	6 Mbps
$TXOP_0$	1.504 ms	$TXOP_1$	3.008 ms

Figure 6.8 shows the normalized throughput of $AC0$ and $AC1$ as a function of packet arrival rate. We set the number of vehicles in the RSU's transmission range to 4 and

L to 512 bytes. We observe that our model allows both AC_0 and AC_1 to have higher throughput compared to the standard thanks to the use of TXOP. We also observe that the normalized throughput has the tendency to stabilize as the packet arrival rate increases for both $AC0$ and $AC1$. Indeed, when λ_i increases, ACs have more packets buffered in their queues (i.e., saturation condition). As a result, they continually contend for the channel. This is compatible with the findings of our first model.

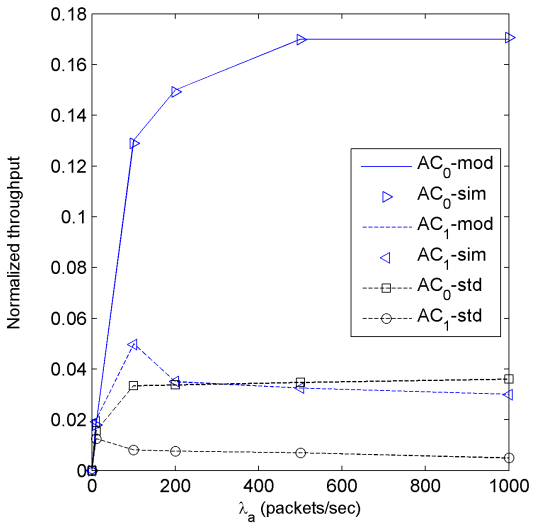

Figure 6.8: Normalized throughput vs. packet arrival rate

Figure 6.9 shows the normalized throughput as a function of the number of stations per AC. We set $L = 512$ bytes and $\lambda_i = 4$ Mbps. As expected, our model incurs higher normalized throughput compared to IEEE 802.11p. In addition, we observe that the normalized throughput decreases with the increase in the number stations. This is because as the number of stations increases, more ACs will contend for the channel, leading to higher number of collisions. Consequently, τ_i decreases, reducing therefore the normalized throughput.

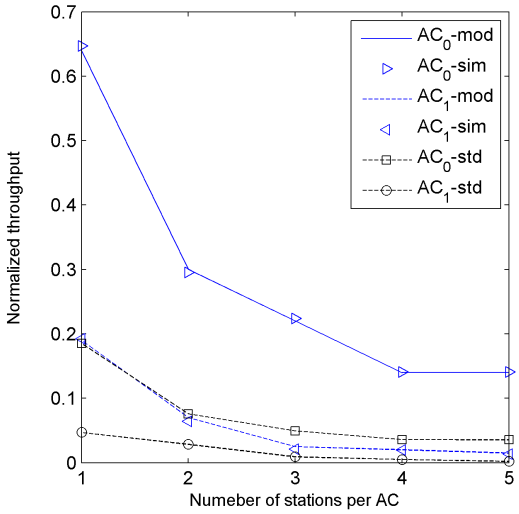

Figure 6.9: Normalized throughput vs. number of stations per AC

Finally, Figure 6.10 depicts the normalized throughput as a function of the packet size. Here, we set the number of vehicles in the RSU's transmission range to 4 and $\lambda_i = 0.5$ Mbps. Again, we see that using TXOP enhances the normalized throughput of both AC_0 and AC_1 in comparison to the IEEE 802.11p standard. This is due to the fact that transmitting multiple packets per channel access allows for the transmission of a higher number of data bytes, augmenting therefore the normalized throughput.

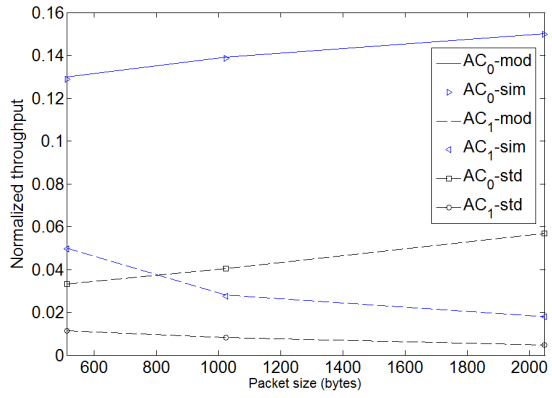

Figure 6.10: Normalized throughput vs. packet size

6.5 Chapter Summary

In this chapter, we developed two stochastic models to analyze the performance of IEEE 802.11p EDCA for infotainment applications. In the first model, two Markov chains were proposed. One illustrating the backoff procedure for each AC while the other portraying the contention phase after a busy period. Both chains consider the backoff counter freezing as well as internal and external collisions. They also consider the busy channel at zero, which is not taken into account by almost all existing schemes. In the second model, we took into consideration TXOP, unused by IEEE 802.11p, in order to enhance the throughput of infotainment applications. Simulation results show that our first model perfectly represents the throughput of different ACs. Simulation results also show that using TXOP can increase the throughput of infotainment applications, allowing for better QoS.

CHAPTER 7

CONCLUSIONS AND PERSPECTIVES

7.1 Conclusions

VANET has seized the attention of different governments, industries, and academic institutions since it offers tremendous potential for new business opportunities in terms of traffic efficiency, convenience, and passengers' infotainment. Yet, it has particular challenges that may hinder its real-life deployment. The main objective of this research project was to design new mechanisms for QoS support of infotainment applications in VANET. To accomplish this goals, this dissertation proposes an efficient routing protocol for urban VANET (SCRP), a service channel selection scheme (ASSCH), and two stochastic models to analyze the performance of the IEEE 802.11p EDCA mechanism.

In SCRP, information included in beacon messages is used to build backbones over road segments, favoring vehicles moving with low relative speeds. Once backbones are built, special nodes at intersections, labeled bridge nodes, are selected based on how long they will stay at the junctions. These nodes will then collect information (i.e., number of hops, delay, and connectivity) using a new control packet, called RAP. This information is then used to assign weights to road segments. To control RAP size, the city is divided into zones and an articulation junction is selected in each one of them. The articulation junction is connected to most intersections in its zone and has up-to-date information about connectivity and delay in its respective zone. By probing bridge nodes at articulation junctions, possible routes between source and destination are constructed. Routes with the lowest aggregated weights are selected to forward data packets. Simulation results show that SCRP achieves better performance compared to existing greedy-based schemes in terms of E2ED and packet delivery ratio.

ASSCH is a hybrid service channel selection scheme designed for V2V infotainment applications. It is a WAVE-compliant mechanism that assists providers in selecting the least congested/used SCHs when setting up their WBSS. It starts by collecting real-time

SCHs state information and updating CSTs accordingly. This is done throughout SI. During CCI, vehicles keep track of received WSA to update their CSTs. During SCI, providers select monitors to listen to different SCHs. SCHs state information is then fed to a Markovian model in order to predict SCHs state in the near future. Finally, SCHs are categorized based on their predicted states and the least used SCHs are selected. Simulation results show that ASSCH outperforms existing allocation-based schemes and performs as good as prediction-based schemes since it allows for quicker access to service channels, handles the overlapping WBSS problem better, and incurs higher throughput and success rate.

Finally, we mathematically analyze the performance of IEEE 802.11p EDCA for V2V infotainment applications. Two stochastic models are proposed. Both models take into consideration the ACs parameter sets, the backoff counter freezing, the busy channel at zero, and the internal and external collisions. The first model includes two Markov chains that describe the backoff procedure and the contention phase of the different access categories. The second model extends the first model by considering TXOP, unexploited in IEEE 802.11p, in order to enhance the throughput of infotainment applications. Simulation results show that our first proposed model perfectly represents the throughput of different ACs. They also show that using $TXOP$ can increase the throughput of the different infotainment applications, allowing for better QoS.

7.2 Limitations

SCRP: During the initial phase of VANET's deployment, not all vehicles will be equipped with WAVE devices which may impact the performance of SCRP as it will not be able to: 1) precisely compute the stability factor to select vehicles to be included into backbones; 2) accurately estimate the information regarding connectivity and delay to attribute weights to road segments; and 3) quickly select articulation junctions.

ASSCH: To predict the state of SCHs in the next SCI, ASSCH uses the Markovian model described in Chapter 5. This Markovian model is executed by providers that want to establish WBSS in every SCI even though we made the service time of providers with

different priorities known to all vehicles. This increases the complexity of ASSCH.

EDCA Analysis Model: Due to time constraints, we limited the number of contending ACs to 5. Also, we made providers transmit their packets on the same service channel, instead of using different ones, in order to simulate the contention phase.

7.3 Perspectives

SCRP deployment in cities with irregular road topologies: In Chapter 4, one of SCRP key components is the selection of articulation junctions. We did so by dividing a city, with regular topology (i.e., grid topology) into zones of 3×3 blocks. Yet, we did not consider cities with irregular road topology. Therefore, an extension to SCRP would be to specify a mechanism to select articulation junctions in cities with irregular topologies. A possible solution would be to divide the city into cells of radius r and use the same process described in Chapter 5 to select the articulation junctions. The value of r, however, should reflect the tradeoff between convergence time and routing overhead. On the one hand, a large value of r means that cells will contain many junctions. This implies that the overhead for establishing routes will be low, but the scheme will converge slowly as several rounds of RAP exchanges are needed to select the articulation junctions. On the other hand, having a small value of r will yield a rapid selection of the articulation junctions. Yet, the overhead for route construction will be high since several articulation junctions may be prompted.

Dynamic Switching to freshly available SCHs: In ASSCH, high priority providers can share SCHs with low priority providers in case all SCHs are occupied. Still, once one of the SCHs becomes available, ASSCH does not allocate the freshly available SCH to one of the providers sharing a service channel. As an extension to ASSCH, providers sharing SCHs can be allowed to dynamically switch to the freshly available SCH, improving therefore their service quality. Questions to be addressed are: which provider should switch to the newly available SCH (i.e., considering priority, WBSS lifetime, and the occupants of adjacent SCHs) and how to inform users of the eventual SCH switching.

Adaptive mechanism to dynamically select the best TXOP value: It was shown

in this dissertation that the performance of infotainment applications can be improved if TXOP is considered. Nevertheless, the values of TXOP used in this dissertation are similar to the ones used by IEEE 802.11e. An extension of this study would analytically determine which parameters to consider when deciding whether a provider should change its TXOP value. Another extension would be to implement this approach in Veins [81], allowing for results' verification.

7.4 Future Research Direction

Cross-layer approach for multihop infotainment applications: An interesting buildup to the work done in this dissertation would be to design a cross-layer approach to further enhance multihop non-safety applications' QoS. Indeed, this approach should enable data forwarding of non-safety applications in a multihop fashion and should support both V2V and V2I communication modes. When a provider wants to transmit data to a far away user, the cross-layer approach will be deployed. On the one hand, the MAC layer will be in charge of selecting the best available SCH (i.e., least used or least prone to interferences) and dynamically switch to a freshly available SCH if the current used SCH is shared. The network layer, on the other hand, is responsible for selecting the best routing paths, depending on the application requirements (i.e., paths with low E2ED or high throughput).

7.5 Articles Published/Submitted

The list of journal articles and conference papers produced during this thesis is as follows:

1. M. A. Togou, A. S. Hafid and L. Khoukhi, "SCRP: Stable CDS-Based Routing Protocol for Urban Vehicular Ad Hoc Networks," in IEEE Transactions on Intelligent Transportation Systems, vol. 17, no. 5, pp. 1298-1307, May 2016.
2. M.A. Togou, L. Khoukhi and A. S. Hafid, "Performance Analysis and Enhancement of WAVE for V2V Infotainment Applications," Submitted to IEEE Transactions on Intelligent Transportation Systems.

3. M. A. Togou, L. Khoukhi and A. S. Hafid, "An Altruistic Service Channel Selection Scheme for V2V Infotainment Applications," Accepted in IEEE International Conference on Communications (ICC), Paris, France (21-25 May, 2017).
4. M. A. Togou, L. Khoukhi and A. S. Hafid, "IEEE 802.11p EDCA Performance Analysis for Vehicle-to-Vehicle Infotainment Applications," Accepted in IEEE International Conference on Communications (ICC), Paris, France (21-25 May, 2017).
5. M. A. Togou, L. Khoukhi and A. S. Hafid, "Throughput analysis of IEEE802.11p EDCA considering transmission opportunity for non-safety applications," 2016 IEEE International Conference on Communications (ICC), Kuala Lumpur, 2016, pp. 1-6.
6. M. A. Togou, A. S. Hafid and L. Khoukhi, "A Novel CDS-based Routing Protocol for Vehicular ad hoc Networks in Urban Environment," Global Communications (GLOBECOM), 2015 IEEE Conference on, 6-10 Dec. 2015.
7. M. A. Togou, A. S. Hafid and P.K. Sahu, "A stable minimum velocity CDS-based virtual backbone for VANET in city environment," Local Computer Networks (LCN), 2014 IEEE 39th Conference on , vol., no., pp.510,513, 8-11 Sept. 2014.

BIBLIOGRAPHY

[1] J. Nzouonta, N. Rajgure, G. Wang, and C. Borcea, "Vanet routing on city roads using real-time vehicular traffic information," *Vehicular Technology, IEEE Transactions on*, vol. 58, no. 7, pp. 3609–3626, Sept 2009.

[2] S. Al-Sultan, M. M. Al-Doori, A. H. Al-Bayatti, and H. Zedan, "A comprehensive survey on vehicular ad hoc network," *J. Netw. Comput. Appl.*, vol. 37, pp. 380–392, Jan. 2014.

[3] T. Cars, "What's the average life expectancy of a car battery?" http://www.telegraph.co.uk/cars/advice/, August 2016, [Online; posted 18-August-2016].

[4] R. R.S., K. M., and S. N., "Security challenges, issues and their solutions for vanet," *Inter. J. Net. Sec. and App. (IJNSA)*, vol. 5, no. 15, 2013.

[5] J. B. Kenney, "Dedicated short-range communications (dsrc) standards in the united states," *Proceedings of the IEEE*, vol. 99, no. 7, pp. 1162–1182, July 2011.

[6] H. H. and L. K.P., *Introduction*. John Wiley and Sons, Ltd, 2009.

[7] C. Campolo and A. Molinaro, "Multichannel communications in vehicular ad hoc networks: a survey," *IEEE Communications Magazine*, vol. 51, no. 5, pp. 158–169, May 2013.

[8] A. Festag, G. Noecker, M. Strassberger, A. Lubke, B. Bochow, M. T.-M. amd S. Schnaufer, R. Eigner, C. Catrinescu, and J. Kunisch, "NowâĂŤnetwork on wheels: Project objectives, technology and achievements," in *Proceedings of the 6th International Workshop on Intelligent Transportation*, 2008.

[9] S. Kumar and A. K. Verma, "Position based routing protocols in vanet: A survey," *Wireless Personal Communications*, vol. 83, no. 4, pp. 2747–2772, 2015.

[10] B. Karp and H. T. Kung, "Gpsr: Greedy perimeter stateless routing for wireless networks," in *Proceedings of the 6th Annual International Conference on Mobile Computing and Networking*, ser. MobiCom '00, 2000, pp. 243–254.

[11] C. Lochert, H. Hartenstein, J. Tian, H. Fussler, D. Hermann, and M. Mauve, "A routing strategy for vehicular ad hoc networks in city environments," in *Intelligent Vehicles Symposium, 2003. Proceedings. IEEE*, June 2003, pp. 156–161.

[12] C. Lochert, M. Mauve, H. Fussler, and H. Hartenstein, "Geographic routing in city scenarios," *SIGMOBILE Mob. Comput. Commun. Rev.*, vol. 9, no. 1, pp. 69–72, Jan. 2005.

[13] G. Liu, B.-S. Lee, B.-C. Seet, C.-H. Foh, K.-J. Wong, and K.-K. Lee, "A routing strategy for metropolis vehicular communications," in *Information Networking. Networking Technologies for Broadband and Mobile Networks*, ser. Lecture Notes in Computer Science. Springer Berlin Heidelberg, 2004, vol. 3090, pp. 134–143.

[14] V. Naumov and T. Gross, "Connectivity-aware routing (car) in vehicular ad-hoc networks," in *INFOCOM 2007. 26th IEEE International Conference on Computer Communications. IEEE*, May 2007, pp. 1919–1927.

[15] M. Jerbi, S.-M. Senouci, R. Meraihi, and Y. Ghamri-Doudane, "An improved vehicular ad hoc routing protocol for city environments," in *Communications, 2007. ICC '07. IEEE International Conference on*, June 2007, pp. 3972–3979.

[16] H. Wu, R. Fujimoto, R. Guensler, and M. Hunter, "Mddv: A mobility-centric data dissemination algorithm for vehicular networks," in *Proceedings of the 1st ACM International Workshop on Vehicular Ad Hoc Networks*, ser. VANET '04, 2004, pp. 47–56.

[17] J. Zhao and G. Cao, "Vadd: Vehicle-assisted data delivery in vehicular ad hoc networks," *Vehicular Technology, IEEE Transactions on*, vol. 57, no. 3, pp. 1910–1922, May 2008.

[18] H. Saleet, R. Langar, K. Naik, R. Boutaba, A. Nayak, and N. Goel, "Intersection-based geographical routing protocol for vanets: A proposal and analysis," *Vehicular Technology, IEEE Transactions on*, vol. 60, no. 9, pp. 4560–4574, Nov 2011.

[19] N. Alsharif, S. Cespedes, and X. Shen, "icar: Intersection-based connectivity aware routing in vehicular ad hoc networks," in *Communications (ICC), 2013 IEEE International Conference on*, June 2013, pp. 1736–1741.

[20] P. Sahu, E. Wu, J. Sahoo, and M. Gerla, "Bahg: Back-bone-assisted hop greedy routing for vanet's city environments," *Intelligent Transportation Systems, IEEE Transactions on*, vol. 14, no. 1, pp. 199–213, March 2013.

[21] N. Sofra, A. Gkelias, and K. Leung, "Route construction for long lifetime in vanets," *Vehicular Technology, IEEE Transactions on*, vol. 60, no. 7, pp. 3450–3461, Sept 2011.

[22] C. Campolo, A. Cortese, and A. Molinaro, "Crasch: A cooperative scheme for service channel reservation in 802.11p/wave vehicular ad hoc networks," in *Ultra Modern Telecommunications Workshops, 2009. ICUMT '09. International Conference on*, Oct 2009, pp. 1–8.

[23] C.-C. T. Kuo-Lung Wang, Tsan-Pin Wang, "A fair scheme for multi-channel selection in vehicular wireless networks," *Wireless Personal Communications*, vol. 73, no. 3, pp. 1049–1065, 2013.

[24] J. Shi, T. Salonidis, and E. W. Knightly, "Starvation mitigation through multi-channel coordination in csma multi-hop wireless networks," in *Proceedings of the 7th ACM International Symposium on Mobile Ad Hoc Networking and Computing*, ser. MobiHoc '06, 2006, pp. 214–225.

[25] C. Han, M. Dianati, R. Tafazolli, and R. Kernchen, "Asynchronous multi-channel mac for vehicular ad hoc networks," in *Vehicular Networking Conference (VNC), 2011 IEEE*, Nov 2011, pp. 109–115.

[26] N. Lu, X. Wang, P. Wang, P. Lai, and F. Liu, "A distributed reliable multi-channel mac protocol for vehicular ad hoc networks," in *Intelligent Vehicles Symposium, 2009 IEEE*, June 2009, pp. 1078–1082.

[27] N. Lu, Y. Ji, F. Liu, and X. Wang, "A dedicated multi-channel mac protocol design for vanet with adaptive broadcasting," in *Wireless Communications and Networking Conference (WCNC), 2010 IEEE*, April 2010, pp. 1–6.

[28] H. Su and X. Zhang, "Clustering-based multichannel mac protocols for qos provisionings over vehicular ad hoc networks," *Vehicular Technology, IEEE Transactions on*, vol. 56, no. 6, pp. 3309–3323, Nov 2007.

[29] K. Inage, S. Lee, T. Fujii, and O. Altintas, "White space vectors for channel selection in vehicular cognitive networks," in *Vehicular Networking Conference (VNC), 2011 IEEE*, Nov 2011, pp. 55–61.

[30] S. Chen and R. Vuyyuru, "Dynamic channel selection for wireless mobile ad hoc networks: Adaptation and learning," in *Wireless and Mobile Computing, Networking and Communications (WiMob), 2013 IEEE 9th International Conference on*, Oct 2013, pp. 75–82.

[31] B. Radunovic, A. Proutiere, D. Gunawardena, and P. Key, "Dynamic channel, rate selection and scheduling for white spaces," in *Proceedings of the Seventh COnference on Emerging Networking EXperiments and Technologies*, ser. CoNEXT '11, 2011, pp. 2:1–2:12.

[32] I. Brahmi, S. Djahel, and Y. Ghamri-Doudane, "A hidden markov model based scheme for efficient and fast dissemination of safety messages in vanets," in *Global Communications Conference (GLOBECOM), 2012 IEEE*, Dec 2012, pp. 177–182.

[33] F. Mapar and K. Chowdhury, "Predictive decision-making for vehicular cognitive radio networks through hidden markov models," in *Communications (ICC), 2014 IEEE International Conference on*, June 2014, pp. 1537–1542.

[34] A. Boyaci, A. H. Zaim, and C. Sönmez, "A cross-layer adaptive channel selection mechanism for IEEE 802.11p suite," *EURASIP J. Wireless Comm. and Networking*, vol. 2015, p. 214, 2015.

[35] Y. L. Morgan, "Notes on dsrc & wave standards suite: Its architecture, design, and characteristics," *Commun. Surveys Tuts.*, vol. 12, no. 4, pp. 504–518, Oct. 2010.

[36] S. Eichler, "Performance evaluation of the ieee 802.11p wave communication standard," in *Vehicular Technology Conference, 2007. VTC-2007 Fall. 2007 IEEE 66th*, Sept 2007, pp. 2199–2203.

[37] J. Gallardo, D. Makrakis, and H. Mouftah, "Performance analysis of the edca medium access mechanism over the control channel of an ieee 802.11p wave vehicular network," in *Communications, 2009. ICC '09. IEEE International Conference on*, June 2009, pp. 1–6.

[38] F. Kaabi, P. Cataldi, F. Filali, and C. Bonnet, "Performance analysis of ieee 802.11p control channel," in *Mobile Ad-hoc and Sensor Networks (MSN), 2010 Sixth International Conference on*, Dec 2010, pp. 211–214.

[39] C. Han, M. Dianati, R. Tafazolli, R. Kernchen, and X. Shen, "Analytical study of the ieee 802.11p mac sublayer in vehicular networks," *Intelligent Transportation Systems, IEEE Transactions on*, vol. 13, no. 2, pp. 873–886, June 2012.

[40] J. Zheng and Q. Wu, "Performance modeling and analysis of the ieee 802.11p edca mechanism for vanet," *Vehicular Technology, IEEE Transactions on*, vol. PP, no. 99, pp. 1–1, 2015.

[41] V. P. Harigovindan, A. V. Babu, and L. Jacob, "Tuning transmission opportunity (txop) limits for providing bit-based fairness in ieee 802.11p v2i networks," in *Proceedings of the International Conference on Advances in Computing, Communications and Informatics*, ser. ICACCI '12, 2012, pp. 248–254.

[42] K. Xu, Q. Wang, and H. Hassanein, "Performance analysis of differentiated qos supported by ieee 802.11e enhanced distributed coordination function (edcf) in wlan," in *Global Telecommunications Conference, 2003. GLOBECOM '03. IEEE*, vol. 2, Dec 2003, pp. 1048–1053 Vol.2.

[43] M. A. Togou, A. Hafid, and L. Khoukhi, "Scrp: Stable cds-based routing protocol for urban vehicular ad hoc networks," *IEEE Transactions on Intelligent Transportation Systems*, vol. 17, no. 5, pp. 1298–1307, May 2016.

[44] M. A. Togou, L. Khoukhi, and A. S. Hafid, "A novel cds-based routing protocol for vehicular ad hoc networks in urban environments," in *2015 IEEE Global Communications Conference (GLOBECOM)*, Dec 2015, pp. 1–6.

[45] M. A. Togou, L. Khoukhi, and A. Hafid, "Throughput analysis of the ieee802.11p edca considering transmission opportunity for non-safety applications," in *2016 IEEE International Conference on Communications (ICC)*, May 2016, pp. 1–6.

[46] E. C. Eze, S.-J. Zhang, E.-J. Liu, and J. C. Eze, "Advances in vehicular ad-hoc networks (vanets): Challenges and road-map for future development," *International Journal of Automation and Computing*, vol. 13, no. 1, pp. 1–18, 2016.

[47] "Wireless lan medium access control (mac) and physical layer (phy) specifications," *IEEE Std 802.11-2012*, 2012.

[48] F. Bai, D. D. Stancil, and H. Krishnan, "Toward understanding characteristics of dedicated short range communications (dsrc) from a perspective of vehicular network engineers," in *Proceedings of the Sixteenth Annual International Conference on Mobile Computing and Networking*, ser. MobiCom '10, 2010, pp. 329–340.

[49] "Ieee standard for wireless access in vehicular environments (wave)-multi-channel operation," *IEEE Std. 1609.4, Feb. 2011*, Feb 2011.

[50] "Ieee standard for wireless access in vehicular environments (wave) – networking services," *IEEE Std 1609.3-2016 (Revision of IEEE Std 1609.3-2010)*, pp. 1–160, April 2016.

[51] "Ieee standard for wireless access in vehicular environments–security services for applications and management messages," *IEEE Std 1609.2-2016 (Revision of IEEE Std 1609.2-2013)*, pp. 1–240, March 2016.

[52] V. G. Martinez, L. H. Encinas, and S. Avila, "A survey of the elliptic curve integrated encryption scheme," *Journal of Computer Science and Engineering*, vol. 2, no. 2, pp. 7–13, 2010.

[53] "Dedicated short range communication (dsrc) message set dictionnary," *SAE std. J2735*, pp. 1–267, March 2016.

[54] "Draft first annual report: Interoperability issues of vehicle-to-vehicle based safety systems project (v2v-interoperability)," *Vehicle Safety Communications 3 (VSC3) Consortium, Submitted to U.S. Dept. Trans.*, Jan 2011.

[55] I. Chakeres and E. Belding-Royer, "Aodv routing protocol implementation design," in *Distributed Computing Systems Workshops, 2004. Proceedings. 24th International Conference on*, March 2004, pp. 698–703.

[56] S. Wang, C. Lin, Y. Hwang, K. Tao, and C. Chou, "A practical routing protocol for vehicle-formed mobile ad hoc networks on the roads," in *Intelligent Transportation Systems, 2005. Proceedings. 2005 IEEE*, Sept 2005, pp. 161–166.

[57] V. Namboodiri, M. Agarwal, and L. Gao, "A study on the feasibility of mobile gateways for vehicular ad-hoc networks," in *Proceedings of the 1st ACM International Workshop on Vehicular Ad Hoc Networks*, ser. VANET '04, 2004, pp. 66–75.

[58] C.-C. Ooi and N. Fisal, "Implementation of geocast-enhanced aodv-bis routing protocol in manet," in *TENCON 2004. 2004 IEEE Region 10 Conference*, vol. B, Nov 2004, pp. 660–663 Vol. 2.

[59] V. Naumov, R. Baumann, and T. Gross, "An evaluation of inter-vehicle ad hoc networks based on realistic vehicular traces," in *Proceedings of the 7th ACM International Symposium on Mobile Ad Hoc Networking and Computing*, ser. MobiHoc '06, 2006, pp. 108–119.

[60] D. Reichardt, M. Miglietta, L. Moretti, P. Morsink, and W. Schulz, "Cartalk2000: safe and comfortable driving based upon inter-vehiclecommunication," in *Proceedings of IEEE Intelligent Vehicle Symposium*, June 2002, p. 545âĂŞ550.

[61] "Mapmechanics, one-stop shop for gis, data and mapping solutions," http://www.mapmechanics.com/, accessed: 2015-01-28.

[62] "Yahoo maps," https://maps.yahoo.com/smartview, accessed: 2015-01-28.

[63] H. Saleet, O. Basir, R. Langar, and R. Boutaba, "Region-based location-service-management protocol for vanets," *Vehicular Technology, IEEE Transactions on*, vol. 59, no. 2, pp. 917–931, Feb 2010.

[64] D. S. Hochbaum, Ed., *Approximation Algorithms for NP-hard Problems*. Boston, MA, USA: PWS Publishing Co., 1997.

[65] N. Meghanathan, "Use of minimum node velocity based stable connected dominating sets for mobile ad hoc networks," *IJCA Special Issue on MANETs*, no. 2, pp. 89–96, 2010.

[66] M. Boban, T. T. V. Vinhoza, J. Barros, M. Ferreira, and O. K. Tonguz, "Impact of Vehicles as Obstacles in Vehicular Ad Hoc Networks," *IEEE Journal on Selected Areas in Communications*, vol. 29, no. 1, pp. 15–28, January 2011.

[67] A. Nadembega, A. Hafid, and T. Taleb, "Mobility prediction-aware bandwidth reservation scheme for mobile networks," *Vehicular Technology, IEEE Transactions on*, vol. PP, no. 99, pp. 1–17, 2014.

[68] H. Li, Y. Cheng, C. Zhou, and W. Zhuang, "Routing metrics for minimizing end-to-end delay in multiradio multichannel wireless networks," *Parallel and Distributed Systems, IEEE Transactions on*, vol. 24, no. 11, pp. 2293–2303, Nov 2013.

[69] A. Abdrabou and W. Zhuang, "Service time approximation in ieee 802.11 single-hop ad hoc networks," *Wireless Communications, IEEE Transactions on*, vol. 7, no. 1, pp. 305–313, Jan 2008.

[70] Q. Wang, S. Leng, H. Fu, and Y. Zhang, "An ieee 802.11p-based multichannel mac scheme with channel coordination for vehicular ad hoc networks," *Intelligent Transportation Systems, IEEE Transactions on*, vol. 13, no. 2, pp. 449–458, June 2012.

[71] "The network simulator: ns2," http://www.isi.edu/nsnam/ns/, accessed: 2015-01-28.

[72] "Sumo - simulation of urban mobility," http://www.dlr.de/ts/en/desktopdefault.aspx/tabid-9883/, accessed: 2016-01-30.

[73] K.-C. Lan, "Move: A practical simulator for mobility model in vanet," in *Telematcics Communication Technologies and Vehicular Networks: Wireless Architecture and Applications*, Feb 2010, pp. 355–368.

[74] H. Xia, "A simplified analytical model for predicting path loss in urban and suburban environments," *Vehicular Technology, IEEE Transactions on*, vol. 46, no. 4, pp. 1040–1046, Nov 1997.

[75] "Ieee standard for wireless access in vehicular environments (wave)-multi-channel operation," *IEEE Std. 1609.4, Feb. 2011*, Feb 2011.

[76] C.-M. Huang and C. Yuh-Shyan, *Telematics Communication Technologies and Vehicular Networks: Wireless Architectures and Applications*. Hershey, PA: IGI Global, 2010.

[77] M. Amadeo, C. Campolo, and A. Molinaro, "Enhancing ieee 802.11p (wave) to provide infotainment applications in vanets," *Ad Hoc Netw.*, vol. 10, no. 2, pp. 253–269, Mar. 2012.

[78] FCC, "Amendment of the commissionâĂŹs rules regarding dedicated short-range communication services in the 5.850âĂŞ5.925 ghz band (5.9 ghz band)," *FCC Memorandum Opinion and Order*, vol. FCC 06-110, July 2006.

[79] K. Hafeez, L. Zhao, B. Ma, and J. Mark, "Performance analysis and enhancement of the dsrc for vanet's safety applications," *Vehicular Technology, IEEE Transactions on*, vol. 62, no. 7, pp. 3069–3083, Sept 2013.

[80] "Omnet++ discrete event simulator," https://omnetpp.org/, accessed: 2016-01-30.

[81] "Veins - the open source vehicular network simulation framework," http://veins.car2x.org/, accessed: 2016-01-30.

[82] "Wireless lan medium access control (mac) and physical layer (phy) specifications - amendment 8: Medium access control (mac) quality of service enhancements," *IEEE Std 802.11e-2005 (Amendment to IEEE Std 802.11, 1999 Edition (Reaff 2003)*, pp. 1–212, Nov 2005.

[83] G. Bianchi, "Performance analysis of the ieee 802.11 distributed coordination function," *Selected Areas in Communications, IEEE Journal on*, vol. 18, no. 3, pp. 535–547, March 2000.